TORNADO TRACKING BY HIGH FREQUENCY SFERICS

By

HENRY BRADFORD FERGUSON

Bachelor of Science
Oklahoma Agricultural and Mechanical College
Stillwater, Oklahoma
1942

Master of Science
Oklahoma Agricultural and Mechanical College
Stillwater, Oklahoma
1948

Submitted to the faculty of the Graduate School of
the Oklahoma Agricultural and Mechanical College
in partial fulfillment of the requirements
for the degree of
DOCTOR OF PHILOSOPHY
May, 1956

TORNADO TRACKING BY HIGH FREQUENCY SFERICS

Thesis Approved:

Herbert L. Jones
Thesis Advisor

Chas. F. Cameron

E. J. Allen

Harold Trimmer

A. Nader

Robert MacVicar
Dean of the Graduate School

PREFACE

Since man first came into the Great Plains Region of the United States, he has been plagued by tornadoes. The tornado problem has been discussed a great deal by scientists for many years, but, until recently, no one has made significant progress in the study of tornadoes. About eight years ago, a research project was started at Oklahoma Agricultural and Mechanical College under the direction of Dr. H. L. Jones to study the tornado problem. This pioneer research had as its objectives, first, to develop a means for identifying a tornado in the formative stage so that endangered persons might be warned, and, second, to develop a means of preventing the formation of tornadoes. Great strides have been made toward accomplishment of the first objective and there is at present no reason to believe that the second objective will not be successfully attained.

This thesis describes research directed toward the accomplishment of the first objective of the overall program. Early in the program, a sferic method of tornado tracking and identification was developed by Dr. Jones and his associates. However, the early work was handicapped by the lack of a suitable sferic direction finder. The instrument which was available, designated as the AN/GRD-1A, had been developed at the University of Florida to study sferics associated with hurri-

canes. For that work it was well suited, but its use in tornado tracking was limited.

The purpose of the research described in this thesis is threefold; namely, to analyze the AN/GRD-1A as it applies to the detection of tornado-type sferics, to design a High Frequency Direction Finder more suitable for the detection of tornado-type sferics, and to analyze the data obtained with the High Frequency Direction Finder as applied to two specific examples of severe weather activity.

This work was carried out under the able direction of Dr. H. L. Jones who is the man most responsible for the success of the tornado research project. Mr. Ruben Kelly, a project engineer and graduate student of Oklahoma A & M College, did an excellent job of building the High Frequency Direction Finder. He also modified the original design as the work progressed in order to improve its operational characteristics and has assisted in collecting much of the data presented here. Without the guidance of Dr. Jones and the assistance of Mr. Kelly, this thesis would not have been possible.

A word of thanks is due to Mr. Joe Pat Lindsey for permitting the use of some introductory material from his thesis on frequency analysis of the sferic waveform. The author also wishes to thank Mrs. Doris Harding for typing the manuscript.

TABLE OF CONTENTS

LIST OF TABLES

LIST OF ILLUSTRATIONS

CHAPTER I

INTRODUCTION

If you have ever lived in the Great Plains Area of the United States, you can perhaps remember those hot, sultry, cloudy days in late spring when the very stillness of the air is depressing. This is what old timers on the plains call "cyclone weather". In late afternoon or early evening of many such days as this, residents of some community in this vast region have been terrified by a great roar not unlike the sound of many on-rushing freight trains. Those who are familiar with the sound immediately go to the storm cellar or any other place of shelter which may be found. Unfortunately in many cases there is not time to reach shelter or no shelter is available. Within a few minutes the terrible roar has passed leaving a path of death and destruction in any community which may have been unlucky enough to be in its path. This is what happens when a tornado strikes. The tornado, improperly called by many a cyclone, is one of nature's most violent phenomena and leaves a path of destruction as much as a mile in width and often many miles long. Tornadoes have occurred which had a path of more than a hundred miles.

The author lived, as a child, in a small community in Eastern Oklahoma which was almost completely destroyed by a

tornado. That was the famous Peggs, Oklahoma tornado of May 2, 1920[1]. Seventy-one people were killed and property losses amounted to $175,000.00. The Peggs tornado was the fourth most destructive tornado, in terms of loss of life, in the history of the state.

In recent years much research has been done on the meteorological conditions which must exist for a tornado to occur. Among the leaders in this field are Colonel E. J. Fawbush and Major R. C. Miller of the Air Force Weather Service at Tinker Air Force Base, Oklahoma[2]. Great progress has been made along this line and it is now possible, from a study of weather conditions to determine that conditions are favorable over a large area for buildup of a tornado and that the occurrence of a tornado is probable. Tornadoes usually occur when cold dry air with a steep lapse rate from the west or northwest is overrun by warm moist air from the south or southwest. The topography of the broad plains region east of the Rocky Mountains is more favorable for these conditions than any other place in the world.

The formation of tornadoes is so rapid that a method of forcasting is desirable which is much more rapid than the

---

[1]Snowden D. Flora, Tornadoes of the United States, (University of Oklahoma Press, Norman, 1953) p. 137

[2]Major E. J. Fawbush, Captain R. C. Miller, and Captain L. C. Starrett, "An Empirical Method of Forecasting Tornado Development". Bulletin of the American Meteorological Society, January, 1951, pp. 1-9

application of conventional weather observations. A research group at Oklahoma A & M College under the direction of Dr. Herbert L. Jones has been working on this problem for the past few years and has produced excellent results[3]. A method has been devised which is both rapid and accurate for detecting the location of a tornado.

The method devised by Dr. Jones is to observe the electromagnetic radiation from the lightning flashes which take place both while the tornado is building up and while it is active. It has been found that the number of lightning strokes per second increases slowly as the tornado is formed, reaching a maximum just prior to the time when the tornado becomes active, decreases slightly during the active life of the tornado and decreases rapidly as the fury of the tornado is spent. Observation of the lightning strokes for this method is accomplished by an instrument called a sferic direction finder which visually displays the direction of the event on an oscilloscope. By counting the strokes from a given direction, any buildup of tornadic conditions can be noted. Since tornadoes are always associated with squall lines, a dangerous situation can be identified at a point where an azimuth of high sferics count crosses a squall line. A radar set is used to locate the position of squall lines. This method has

---

[3] "Research on Tornado Identification", Sixth Quarterly Progress Report, Signal Corps Research Project No. 172B-0 1953, pp. 18-19

been successfully used to identify and track a number of active tornadoes as well as many thunderstorms which did not reach the tornado stage. Tables I and II are examples of high sferics count associated with tornadoes[4]. During the Pawnee tornado the sferics count reached 28 per second and during the Meeker tornado the maximum count was 27 strokes per second.

An interesting aspect of the study of sferics is the variations in frequency within the sferic waveform from different types of storms. Low power storms such as thunderstorms usually produce sferics with a peak frequency in the neighborhood of 10,000 cycles per second. The sferics rate from such a storm rarely exceeds 15 per second. On the other hand, sferics from tornadoes have been recorded which had a peak frequency well in excess of 100,000 cycles per second. Thus, not only does the sferics rate go up as tornadic conditions are approached but also the frequency within the waveform itself increases. These effects are graphically shown in Figures 1, 2 and 3[5]. (These figures are taken directly from the thesis of Joe Pat Lindsey). Figure 1 shows a typical low frequency waveform and its frequency

---

[4]"Research on Tornado Identification", Tenth Quarterly Progress Report, Signal Corps Research, Project No. 172B-0, 1954, p. 27

[5]Joe Pat Lindsey, "An Analysis of the Sferic Waveform", Unpublished Masters Thesis, Oklahoma A & M College, (1954), pp. 41-43

TABLE I

Pawnee Tornado

Pre-Tornado Counts						Reported Time of Tornado
5:10 p.m.	5:15 p.m.	5:20 p.m.	5:25 p.m.	5:30 p.m.	5:35 p.m.	5:40 p.m.
14*	19	20	21	24	21	27
12	19	14	22	19	26	24
21	13	16	16	18	20	23
16	16	17	21	23	26	30
12	20	23	15	22	24	25
19	14	19	20	18	17	30
18	18	25	16	20	20	26
21	23	22	12	23	27	24
Ave. 17	18	19	18	21	23	26

Tornado and Post-Tornado Counts						
5:45 p.m.	5:50 p.m.	5:55 p.m.	6:00 p.m.	6:05 p.m.	6:10 p.m.	6:15 p.m.
26	22	26	21	19	16	15
32	24	24	25	20	14	12
29	26	24	21	21	14	12
21	27	22	18	20	11	9
27	26	22	19	16	18	15
24	38	21	17	17	14	11
28	26	24	22	23	13	15
25	33	23	21	19	15	16
Ave. 27	28	23	21	19	14	13

* Each one of these readings covers the stroke count over a one second interval.

TABLE II

Meeker Tornado

Pre-Tornado Counts			Reported** Time of Tornado
6:15 p.m.	6:20 p.m.	6:25 p.m.	6:30 p.m.
16*	21	24	29
19	17	24	24
15	22	36	27
25	18	20	28
19	25	20	27
14	20	25	25
18	19	22	30
23	21	19	24
Ave. 18	20	24	27

Tornado and Post-Tornado Counts					
6:35 p.m.	6:40 p.m.	6:45 p.m.	6:47 p.m.	6:50 p.m.	6:55 p.m.
27	31	23	18	16	23
24	30	26	24	23	18
23	25	26	20	19	9
25	27	27	27	19	16
27	27	23	21	24	26
29	22	25	23	24	19
28	27	27	20	22	12
24	23	24	18		19
Ave. 26	27	25	21	21	18

* Each one of these readings covers the stroke count over a one second interval.

** Quoted from the Daily Oklahoma.

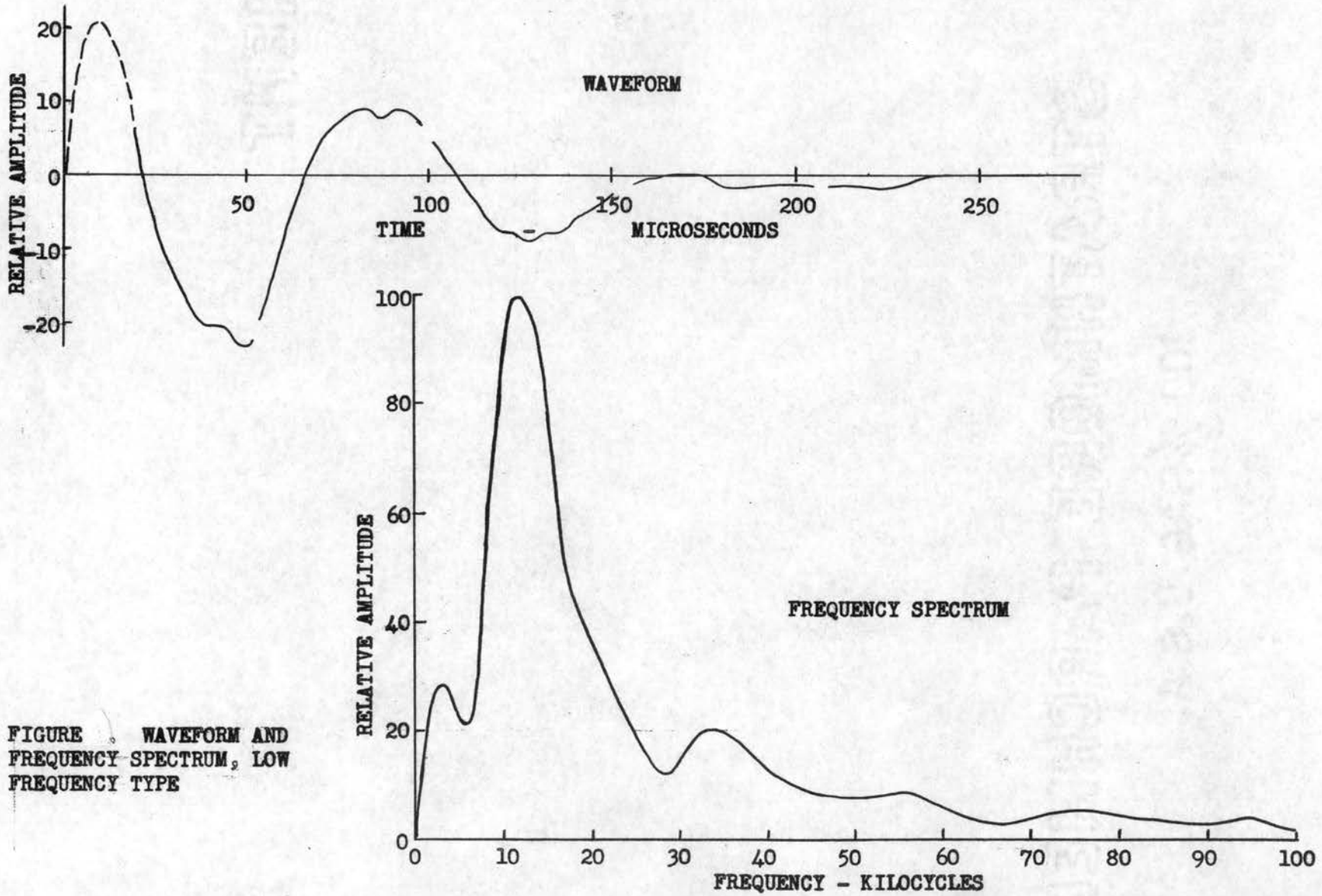

FIGURE . WAVEFORM AND FREQUENCY SPECTRUM, LOW FREQUENCY TYPE

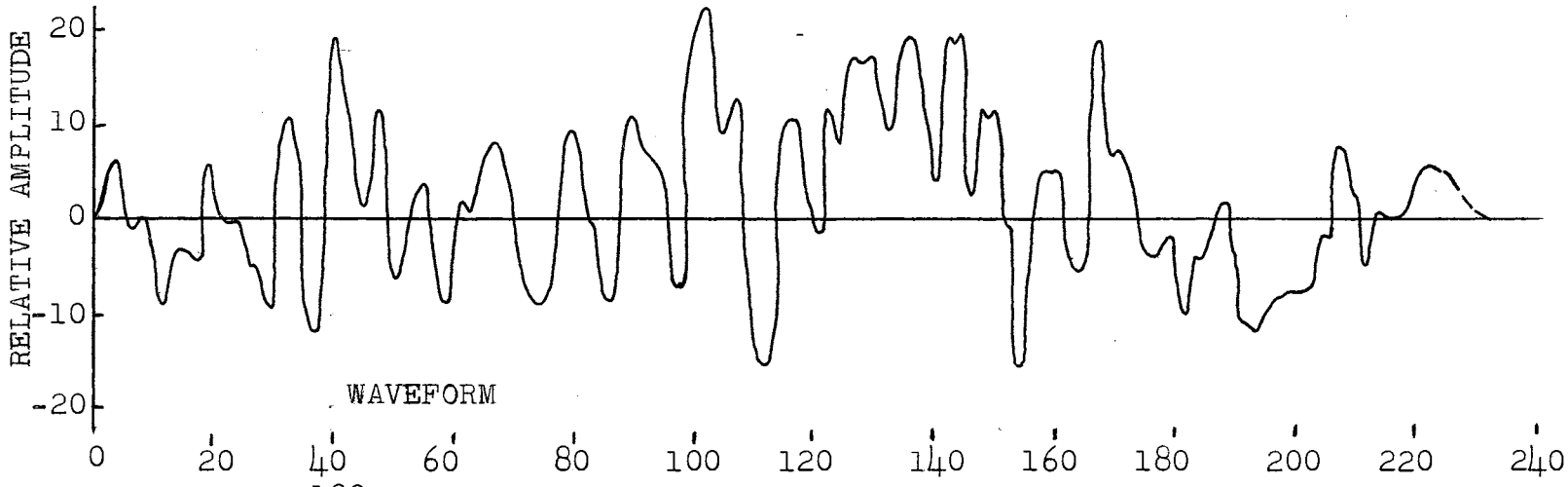

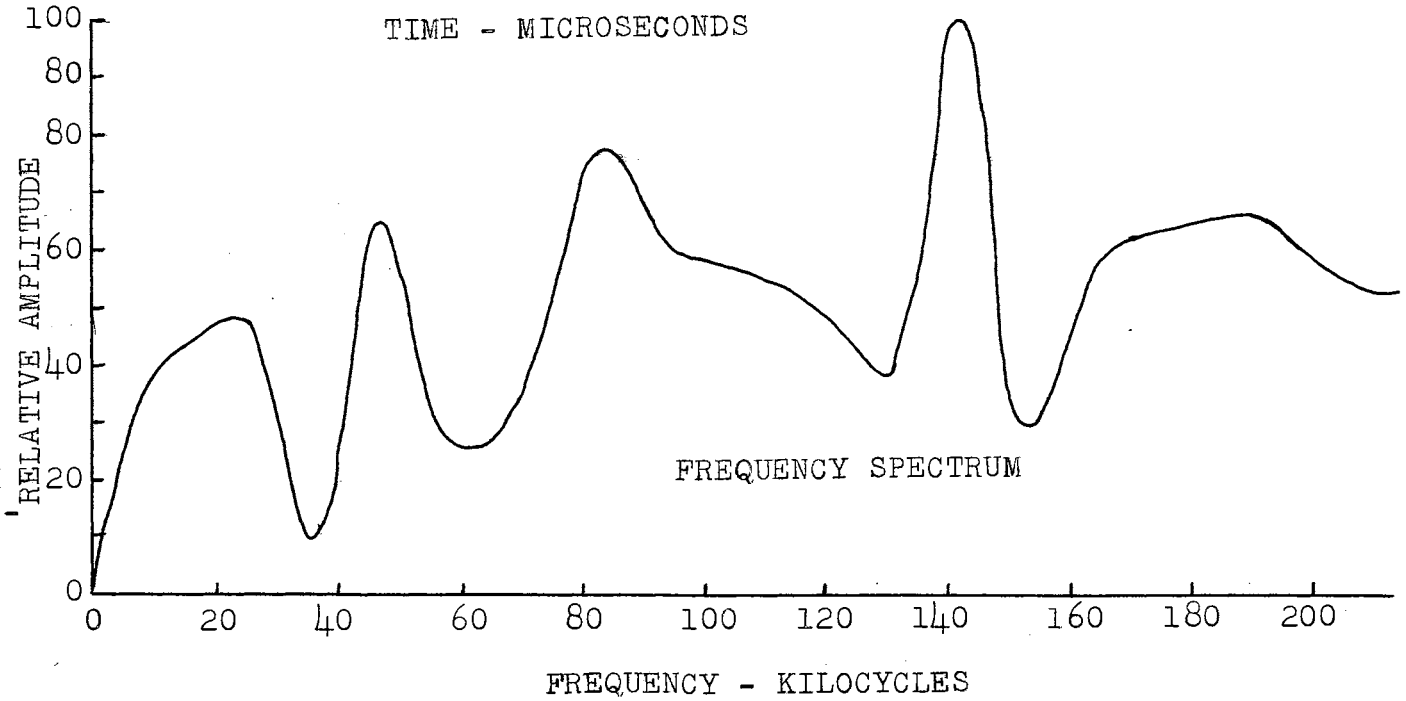

FIGURE 2. WAVEFORM AND FREQUENCY SPECTRUM, HIGHER FREQUENCY TYPE

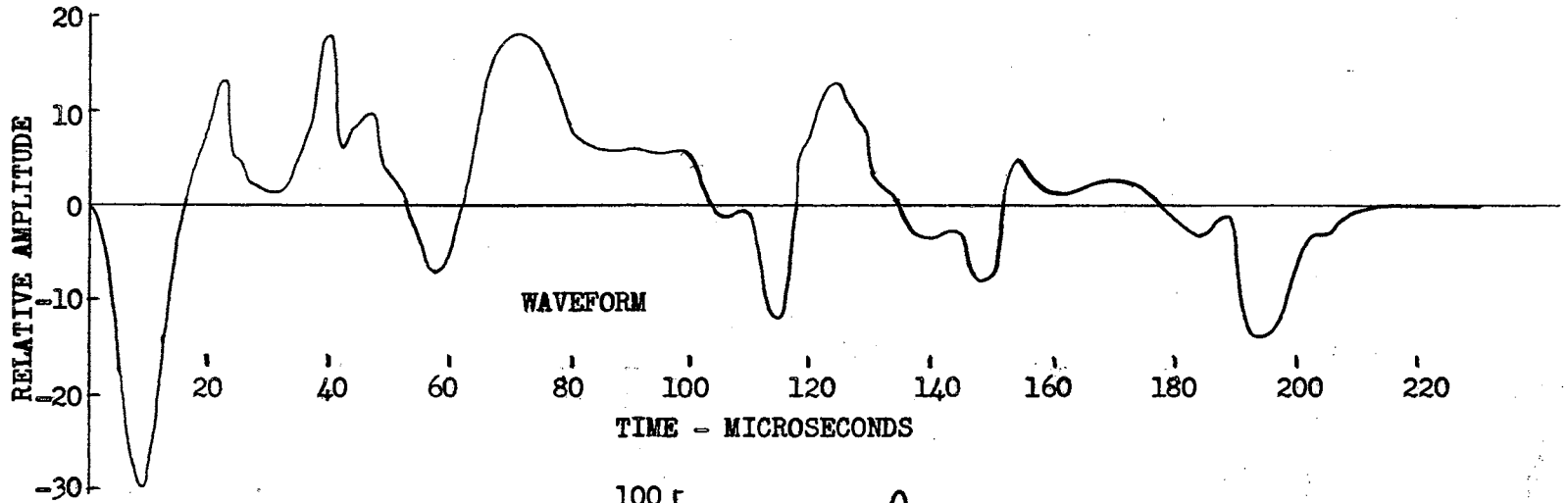

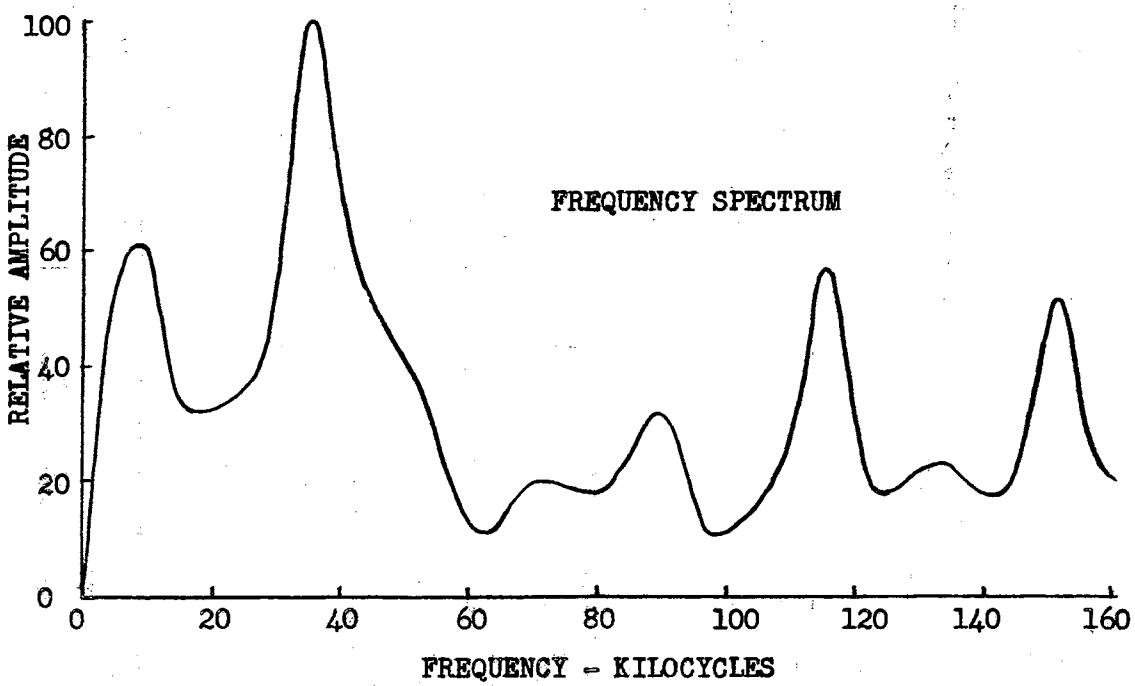

FIGURE 3. WAVEFORM AND FREQUENCY SPECTRUM, MEDIUM FREQUENCY TYPE

spectrum which is peaked at 12,000 cycles per second. This type sferic is usually associated with simple thunderstorms. Figure 2 shows a typical tornado type high frequency sferic with its spectrum peaked at 145,000 cycles per second. Figure 3 shows a medium frequency waveform and spectrum peaked at about 40,000 cycles per second. This sferic may be from either a thunderstorm or a tornado, or from the storm when the tornado is in the formative stage.

An instrument for observation of sferics, designated as the AN/GRD-1A static direction finder, was developed at the University of Florida and has been used effectively in the study of low frequency sferics originating from electrical disturbances associated with hurricanes[6]. However, when the instrument was used in tornado research at Oklahoma A & M College a number of limitations became apparent. First, the frequency response is much too low to record faithfully the high frequency sferics which are associated with tornadoes. In addition, the equipment produces some effects which are not entirely due to the limited frequency response. Figures 4, 5, and 6 are reproductions from moving film strips on which are recorded the output of two direction finders[7].

---

[6] "Static Direction Finder AN/GRD-1A" War Department Technical Manual TM 11-2693, September, 1945

[7] "Research on Tornado Identification", Eleventh Quarterly Progress Report, Signal Corps Research Project No. 172B-0, 1954, pp. 16-18

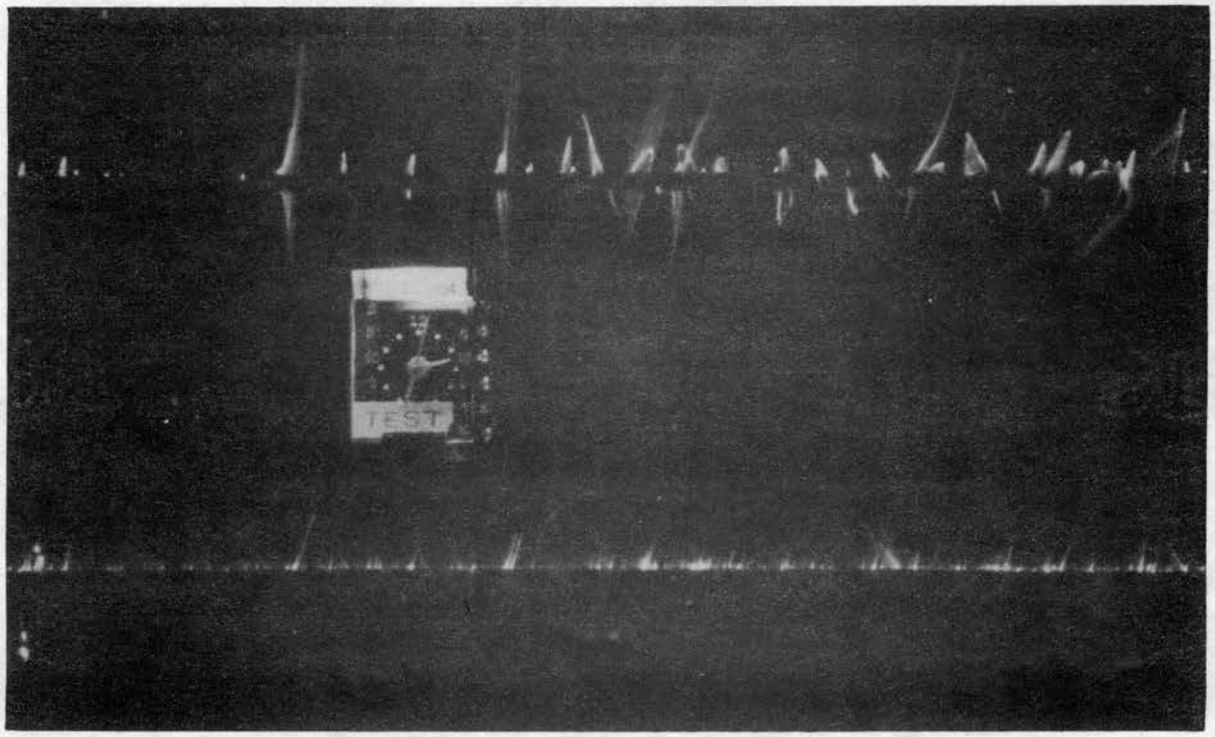

Figure 4. DF records for 1433 CST, Oct.11, 1954.

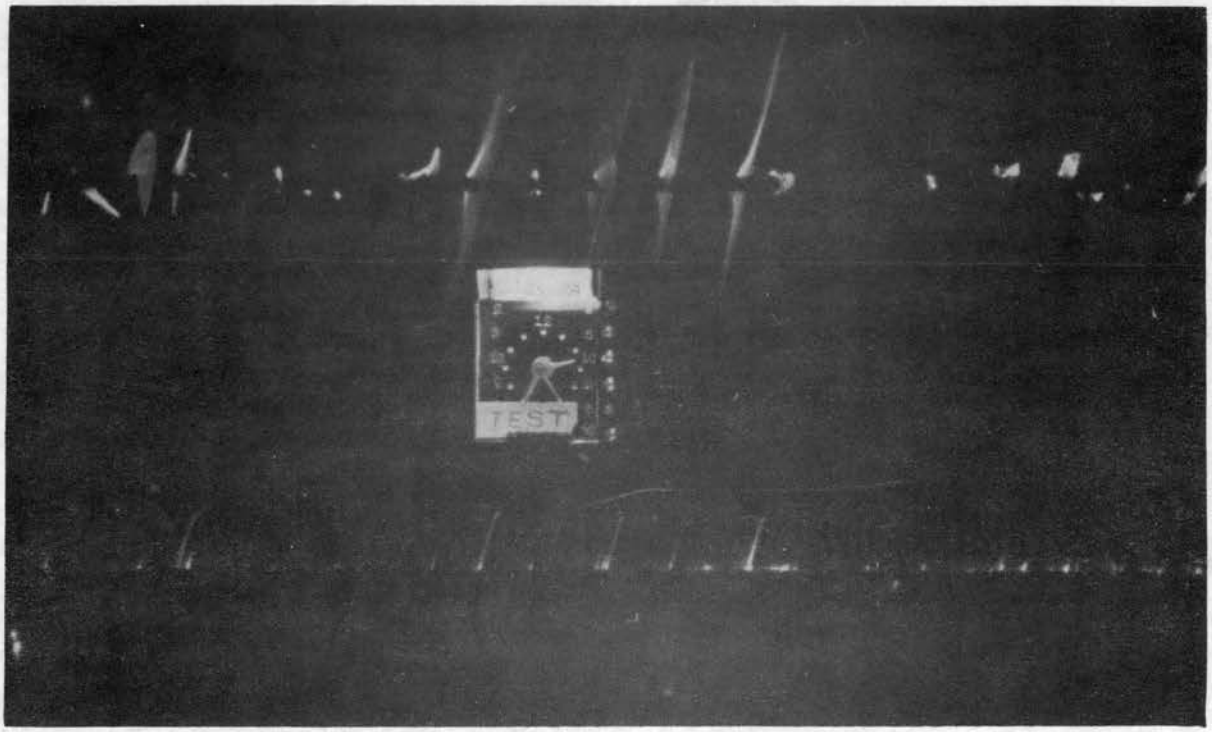

Figure 5. DF records for 1435 CST, Oct. 11, 1954.

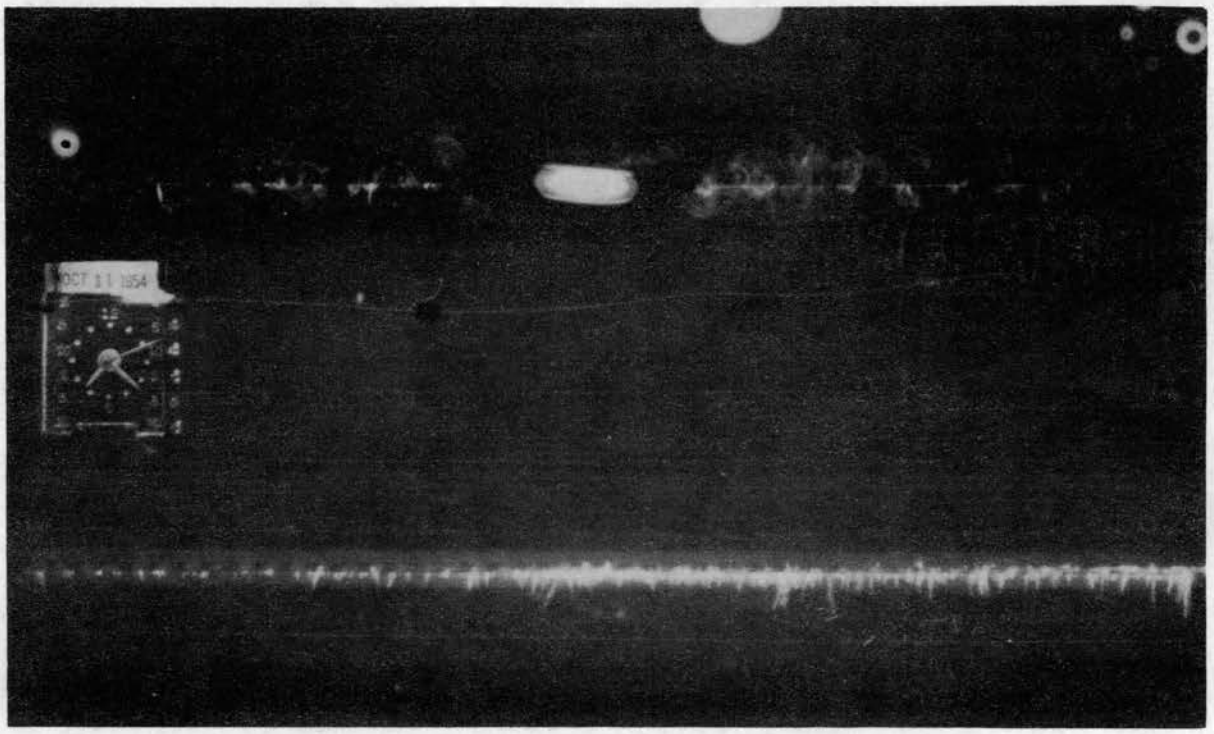

Figure 6. DF records for 1922 CST, Oct. 11, 1954

At the top in each Figure is recorded the output of the AN/GRD-1A direction finder at different instants of time. The recordings at the bottom of the film strips will be discussed later. Ideally these recordings would be a series of straight lines pointing in the direction from which the disturbance came. Instead of a straight line each sferic direction is indicated by a series of ellipses which makes it difficult to determine the direction from which the disturbance came and makes it even more difficult to count the rate at which the sferics occur. The record shown in Figure 6 is particularly bad in this respect. The conclusion should not be made that the AN/GRD-1A is not usable for determining the direction and rate of sferics for indeed it has been used successfully both in tracking thunderstorms with low frequency sferics and in some cases in tracking tornadoes with high frequency sferics. The records shown here are from extreme conditions and are shown to point out the limitations of the equipment and to show the need for an improved sferic direction finder.

This study has three main objectives as follows:

1. To analyze the AN/GRD-1A system to determine its suitability for the study of tornado-type sferics and to determine the cause of the ellipse patterns shown in Figures 4, 5, and 6.
2. To design a sferic direction finder to operate in the frequency range of 100 kilocycles per second

to 300 kilocycles per second.

3. To study the relationship of high frequency sferics, as recorded with the HFDF (high frequency direction finder), to severe weather activity.

CHAPTER II

ANALYSIS OF THE AN/GRD-1A SYSTEM

General Description of the System

The AN/GRD-1A system consists of a set of crossed loop antennas, a dual amplification system, a cathode ray tube indicator and photographic recording equipment. The system is described in detail in War Department Technical Manual TM 11-2693, but a brief description will be given here for completeness.

Figure 7 is a schematic diagram of the AN/GRD-1A system. The antenna loops are fixed on true compass points and connected through their respective amplifiers to the vertical and horizontal plates of an oscilloscope. When a lightning discharge occurs an electromagnetic wave is propagated in all directions from the location of the discharge just as a radio wave is propagated from a transmitting antenna. This wave is detected by the crossed loop antennas and relayed to the oscilloscope where it is registered as a "flash". The voltage induced in each loop of the antenna is a function of the intensity of the incoming electromagnetic wave and the cosine of the angle the wave makes

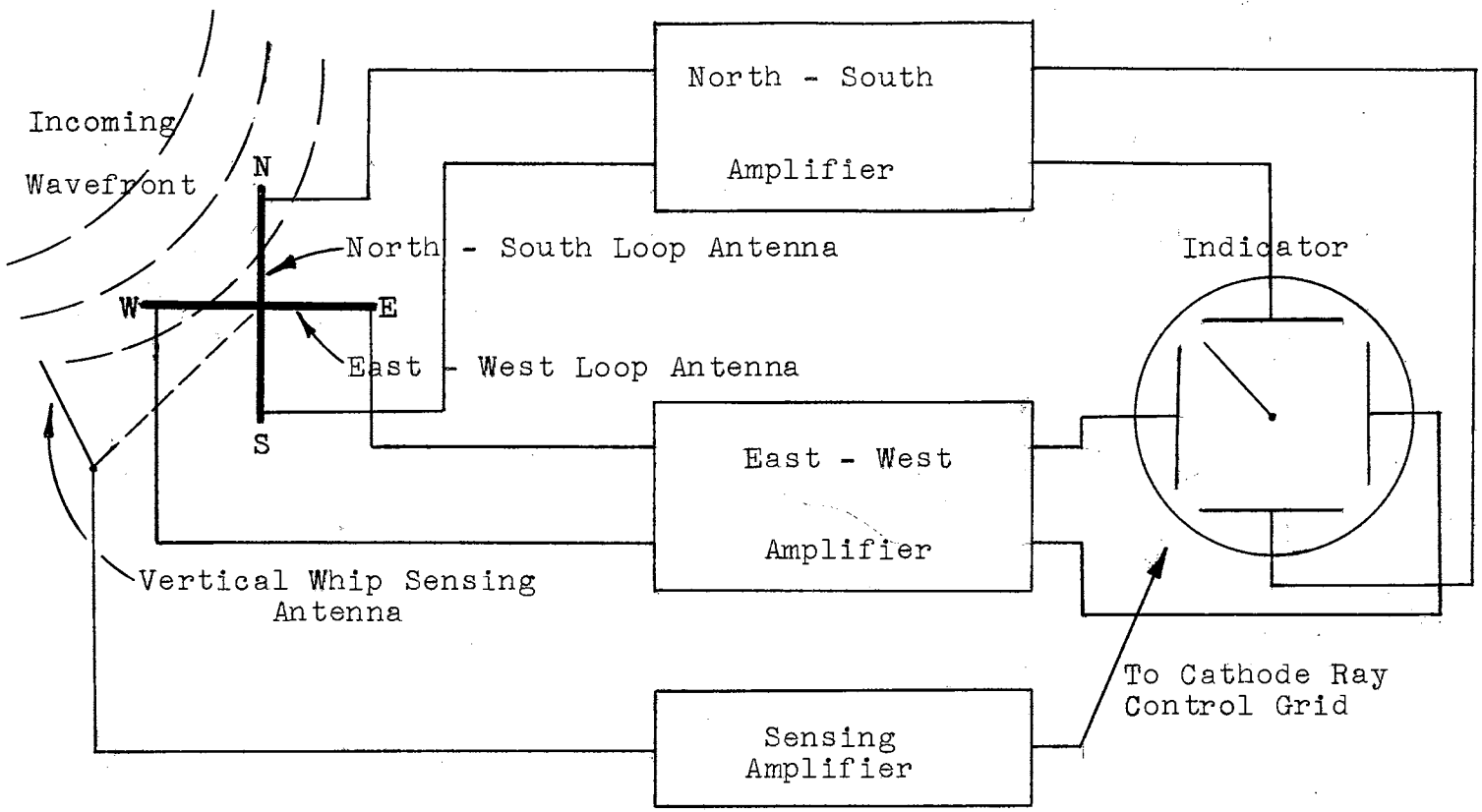

Figure 7. AN/GRD-1A System Block Diagram

with the plane of the loop[1]. Stated mathematically,

$$v_1(t) = E(t) \cos \theta_1,$$

and

$$v_2(t) = E(t) \cos \theta_2,$$

where $E(t)$ is the intensity, $v_1(t)$ and $v_2(t)$ are the voltages generated in loops 1 and 2 respectively, and θ_1 and θ_2 are the respective angles of the incoming wavefront with the planes of the loops. The effect of voltages $v_1(t)$ and $v_2(t)$ on the two sets of oscilloscope deflection plates will thus product a flash in the direction of travel of the wavefront. In the example shown in Figure 7 the flash will thus extend across the scope face from northwest to southeast as shown. A special vertical whip antenna is used to remove the 180° ambiguity which would otherwise result. This is accomplished by amplifying the voltage induced in the sensing antenna and applying it to the control grid of the oscilloscope tube. A wavefront arriving from a given direction produces a voltage in the sensing antenna of one polarity; a voltage from the opposite direction induces a voltage of the opposite polarity. If the intensity of the cathode ray tube is adjusted so that is is very faint at zero signal from the sensing amplifier, the positive peaks of voltage will intensify the trace and the negative peaks

---

[1]Sergei A. Schelkunoff, Harald T. Friis, Antennas Theory and Practice, (John Wiley and Sons, New York, 1952), pp. 503-508.

will "blank" the trace. The oscilloscope trace will thus be intensified in the direction from which the wavefront came, as shown in Figure 7 and the 180° ambiguity is removed.

A block diagram of one of the AN/GRD-1A amplifiers is shown in Figure 8. The North-South and East-West amplifiers are identical. Each amplifier consists of a cathode-follower input stage, an amplifier stage, a tuned-amplifier stage and an output stage to couple to the plates of the indicator oscilloscope tube. There are a number of appropriate gain and frequency control elements in the amplifier which are important from an operational viewpoint. However, the purpose of this study is to make a technical analysis of the amplifier and such operational controls will not be discussed except as they apply to the technical problems under consideration.

Analysis of the Filter Section

One of the characteristics most important in determining the performance of an amplifier, or transmission network, is the transient response of the system. A second important characteristic of an amplifier is the dynamic range of the system. The dynamic range is the variation in signal level that can be faithfully transmitted through the system without excessive noise or distortion. The lower limit of the useful dynamic range of a system is the

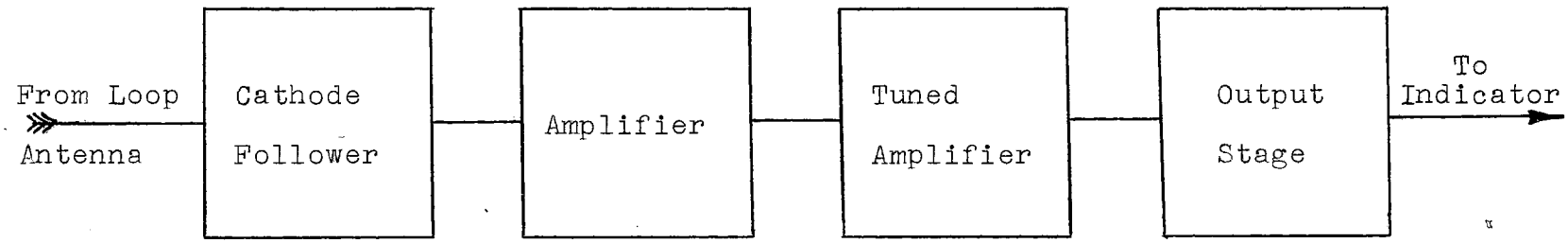

Figure 8. Amplifier Block Diagram

inherent noise of the first stage or element, and the upper end of the range is at the signal level where harmonic distortion of the signal occurs. Both transient response and dynamic range are important considerations in the analysis of the AN/GRD-1A direction finder. An inspection of the amplifier circuit diagram shows that the two sections which limit the transient response and dynamic range are the filter section and the output stage. The cathode-follower input stage and the video amplifier are broad-band amplifiers and the tubes used are powerful enough to produce good dynamic range. Consequently, the emphasis here will be placed on the filter, or tuned-amplifier, section and the output stage.

The transient response of an electrical network may best be determined by use of the Laplace transformation. The Laplace transformation of a function $f(t)$ is defined as[2]

$$F(p) = \int_0^\infty f(t)\, e^{-pt}\, dt = \mathcal{L} f(t).$$

By means of the Laplace transformation, differential and integro differential equations in t may be transformed into algebraic equations in p, where p is a complex variable, that is,

$$p = \lambda + j\omega.$$

---

[2]Stanford Goldman, Transformation Calculus and Electrical Transients, (Prentice-Hall, Inc., New York, 1949), pp. 58-62.

Two special transforms are of importance in network theory. They are

$$\int_0^\infty \frac{d}{dt}\left[f(t)\right] e^{-pt}\, dt = p\, F(p) - f(0+)$$

and

$$\int_0^\infty \left\{\int_0^t f(t)\, dt\right\} e^{-pt}\, dt = \frac{F(p)}{p} + \frac{f^{-1}(0+)}{p},$$

where $f(0+)$ is the value of $f(t)$ as t approaches zero from a positive direction, and $f^{-1}(0+)$ is the value of the indefinite integral $\int f(t)dt$ as t approaches zero from the positive direction. If the system under study is at rest at $t = 0$, as will be the case in this study, $f(0+)$ and $f^{-1}(0+)$ will be zero and

$$L\left[\frac{df(t)}{dt}\right] = p\, F(p)$$

and

$$L\left[\int_0^t f(t)\, dt\right] = \frac{F(p)}{p}.$$

The schematic circuit diagram of the tuned-amplifier circuit of the AN/GRD-1A is shown in Figure 9. In Figure 10 is shown the exact equivalent circuit for Figure 9 and also the approximate equivalent circuit which is adequate for this analysis. In the approximate equivalent circuit each element has been replaced by the Laplace transform which will appear in the equation of response of the network[3].

---

[3] G. E. Valley, Jr., Henry Wallman, Vacuum Tube Amplifiers, (McGraw-Hill Book Company, Inc., New York, 1948), p. 44.

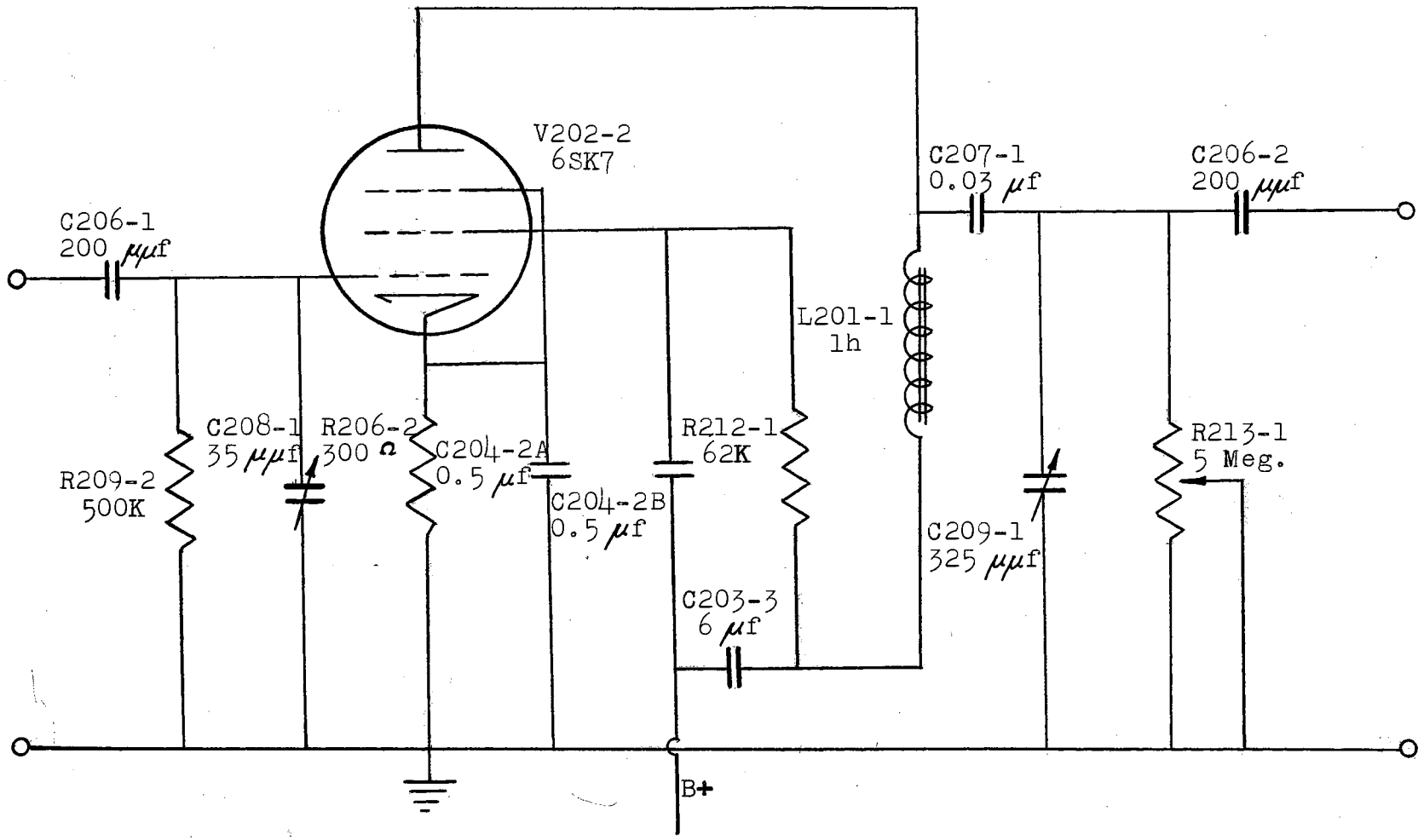

Figure 9. Tuned Amplifier Circuit

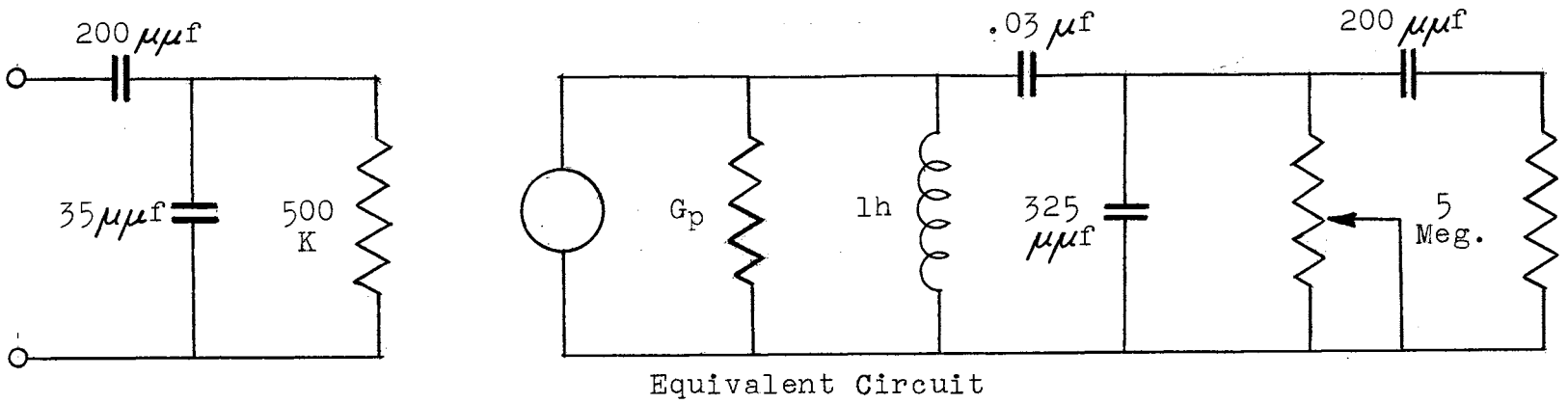

Equivalent Circuit

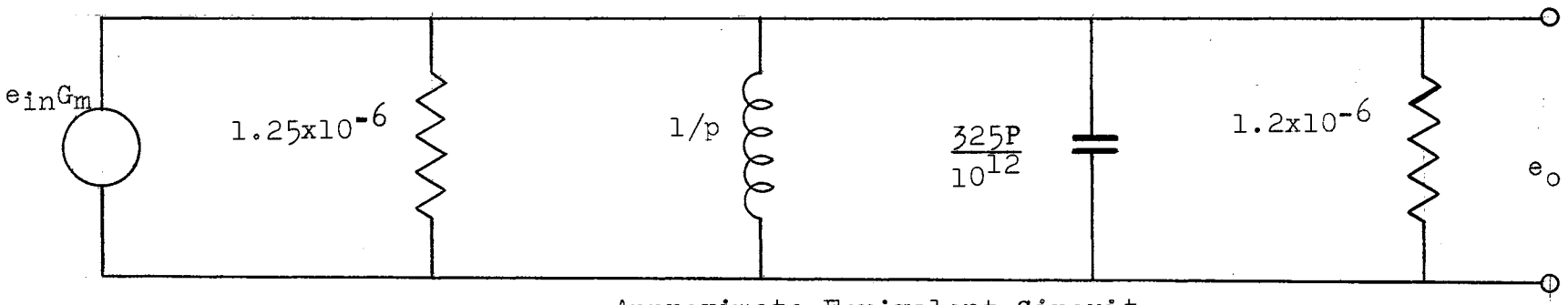

Approximate Equivalent Circuit

Figure 10. Equivalent Circuits of Tuned Amplifier

The equations expressing the response of the equivalent circuit by nodal analysis are as follows:

$$e_{in}\, g_m = e_o \left(1.25 \times 10^{-6} + \frac{1}{p} + \frac{325}{10^{12}}\, p + 1.2 \times 10^{-6}\right),$$

$$\frac{e_o}{e_{in}\, g_m} = \frac{p}{\left(\frac{325}{10^{12}}\, p^2 + 2.45 \times 10^{-6}\, p + 1\right)},$$

or

$$\frac{e_o}{e_{in}\, g_m} = \frac{10^{12}\, p}{325(p^2 + 7.5 \times 10^3\, p + 3.07 \times 10^9)}\ .$$

F(p) is thus the Laplace transform of the transfer function of the tuned amplifier shown in Figure 9. The amplitude and phase response of the transfer function may be obtained by considering F(p) as a function of the imaginary part of p[4]. The frequency response is

$$F(j\omega) = \frac{10^{12}}{325} \times \frac{j\omega}{\left[(j\omega)^2 + 7.5 \times 10^3 (j\omega) + 3.07 \times 10^9\right]}$$

or

$$F(j\omega) = \frac{10^{12}}{325} \times \frac{j\omega}{\left[(3.07 \times 10^9 - \omega^2) - j\, 7.5 \times 10^3 \omega\right]}\ .$$

The above equation may be written $F(j\omega) = A(\omega)\, e^{j\theta(\omega)}$,

where $A(\omega)$ is commonly called the amplitude response of the network and $\theta(\omega)$ is the phase response. Numerical values are given by

$$\omega_o = \sqrt{3070} \times 10^3 = 55.3 \times 10^3 \text{ radians/sec.}$$

and

$$f_o = \frac{55.3}{2\pi} \times 10^3 = 8.81 \times 10^3 \text{ cycles/sec.},$$

---

[4]H. W. Bode, Network Analysis and Feedback Amplifier Design, (D. Van Nostrand Company, Inc., New York, 1945), pp. 22-30.

where f_o is the resonant frequency of the tuned amplifier.

The amplitude response of the tuned amplifier as a function of frequency is shown in Figure 11 and the phase response is shown in Figure 12. The data from which Figures 11 and 12 are plotted are shown in Table III. Examination of Figures 11 and 12 shows no anomalous conditions such as spurious peaks in the amplitude response or sudden reversals in the phase response.

The response of the tuned amplifier to an arbitrary input may be determined by considering the complex poles and zeros of the transfer function. Examination of the equation for F(p) shows that it has no zero except at $p = 0$. The poles of F(p) are the values of the complex variable p where the denominator of the equation of F(p) is equal to zero. To calculate these values, let

$$p^2 + 7.5 \times 10^3 p + 3.07 \times 10^9 = 0 ,$$

whence, $$P_o = (-7.5 \times 10^3 \pm \sqrt{(7.5)^2 \times 10^6 - 4 \times 3.07 \times 10^9}),$$

or $$P_o = -3.75 \times 10^3 \pm j\, 5.5 \times 10^4.$$

The transfer function thus has one pair of conjugate poles at $-3.75 \times 10^3 + j\, 5.5 \times 10^4$ and $-3.75 \times 10^3 - j\, 5.5 \times 10^4$. The poles of F(p) are shown plotted in Figure 13.

The response of a network to a unit impulse is very informative. From the unit impulse response the recovery

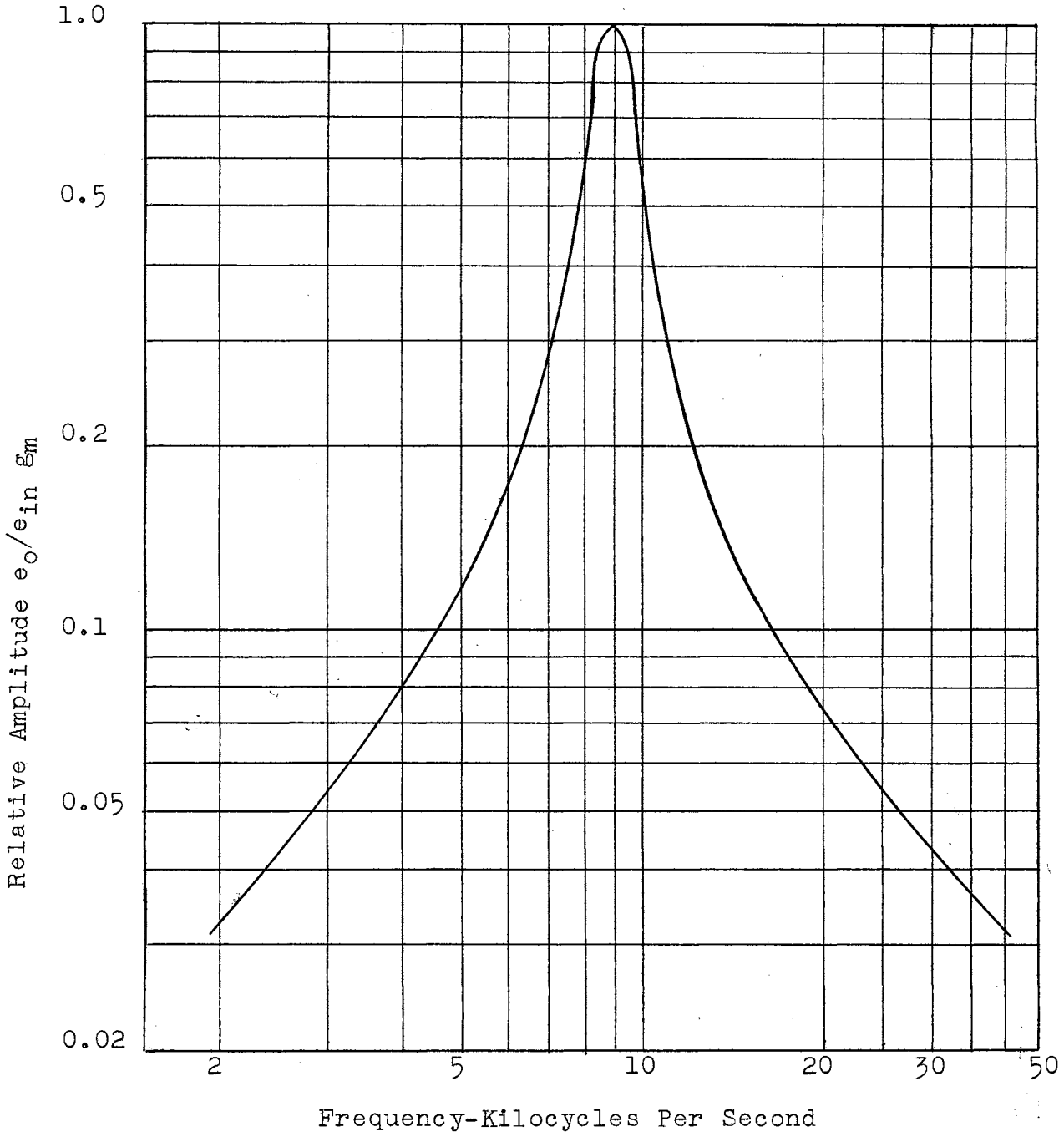

Figure 11. Amplitude Response-Tuned Amplifier

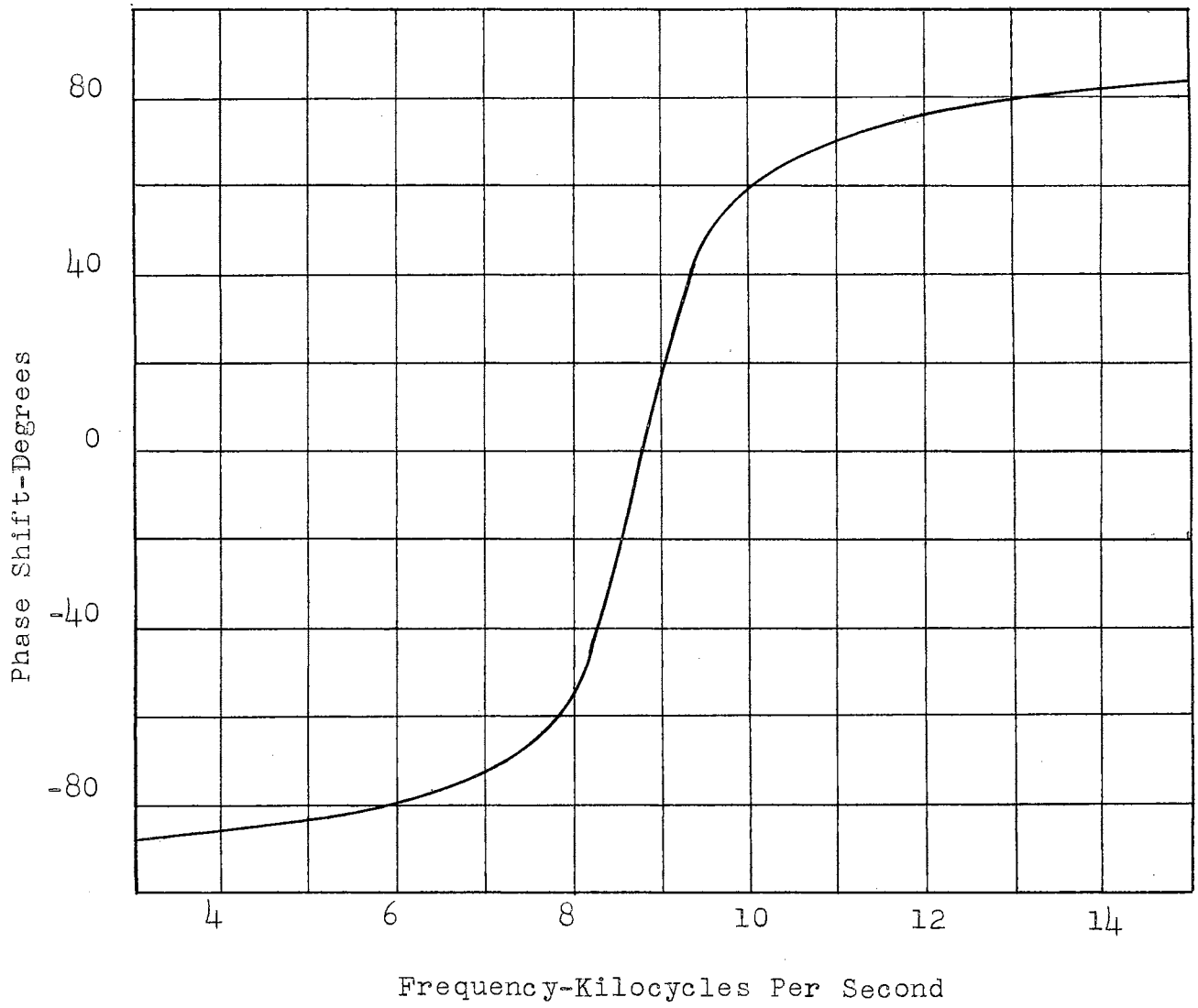

Figure 12. Phase Response-Tuned Amplifier

TABLE III

Amplitude and Phase Response Data - Tuned Amplifier

f kc	ω x10^3	ω^2 10^6	a 10^6	jb 10^6	A 10^6	$\angle\theta$	$\frac{\omega}{A}$ x10^6	$\angle$-90-θ	$\frac{e_o}{e_{in}}$ g_m	$\angle\phi^\circ$	db
2	12.6	158	2912	-94.5	2912	-0	4.32	-90	.0324	-90	29.8
3	18.8	355	2525	-141	2525	0	7.45	-90	.056	-90	25.0
4	25.1	632	2448	-188	2448	-0	10.2	-90	.0765	-90	22.3
5	31.4	990	2080	-236	2095	-6.5	15	-83.5	.113	-83.5	18.9
6	37.7	1420	1650	-283	1670	-9.7	22.6	-80.3	.17	-80.3	15.4
7	4.4	1940	1130	-330	1180	-16.3	37.2	-73.7	.28	-73.7	11.0
8	50.2	2530	540	-376	657	-34.9	76.5	-55.1	.575	-55.1	4.8
8.5	53.3	2850	220	-400	447	-63.4	119	-26.6	.895	-26.6	1.0
8.81	55.3	3070	0	-412	412	-90	133		1		
9.5	59.6	3570	- 500	-447	670	221.8	89	48.2	.67	48	3.5
10	62.5	3950	- 880	-471	1000	208.2	62.8	61.8	.472	61.8	6.5
12	75.5	5700	-2630	-566	2690	192.2	28.0	77.8	.21	77.8	13.5
14	88	7750	-4680	-660	4740	188	18.6	82	.14	82	17.1
16	100	10000	-6930	-750	6960	186.2	14.35	83.8	.1075	83.8	19.4
18	113	12800	-9730	-850	9730	180	11.6	90	.087	90	21.2
20	126	15800	-12730	-945	12730	180	9.9	90	.074	90	22.6
40	252	63500	-60430		60430		4.17	90	.0314	90	30.1
100	628	395000	391000		391000		1.6		.012		38.4

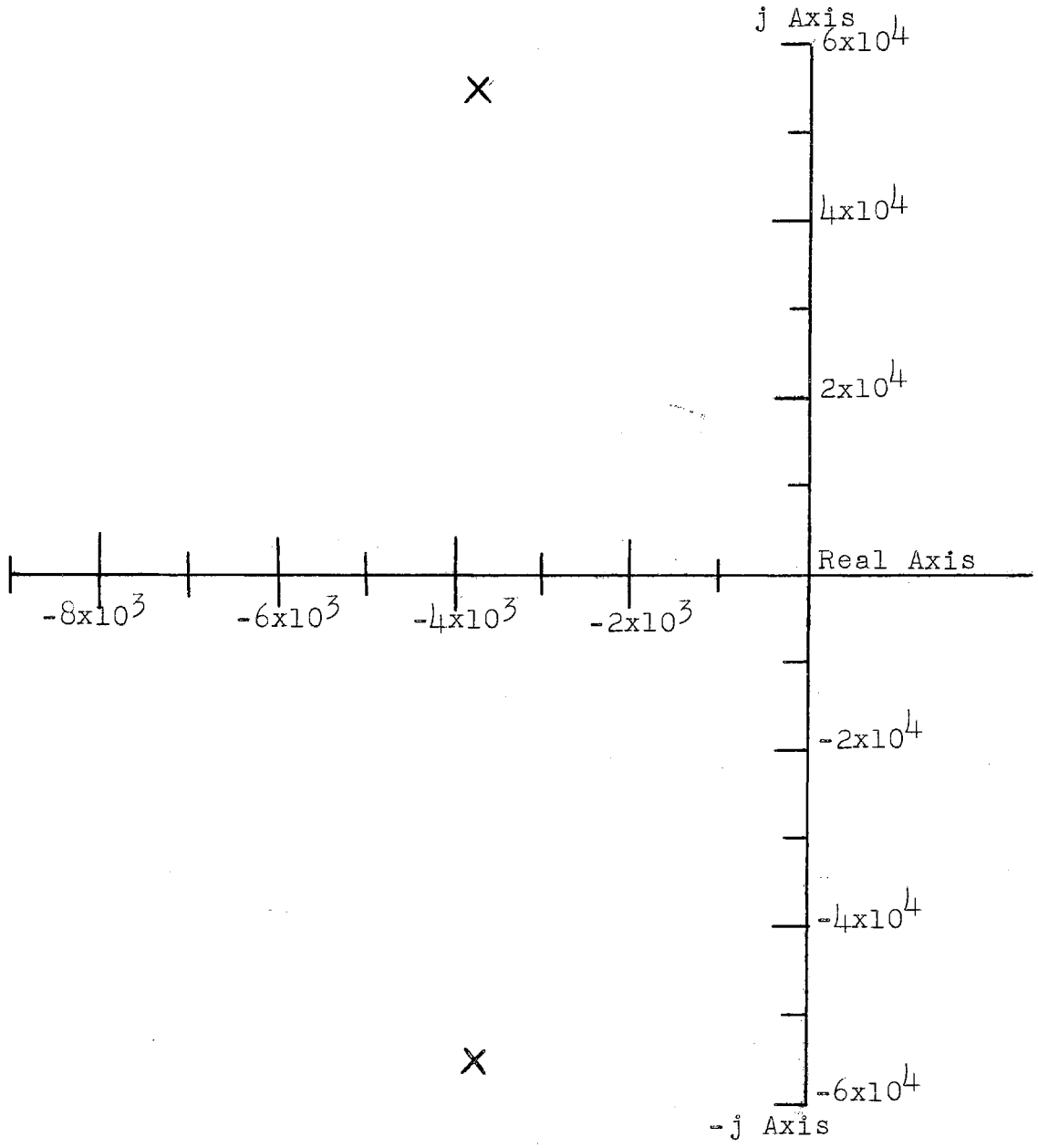

Figure 13. Location of Poles-Tuned Amplifier

time of the network and other useful information can be gained. A unit impulse is a function whose value is zero except in an arbitrarily small interval around t = 0, where it becomes infinite in such a way that

$$\int_a^b \delta(t)\, dt = 1.$$

It is shown by Goldman[5] that $L\left[\delta(t)\right] = 1$.

Therefore,

$$L\left[f(t)\, \delta(t) \right] = F(p).$$

The response of the network to a unit impulse is thus the inverse transform of the transfer function of the network, that is,

$$f(t) = L^{-1}\left[F(p)\right]$$

where f(t) is the response of the network to a unit impulse.

It is also shown by Goldman that

$$f(t) = \frac{1}{2\pi j} \oint F(p)\, e^{pt}\, dp$$

and can be evaluated from the sum of the residues of the function $F(p)\, e^{pt}$ at the poles. Thus,

$$f(t) = R_1 + R_2 .$$

Evaluation gives

$$R_1 = \left[\frac{10^{12}\, p\, e^{pt}}{325 \frac{d}{dp} (p^2 + 7.5 \times 10^3 p + 3.07 \times 10^9)} \right] p = -3.75 \times 10^3 + j5.5 \times 10^4$$

and

$$R_2 = \left[\frac{10^{12}\, p\, e^{pt}}{325 \frac{d}{dp} (p^2 + 7.5 \times 10^3 p + 3.07 \times 10^9)} \right] p = -3.75 \times 10^3 - j5.5 \times 10^4.$$

Numerical solution of the above equation gives,

$$f(t) = 55.4 \times 10^3\, e^{-3.75 \times 10^3 t} \sin (55.4 \times 10^3 t + \theta)$$

---

[5] Goldman, p. 102

where, $\theta = \tan^{-1} 14.75$.

The response of the tuned amplifier to a unit impulse is shown in Figure 14. Although the circuit rings when a waveform strikes, the total recovery time is relatively short, being less than one millisecond. It should, therefore, be possible to count lightning strokes accurately were it not for the elliptical patterns observed on the oscilloscope during severe storms.

It may be concluded that there is nothing inherent in the tuned amplifier which would cause the observed elliptical patterns.

Analysis of the Output Section

The output stage of the AN/GRD-1A is a 6J5 amplifier tube which is transformer coupled to the plates of the cathode ray tube. The circuit is shown schematically in Figure 15. There are not enough data given in the AN/GRD-1A manual to analyze the output circuit, so measurements have been made from which the performance of the circuit can be calculated. Figure 16 shows the equivalent circuit of the output stage. The following relations refer to the equivalent circuit:

$$Z_1 = \frac{e_{in}}{I_1}, \quad Z_2 = \frac{e_o}{I_2} \quad \text{and} \quad Z_3 = j\omega M \ .$$

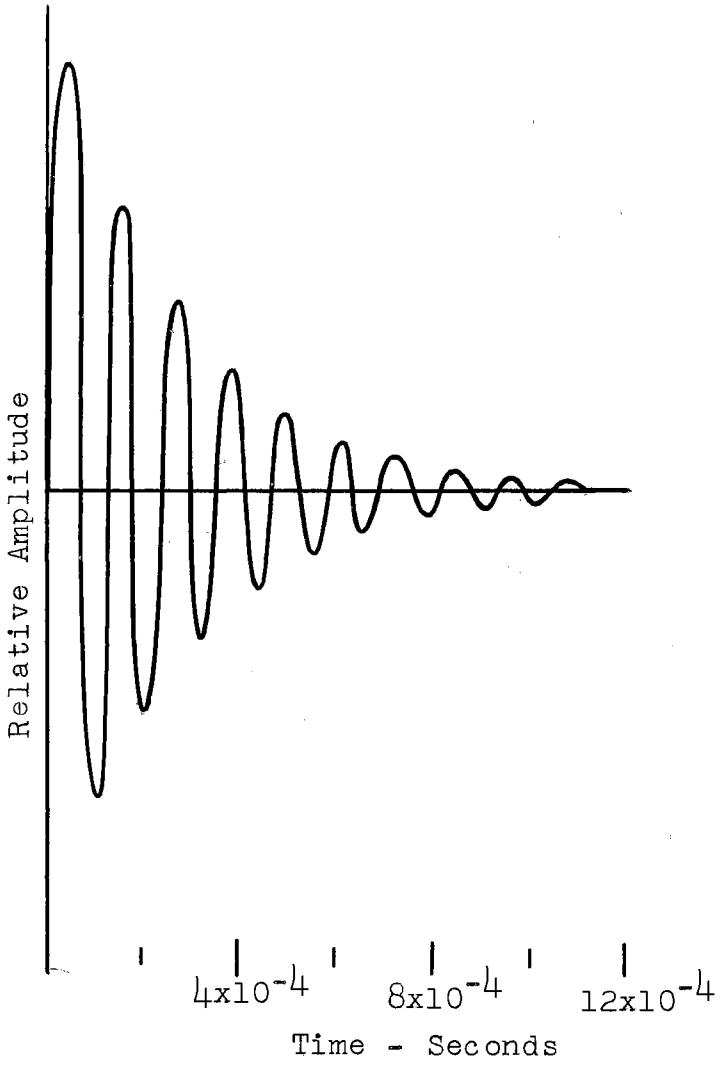

Figure 14. Response of Tuned Amplifier to $\delta(t)$

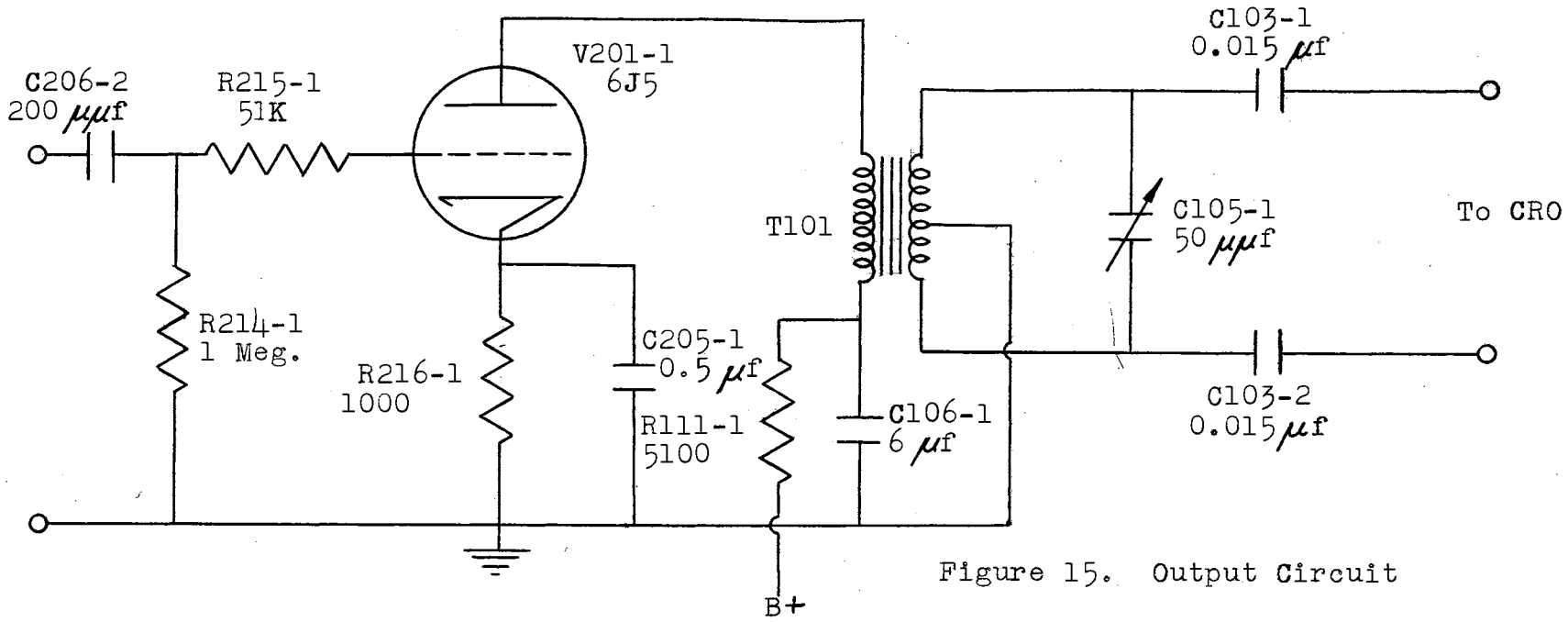

Figure 15. Output Circuit

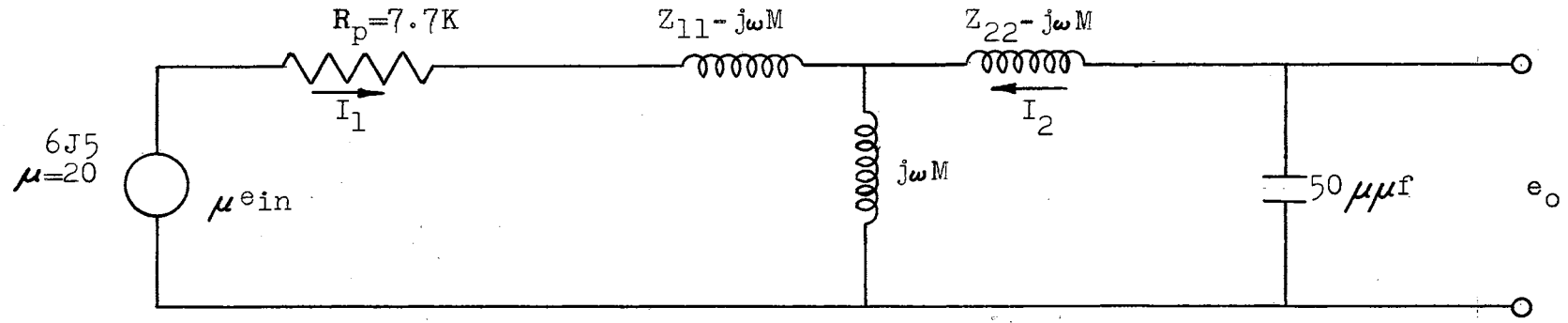

Figure 16. Equivalent Circuit-Output Stage

These parameters may be obtained from measurements as follows:

$$Z_1 = Z_{o1} - \sqrt{Z_{o2}\,(Z_{o1} - Z_{s1})},$$

$$Z_2 = Z_{o2} - \sqrt{Z_{o2}\,(Z_{o1} - Z_{s1})},$$

$$Z_3 = \sqrt{Z_{o2}\,(Z_{o1} - Z_{s1})} = j\omega M,$$

$$Z_{11} = Z_{o1}$$

and

$$Z_{22} = Z_{o2}$$

where Z_{o1} is the measured impedance of the transformer from the primary side with the secondary open, Z_{o2} is the measured impedance of the transformer from the secondary side with the primary open, and Z_{s1} is the measured impedance of the transformer from the primary side with the secondary shorted. The measured parameters of the output transformer are as follows:

D.C. resistance of primary: 1087 ohms

D.C. resistance of secondary: 10,350 ohms

Inductance of primary with secondary open: 11.75 henries

Inductance of secondary with primary open: 79 henries

Inductance of primary with secondary shorted: 225 millihenries.

From the above measurements the amplitude response of the equivalent circuit of the output stage was calculat-

ed by means of the Laplace transform by evaluating the equation of the transfer function along the $j\omega$-axis of the complex variable, p. The calculations are quite similar to those made in the analysis of the filter section and hence will not be shown in detail here.

The calculated amplitude response of the output section is shown in Figure 17. Inspection of the amplitude response may offer some clue to the cause of the ellipses as shown in Figures 4, 5, and 6. The output circuit peaks at about 8000 cycles per second and falls off rather rapidly at higher frequencies. This means that the frequency components of a sferic which are in the neighborhood of 10,000 cycles or above are highly attenuated in the output stage even though they may pass through the tuned amplifier without undue attenuation. This effectively reduces the dynamic range of the amplifier and may result in overloading of the circuits when the sferic frequencies are high.

As the amplitude response of the output stage falls off rapidly above 10,000 cycles per second, the relative phase shift of the output voltage with respect to the input voltage is also changing rapidly. This means that the phase adjustment is critical even at the peak frequency of the filter section. This may add to the ellipse problem since the phase response of the East-West and North-South channels must be identical for accurate measurements of the

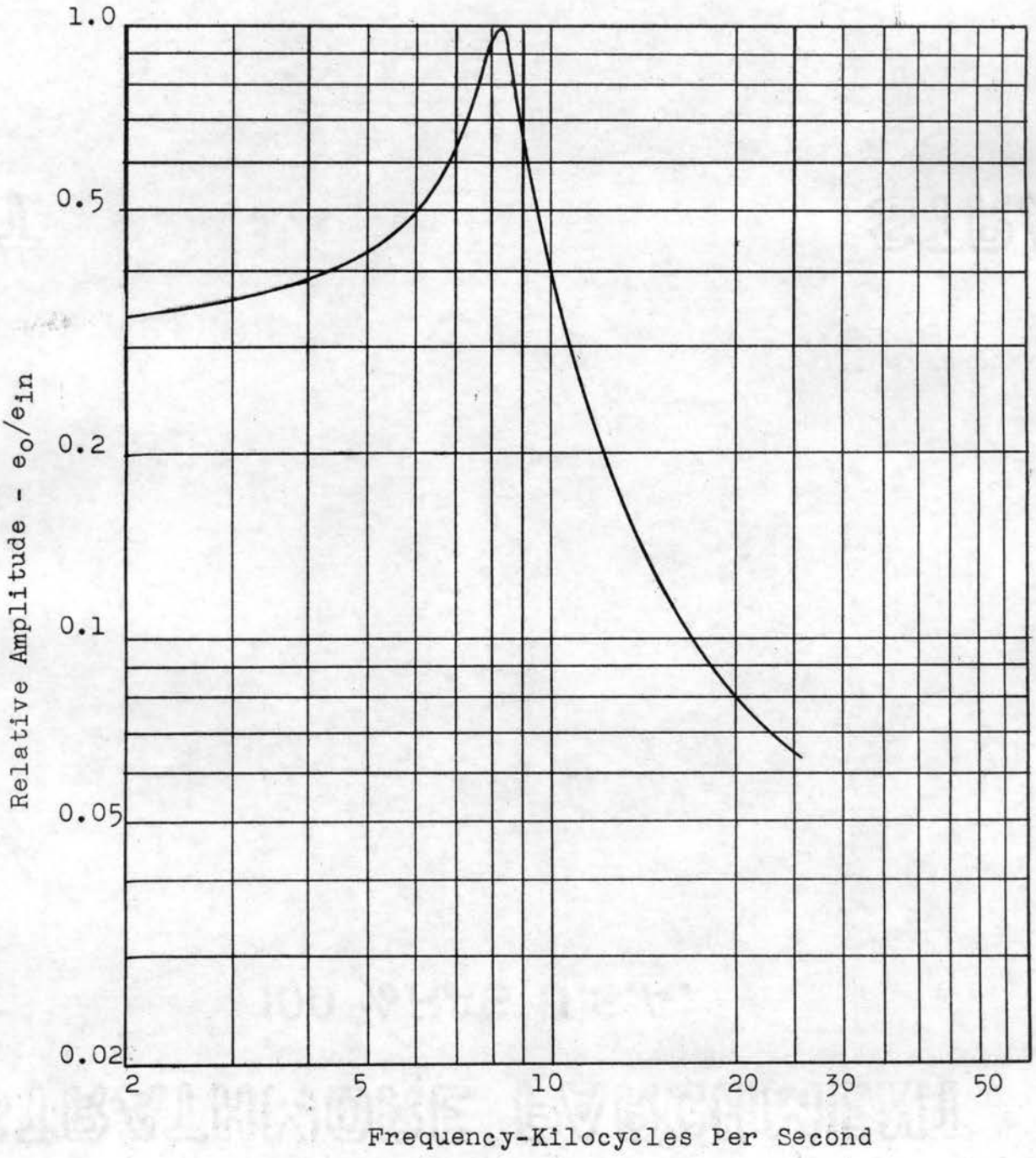

Figure 17. Amplitude Response-Output Circuit

direction of arrival of sferics. Since the phase shift of the amplifiers is varying rapidly at higher frequencies, there is a greater chance for the phases of the two amplifiers to be different.

It is concluded that the two most probable causes of elliptical patterns of the AN/GRD-1A are (1) overloading and (2) phase shift errors in the output circuit.

CHAPTER III.

DESIGN OF A HIGH FREQUENCY DIRECTION FINDER

Specifications of the System

After considering the shortcomings of the AN/GRD-1A system and after analysis of the sferic waveforms associated with tornadoes, it became apparent that a new instrument for accurately tracing tornadoes was needed.

Consideration of the high frequency nature of some observed sferics led to the decision that the new High Frequency Direction Finder should be tuneable over a range of 100 kilocycles per second to 300 kilocycles per second. This is more than one decade higher than the frequency range of the AN/GRD-1A system. Since it was desired to pass waveforms with a peak frequency of 300 kilocycles per second, it was necessary to design the basic amplifier circuits to pass frequencies up to 500 kilocycles per second. Thus video amplifiers were required. This desired high frequency response eliminated the possibility of using transformer coupling to the plates of the cathode-ray tube as was used in the AN/GRD-1A.

The value of observation of angular distribution of sferics, when only one station is in operation, is con-

siderably enhanced if the azimuths of peak sferic activity are compared simultaneously with the radar display of squall lines. With long range sferics equipment, such as the AN/GRD-1A when operated on a frequency of 10 kilocycles per second, it is difficult to establish that the sferics received at the station originate from a given echo on the radar screen, even though the azimuthal origin of sferics is comparable to the azimuth of the echo under observation. It is possible that the sferics emanate from a storm area at the same azimuth as the radar echo, but several hundred miles beyond the range of the radar. This is especially true at night when the propagation of sferic radiation fields is enhanced by reflection from the ionosphere. In such cases it is possible, under ideal conditions, to observe sferics originating from as far as 3000 miles. It is therefore desirable that the maximum range of the single-station, sferic direction finder be comparable, but slightly greater than the maximum range of the radar. One of the objectives in the design of the High Frequency Direction Finder was to eliminate the reception of unwanted long range sferics. Experience has shown that the range of the new HFDF should be about 250 miles.

The individual sections of the High Frequency Direction Finder were designed by using well established design principles such as found in Valley and Wallman[1], and in

---

[1]Valley and Wallman, pp. 71-112.

Greenwood, Holdam and MacRae[2]. The detailed design procedure of the individual sections will not be discussed, but a brief description of each section will be given below.

The chassis layout and construction of the experimental model were carried out at the Tornado Laboratory under the direction of the Project Engineer, Mr. R. D. Kelly. The original design was modified as construction progressed, and a number of important additions were made to the original design.

Overall System Description and Operation

A modified block diagram of the High Frequency Direction Finder is shown in Figure 18. Certain features that simplify the tuning process were incorporated so that non-technical personnel can easily tune the unit. The antenna system (not shown) consists of single-turn crossed loops. A single twenty-two foot mast supports both loops at the center, the base of each loop being forty feet. A vertical conductor is attached to the mast and is used as the sense antenna. The two single-turn loops, as well as the sense antenna, are connected into the direction finder as indicated. Three identical high frequency amplifiers are

---

[2] I. A. Greenwood, Jr., J. V. Holdam, Jr., and Duncan MacRae, Jr., Electronic Instruments, (McGraw-Hill Book Company, Inc., New York, 1948), pp. 573-664.

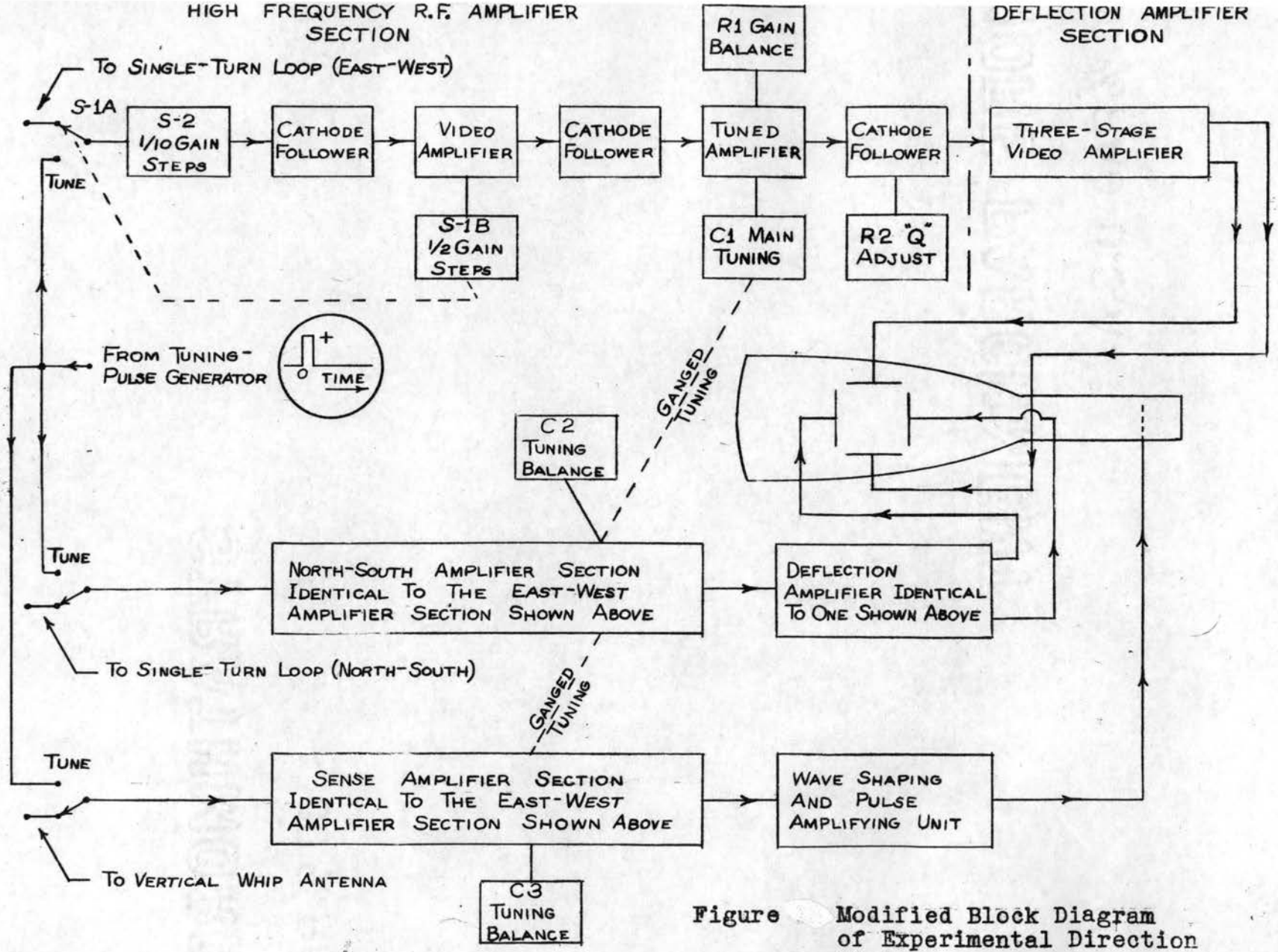

Figure Modified Block Diagram of Experimental Direction Finder

used for the East-West circuit, the North-South circuit, and the Sense Unit. Since the three units are identical, the block diagram shows only the stages of one unit in detail.

The output of the single turn loop is coupled from the base of the antenna mast to the amplifier input by means of a coaxial cable. The termination for the coaxial cable consists of ten equal resistors connected in series. The input to the amplifier may be selected by the switch S-2 from any junction point of the ten resistors. This provides a gain control that varies in increments of 1/10 of the total. The corresponding switch in the other loop amplifier must always be set to the corresponding position.

The percentage of the loop signal selected by switch S-2 is coupled to a cathode-follower stage to isolate the loop from the first video amplifier stage. An additional amplifier gain control is provided in the first video stage giving steps of 1/2, 1/4 and 1/8 increments of the overall amplifier gain.

Each amplifier stage in the radio frequency section is separated from the next by a cathode follower. This is to minimize the effect of input capacitance in producing elliptical scope patterns. Thus, the output of the video amplifier is coupled to the tuned-amplifier stage by a cathode follower.

The tuned-amplifier stage is adjustable over a range

from 100 kilocycles per second to 300 kilocycles per second. The main tuning adjustment, condenser C_1, is ganged to corresponding stages in the other loop section and the sense section to facilitate the adjustment of the operating frequency. Only small trimmer adjustments are necessary on the other loop section and the sense section. One other adjustment is made in the tuned amplifier stage. This is provided by the gain-balancing adjustment, R_1, in order to obtain equal loop voltages that will in turn give equal cathode-ray tube presentations.

The cathode follower immediately succeeding the tuned-amplifier stage has been constructed to perform the "Q" balance adjustment. The tuned-amplifier stage when shocked by a lightning discharge will oscillate for a fraction of a millisecond after the lightning has ceased. This signal continually decreases in magnitude according to the "Q" of the tuned circuit. If the "Q" of both tuned amplifiers for the loops is not identical, an elliptical pattern will be produced.

A principle based upon the pendulum analogy to the electrical circuit has been used to simplify the "Q" balance adjustment. With the loops disconnected from the amplifier sections, an electrical impulse from a tuning-pulse generator is coupled into both radio-frequency amplifier sections simultaneously. This electrical impulse shocks both tuned amplifiers and produces a given cathode-

ray-tube pattern. The "Q" adjust resistor, R_2, is manipulated, as well as the tuning trimmer condenser on the tuned amplifier, until a straight line is produced on the screen of the cathode-ray tube. If the "Q" is out of balance, a family of ellipses will be formed. Each ellipse of the family is smaller than the preceeding and has its major axis rotated from that of the previous ellipse. This produces a stationary elliptical pattern resembling an aeroplane propeller. As the "Q" adjustment approaches balance, the major axes for the smaller ellipses rotate until, under correct adjustment, all are coincident and a straight line presentation can be obtained on the scope when the tuning balance or trimmer condenser is adjusted. If the tuning trimmer is not at the balance point after the "Q" has been adjusted, the pattern obtained is still elliptical, but the major axes of all of the family of ellipses coincide. Proper adjustment of the tuning trimmer then produces a straight line pattern on the cathode-ray tube.

At this point, the only additional requirement to complete the tuning process is to adjust for gain balance in the two amplifier sections by means of R_1. This is indicated on the cathode-ray tube when the straight line presentation occurs at 45°. Thus R_1 is manipulated until the scope pattern occurs at 45° and the entire tuning process is complete. To place the properly tuned amplifier sections into operation it is necessary only to throw switch

S-1 so that the loops are again in the circuit. It will be necessary to set the gain by the 1/10 step adjustment of S-2 and 1/2 step adjustment of S-1B to conform with the intensity of the storm. Once the tuning process is properly completed, the gain adjustments may be made by switches and the tuning need not be repeated. This is not possible with the AN/GRD-1A. The gain of any direction finder should be reduced as the storm approaches the receiver in order to prevent overdriving of the amplifiers with excessive signal strength.

The amplifier section for the vertical deflection plates is identical with that for the horizontal deflection plates. The deflection amplifier was designed to produce a maximum deflection of two inches, peak-to-peak; however, because of the sensing circuit the resultant which is photographed is only one inch long. This limitation of picture size does not prevent accurate indication of azimuth. A problem arises, however, when large amplitude signals from intense lightning strokes occur, because the first inch of the picture gives an accurate indication of azimuth while the rest of the presentation does not. This is indicated on the film when the line representing a certain stroke extends out straight initially and then bends as if to indicate another azimuth. This bending is entirely due to circuit characteristics under conditions of overdriving by excessive signal strength.

The deflection amplifier section was designed to be free of transformers. All stages use resistance-capacitance coupling and are designed to give equal amplification to a given signal as the signal frequency varies over a wide range. This wide range frequency response is indicated by the absence of elliptical scope patterns when the same signal is coupled into each deflection amplifier section and the signal frequency is varied. These units give a linear pattern with no indication of ellipticity over a frequency range from 100 cycles per second to 500,000 cycles per second.

The Wave Shaping and Pulse Amplifying Unit utilizes the output of the Sense Amplifier section. The function of this unit is to switch the electron beam of the cathode-ray tube on and off in accordance with the demands of the sense antenna. It is imperative that the tuned amplifier for the sense unit have the same tuning and same "Q" as the tuned amplifiers for the loop stages. When the loop tuning is adjusted, the input to the sense unit is also connected to the electrical impulse previously mentioned. The scope pattern with proper sensing adjustment will be a 45° line extending from the origin, and without "tails". Existence of tails indicates improper tuning or improper "Q". The "Q" is adjusted to correspond to the "Q" of the loop sections by feeding the output of one properly adjusted loop section and the output of the sense unit into

the two deflection amplifiers and adjusting the sense "Q" by the same method as outlined above for balancing the "Q" for both loop sections. This adjustment is made on the initial installation and need not be repeated for several weeks, or for even longer periods. The respective outputs for the loop and sense sections are then reconnected as shown in Figure 18. The trimmer condenser marked "tuning balance" on the sense section is then adjusted until the tails vanish. This final adjustment of the tuning process provides for complete direction finding with sensing.

The High Frequency Direction Finder has design features that eliminate some of the possible causes for ellipses. Among these features, the following are considered to be of major importance:

1. When two strokes occur at almost the same instant, but at different locations, the direction finder must recover from one indication in a length of time that is sufficiently short to permit successful indication of the second stroke. This is accomplished by the increased frequency of operation. If a length of time corresponding to 50 cycles of the incoming wave train is required to indicate a given stroke, regardless of the operation frequency of the direction finder, then the 10 kilocycle per second system will require a period of 50/10,000 or 5 milliseconds to indicate

the stroke. The 150 kilocycle per second system will require a period of only 50/150,000 or .333 milliseconds to indicate the same stroke. Thus the high frequency system is capable of indicating strokes at a rate that is approximately 15 times as fast as the 10 kilocycle per second system. That this property also allows better integration on certain multiple strokes has been indicated on recorded data.

2. Transformer coupling in amplifiers has been completely eliminated in the new high frequency system.
3. Electrical coupling between vertical amplifier units and horizontal amplifier has been virtually eliminated by using separate shielded-chassis construction. Coupling at switching points is eliminated by having separate switches for each section.

The Filter Section

A simplified schematic diagram of the tuned-amplifier section of the High Frequency Direction Finder is shown in Figure 19. The circuit is an inductance-loaded pentode amplifier with R-C coupling at the input grid. The frequency response of the amplifier is largely determined by the three-millihenry load inductance and the 10 to 365

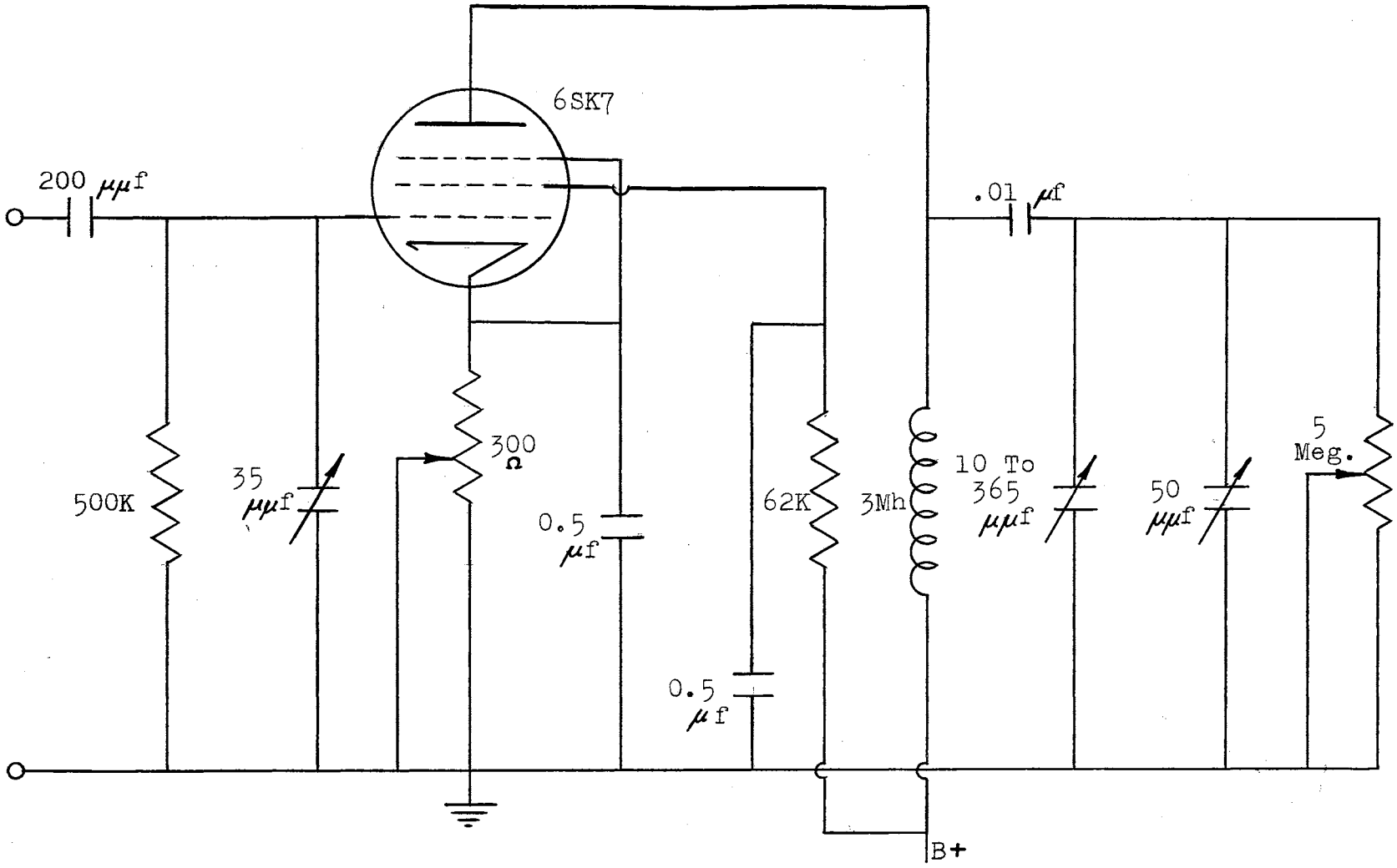

Figure 19. Tuned Amplifier Circuit-High Frequency Direction Finder

tuning condenser in parallel. An analysis was made of the equivalent circuit of the tuned amplifier in the same manner as was made for the tuned amplifier of the AN/GRD-1A Direction Finder. Since the mathematics involved is so similar to that shown in detail in connection with the analysis of the AN/GRD-1A, it will not be shown here.

The amplitude-versus-frequency response of the filter section is shown in Figure 20 with values of tuning capacitance chosen to give a peak frequency of 100 kilocycles per second and 300 kilocycles per second. This represents the practical tuning range of the filter. The phase response curves are similar to that shown for the AN/GRD-1A and, although calculated, are not shown here. The sharpness of these amplitude curves may be varied by means of the "Q" adjustment mentioned previously.

Since the remainder of the amplifier was designed to have a broad frequency response, the amplitude response curves shown here are essentially the curves for the overall amplifiers.

Other Amplifier Features

The remaining sections of the High Frequency Direction Finder amplifier consists of cathode followers, video stages, a phase inverter and a push-pull deflection amplifier. Conventional procedures were used in designing all of these stages.

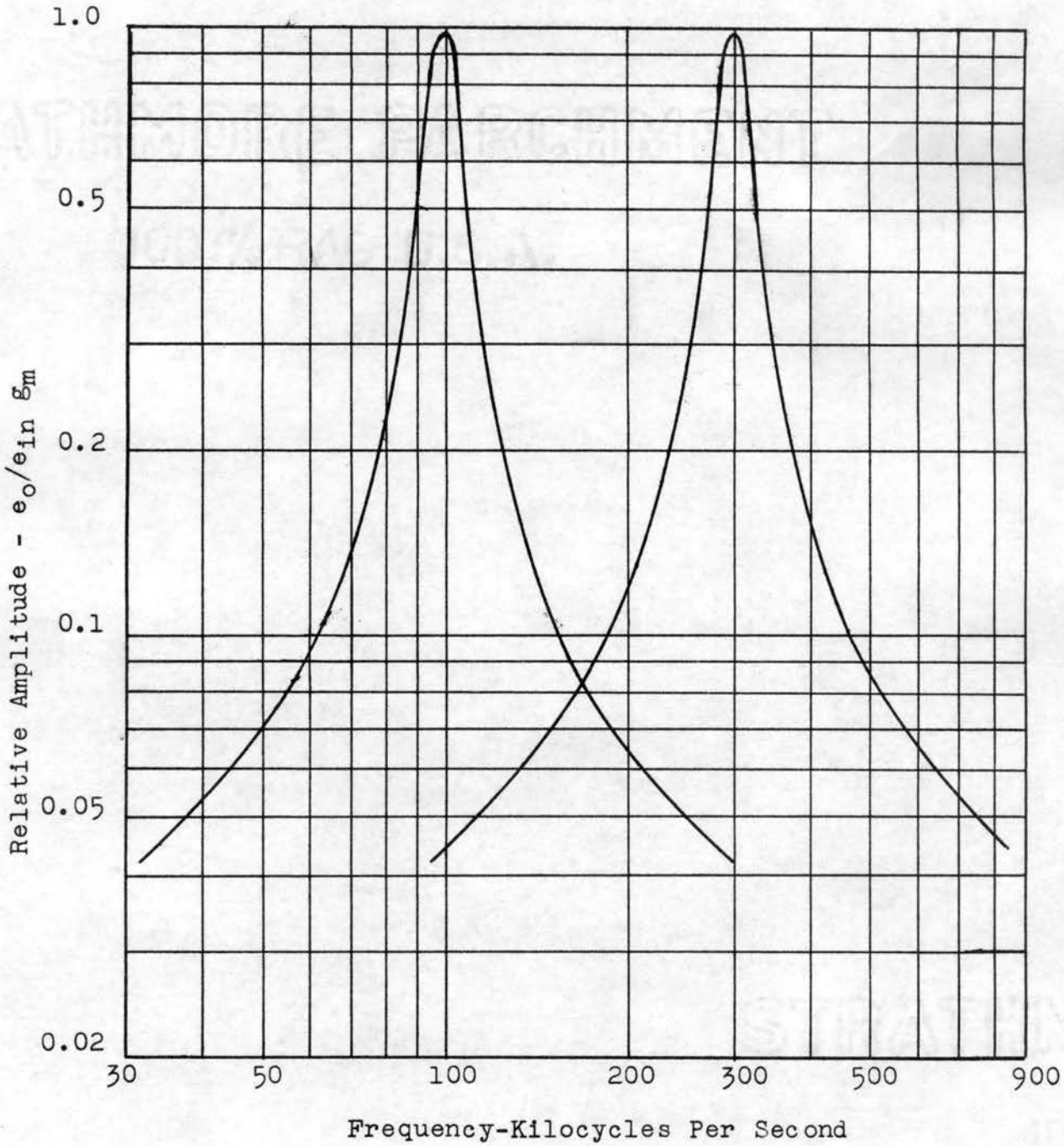

Figure 20. Amplitude Response-High Frequency Direction Finder

A schematic diagram of the prototype High Frequency Direction Finder is shown in Figure 21. As mentioned before, it was necessary to modify the original design in order to obtain satisfactory operation of the system. The modified schematic of the amplifier is shown in Figure 22. These modifications made by Mr. Kelly consisted primarily of placing a cathode follower between each stage to improve the coupling, a more convenient set of tuning adjustments and a more powerful deflection amplifier to adapt to the type of cathode-ray tube used. In Figure 23 are shown the sense, wave-shaping circuit and cathode-ray control circuits designed by Mr. Kelly.

Initial Results

In Figures 4, 5, and 6 were shown film strips showing directional pips recorded from the AN/GRD-1A at the top and from the High Frequency Direction Finder at the bottom. The directional markers from the HFDF are much more easily studied than for the AN/GRD-1A since they are thinner and show no tendency toward the troublesome ellipses of the AN/GRD-1A. The resolution is therefore much better than for the AN/GRD-1A. Even when the sferic activity is extreme as in Figure 6 it is still possible to magnify the film and count the pips from the High Frequency Direction Finder.

Figures 24 to 30 inclusive show results from the Black-

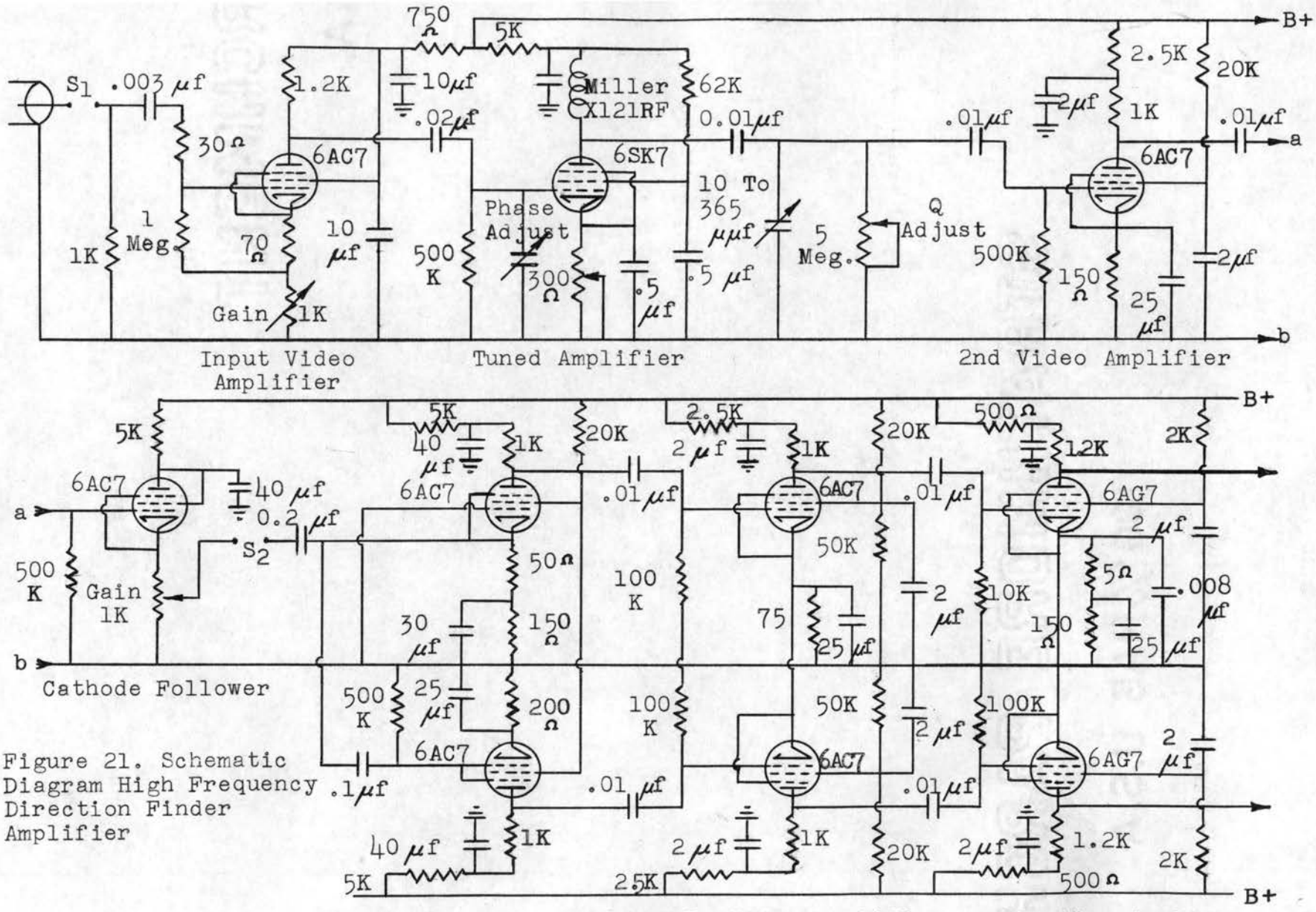

Figure 21. Schematic Diagram High Frequency Direction Finder Amplifier

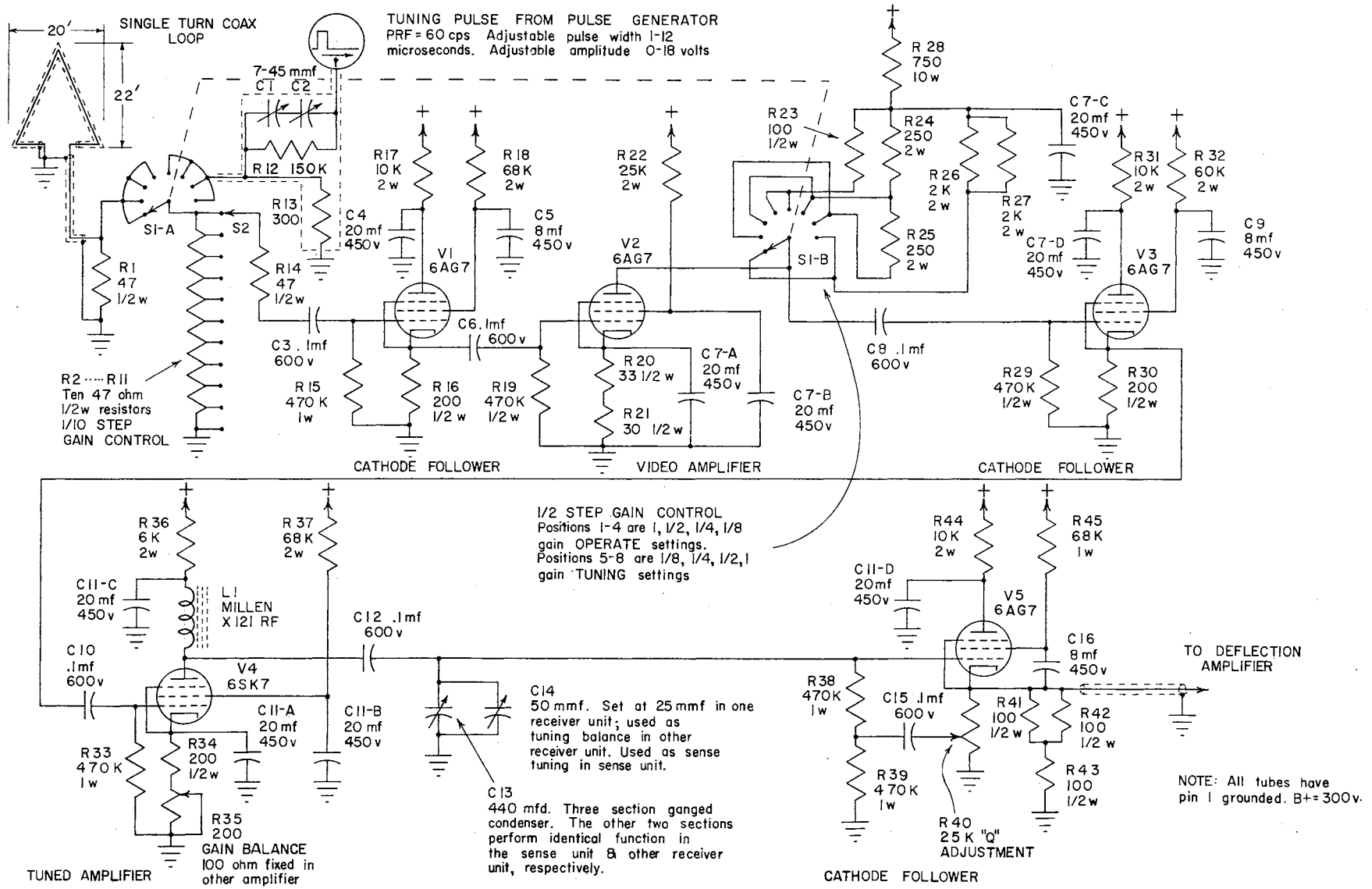

Fig. 22 RECEIVER UNIT FOR THE HIGH FREQUENCY DIRECTION FINDER

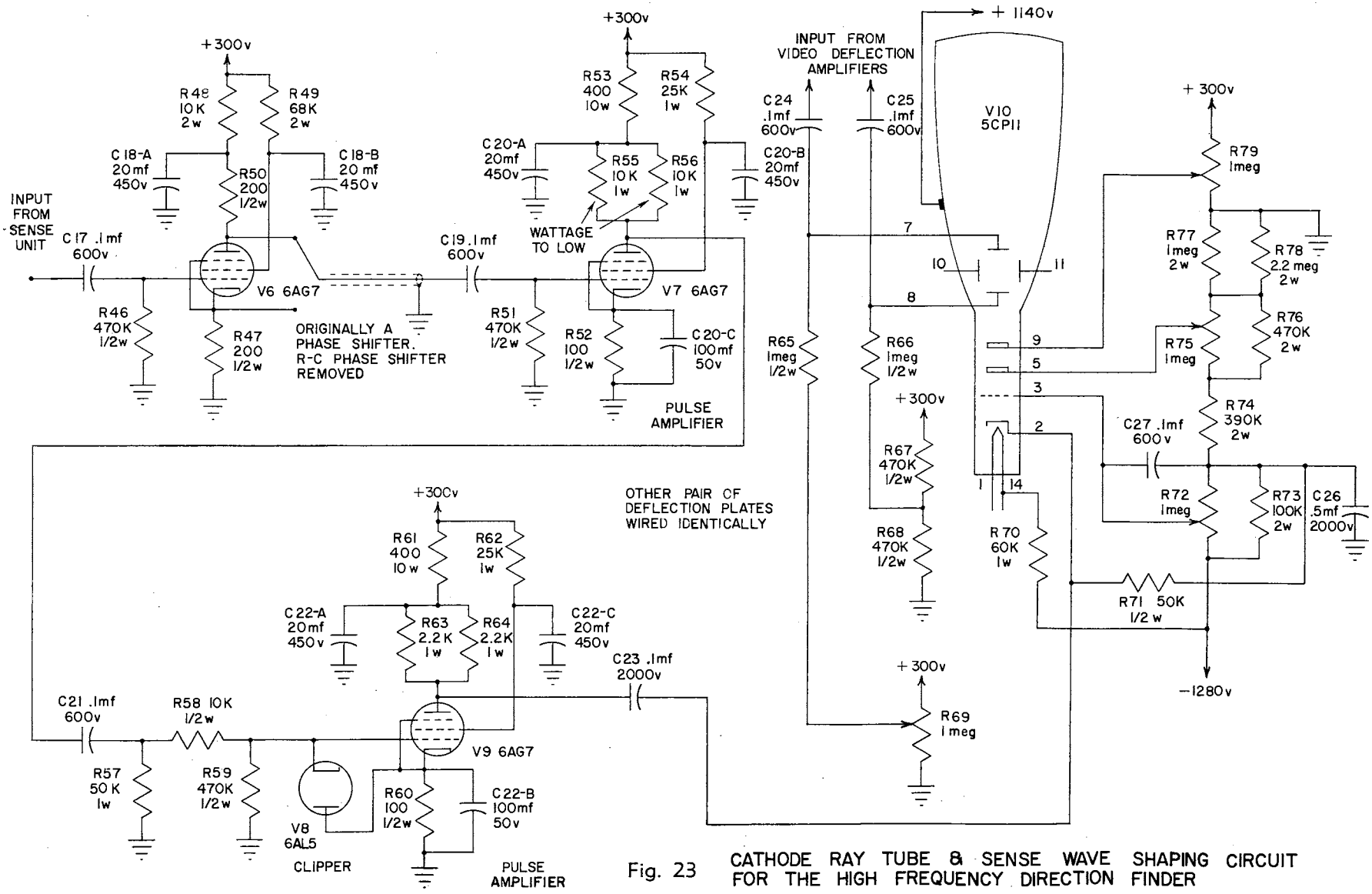

Fig. 23 CATHODE RAY TUBE & SENSE WAVE SHAPING CIRCUIT FOR THE HIGH FREQUENCY DIRECTION FINDER

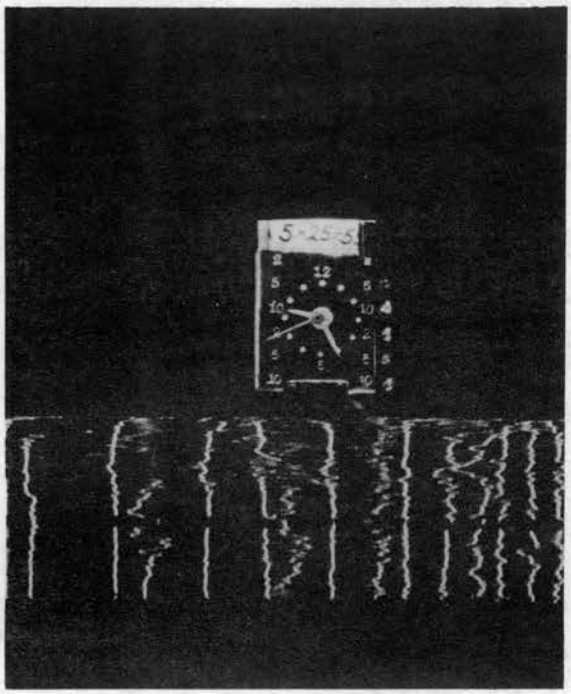

Figure 24. H. F. Wave Forms,
2125 CST, 5-25-55

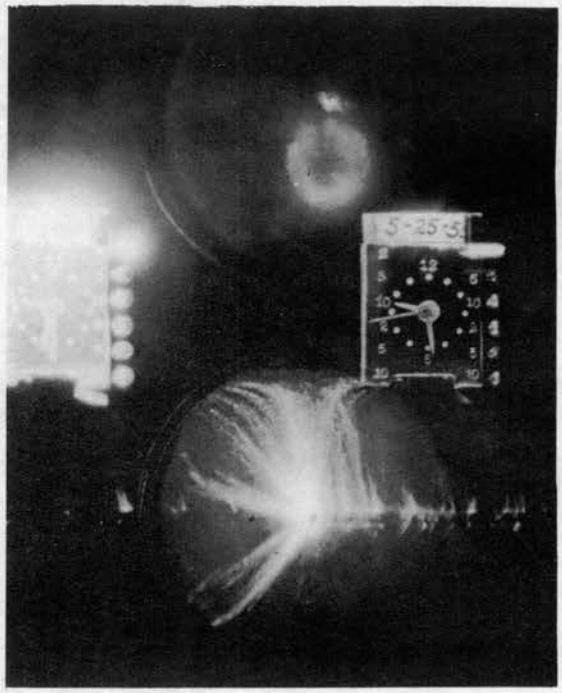

Figure 25. Directional Composite
2129 CST to 2134 CST, 5-25-55

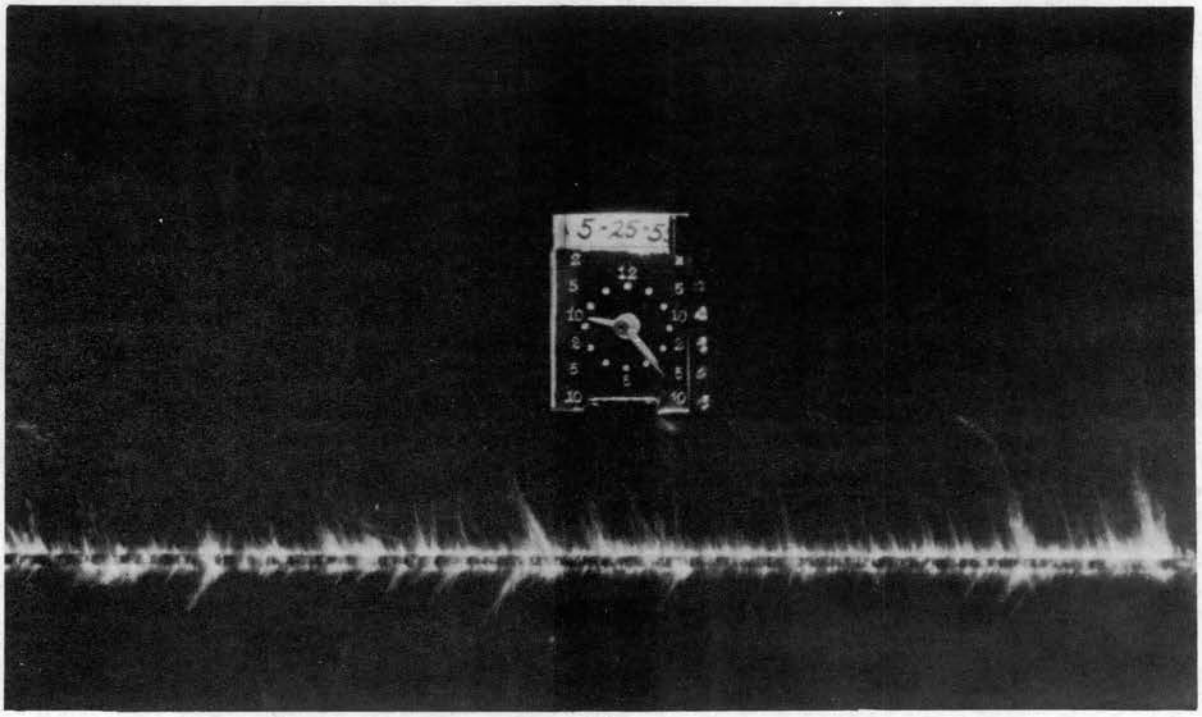

Figure 26. H. F. Directional Characteristics
2123 CST, 5-25-55

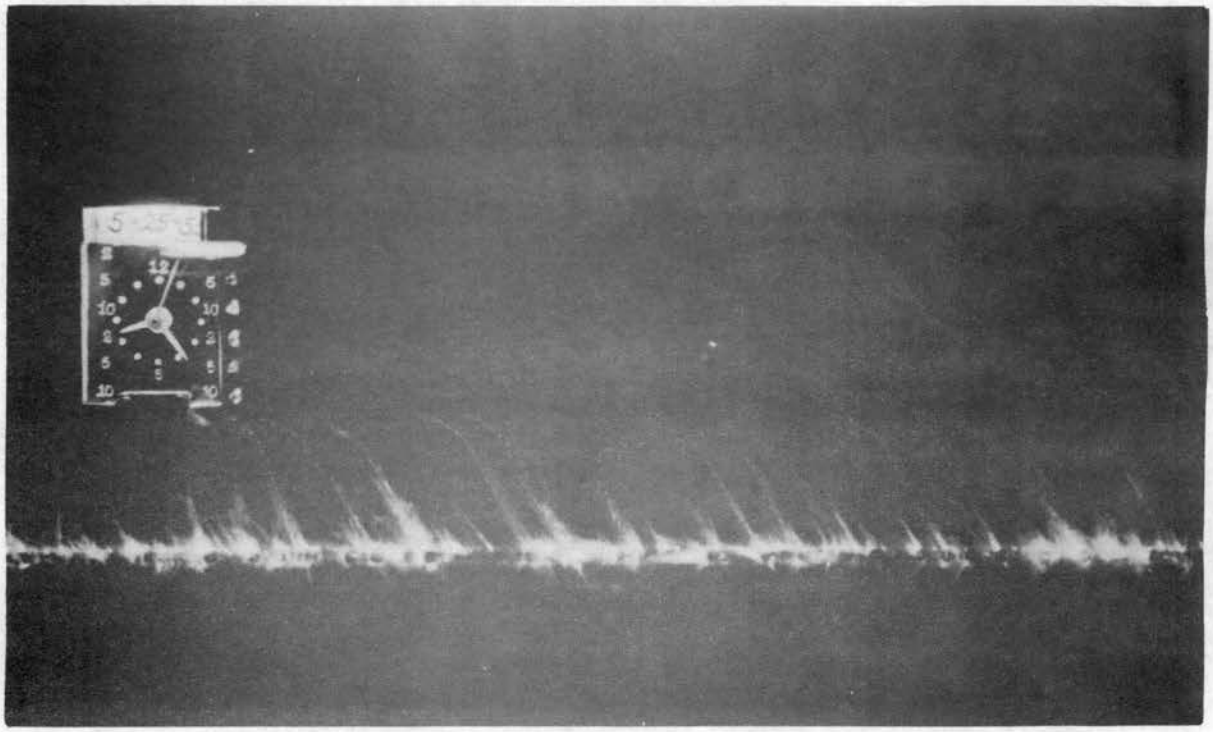

Figure 27. Film record of sferics. May 25, 1955. High intensitv.

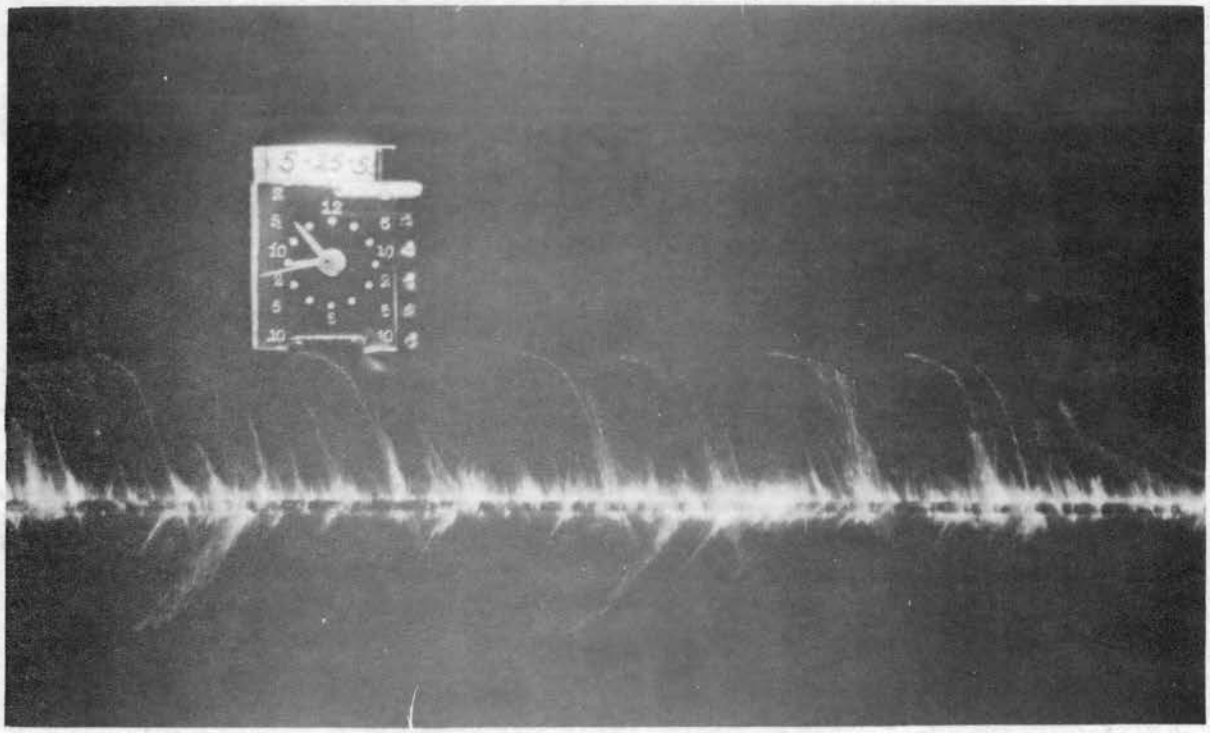

Figure 28. Film record of sferics. May 25, 1955. High intensity.

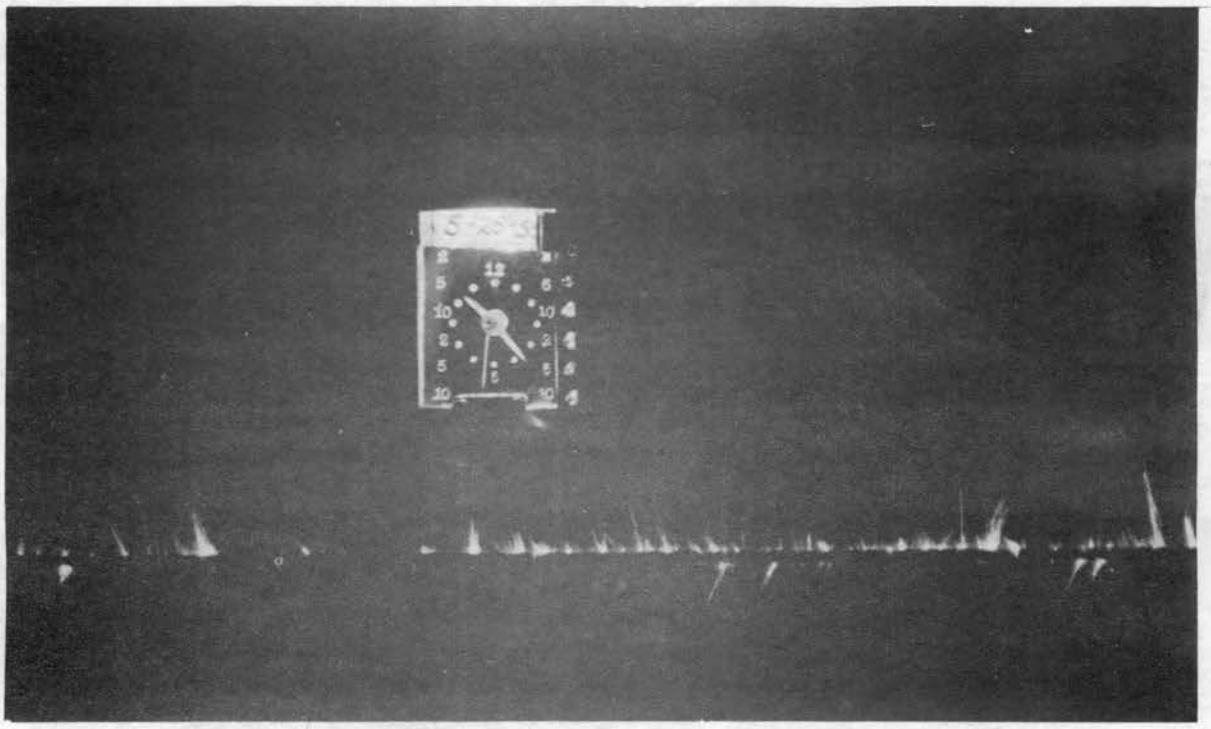

Figure 29. Film record of sferics. May 25, 1955. Low intensity.

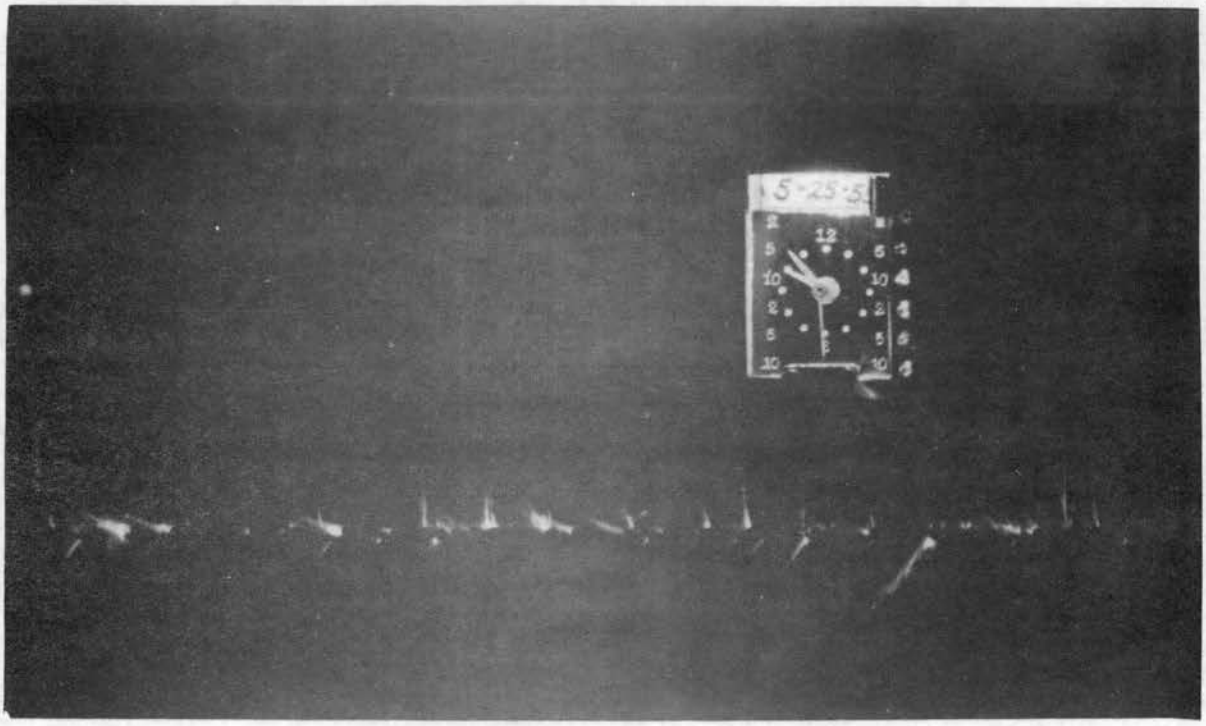

Figure 30. Film record of sferics. May 25, 1955. Low intensity.

well tornado on May 25, 1955. A complete analysis of the Blackwell tornado will be given in Chapter IV. In Figure 24 are shown some of the high frequency wave forms associated with tornadoes. In Figure 25 is shown a directional composite obtained by keeping the film stationary for five minutes and recording the directional pips on top of each other. Figures 26 to 30 inclusive show the directional pips obtained during an extremely active part of the tornado. There is some overloading of the oscilloscope tube shown in Figures 27 and 28 as indicated by the bending of the directional pips near the top. This necessitated a reduction in gain of the amplifier. Subsequent sferic pips are shown in Figures 29 and 30.

It was concluded from these tests that the High Frequency Direction Finder is satisfactory for use as a tornado tracing instrument and meets the design specifications originally set forth.

CHAPTER IV

RESULTS FROM THE TORNADOES OF MAY 25, 1955

General Description

On May 25, 1955, meteorological conditions in Oklahoma were unstable and typical of tornado weather. By late afternoon a complex low pressure system was moving eastward across the Texas Panhandle and into Western Oklahoma. Behind the low pressure system was a large mass of Pacific air centered in Arizona. Covering the state of Oklahoma at the surface was a mass of tropical air. The frontal area between the two masses of air extended from the center of the low pressure area southward across West Texas, where widely scattered thunderstorms, some with damaging wind and hail were reported during the day. Shortly after 1500 CST, a tornado was reported in the Texas Panhandle moving northeasterly into Oklahoma. During the day, after numerous thunderstorms had occurred in the western part of Oklahoma, a severe tornado developed from an isolated thunderstorm complex about 26 nautical miles north-northwest of Stillwater at 2100 CST. The paths of this tornado and a second tornado which formed at about 2200 CST are shown in

Figure 31[1]. The tornado moved in a northerly direction passing 1 mile east of Tonkawa, Oklahoma at 2115 CST. After crossing U. S. Highway 60 east of Tonkawa, the funnel assumed a course a little east of north to a point two and one-half miles southeast of Blackwell where it curved northwest, more or less following the Chikaskia River into the southeastern part of Blackwell. As it passed through the eastern section of Blackwell at about 2130 CST, the funnel curved to the north again and continued in that direction to a point some three and one-half nautical miles south of the Kansas - Oklahoma border. Here the tornado, now of somewhat diminished intensity, assumed a northwesterly direction, passing into Kansas and dissipating in the vicinity of South Haven, Kansas, at about 2200 CST. The average speed of this tornado was 34 knots with little apparent deviation from this average during its entire course.

At about the same time as this tornado dissipated, or slightly before, another funnel touched the ground about 5 nautical miles east of the path of the Blackwell funnel and nine nautical miles southwest of Arkansas City, Kansas. This funnel also moved in a northerly direction passing

---

[1]"Research on Tornado Identification", Second Quarterly Progress Report, Signal Corps Research, Project No. 172B, (1955), p. 17.

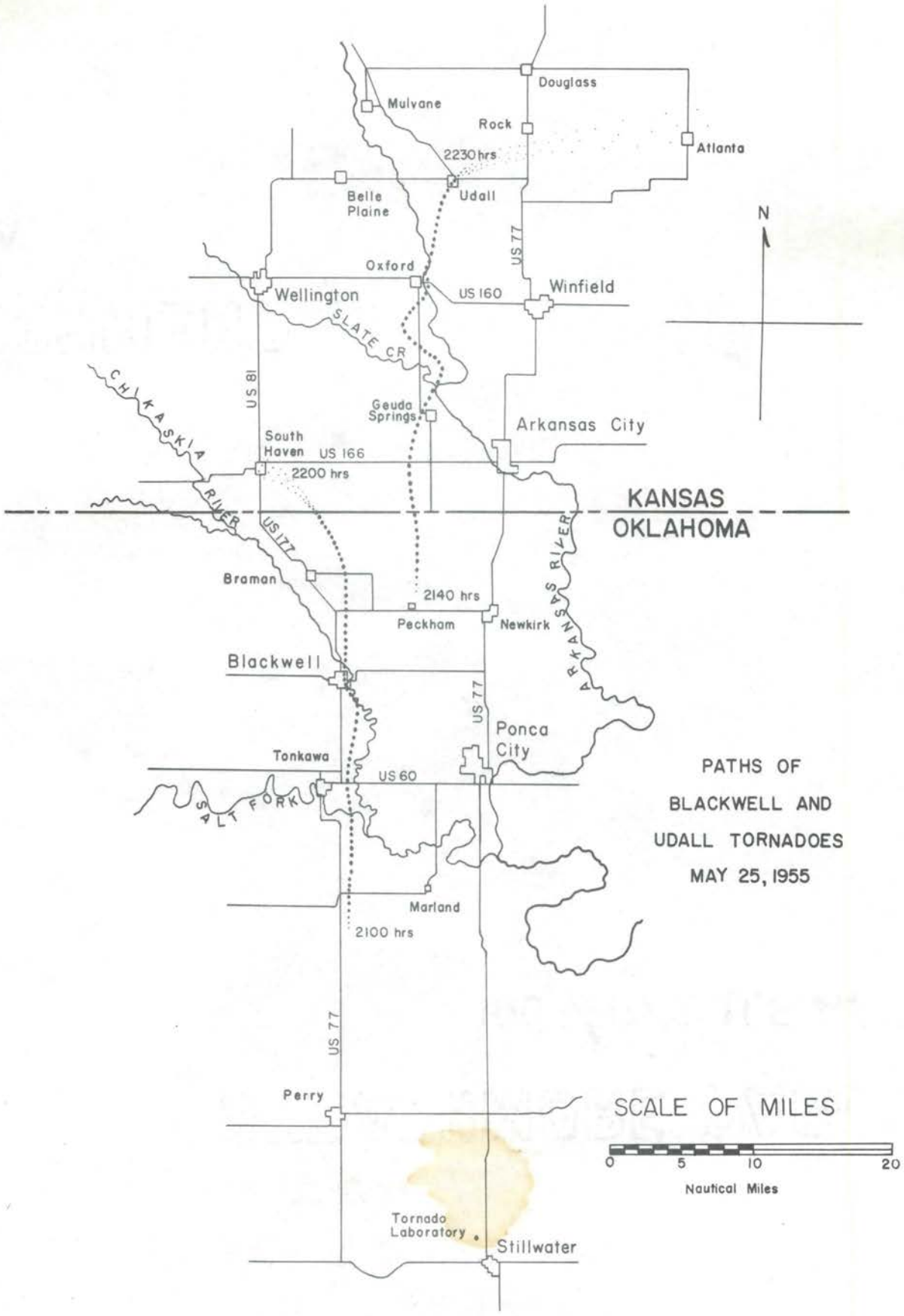

Figure 31. Map showing paths of tornadoes of May 25, 1955

just west of Gouda Springs, Kansas, a little after 2200 CST. At this point it curved northeast for a few miles then to the northwest for several miles and back to the northeast again until it reached the Arkansas River southeast of Oxford, Kansas. Here it followed the river in a general northerly direction for about three miles, passing one-half mile east of Oxford at 2220 CST. After leaving the river two miles north of Oxford, it curved again to the northeast, passing directly over Udall, Kansas, at 2230 CST. Immediately after leaving Udall, it apparently began to dissipate as it continued curving to the east. Beyond Udall, there was little evidence of total destruction, but rather a wide belt of partial destruction extending to the east as far as Atlanta, Kansas. There was considerable discrepancy in the tornado times reported by witnesses along the path of this funnel, and there was some evidence that more than one funnel touched the ground along its course, especially south of Oxford. However, from the best estimates available, the average speed, assuming that the main path of destruction was caused by one funnel continuously on the ground, was about 45 knots. This movement was considerably faster than that of the Blackwell tornado. The length of the path for the Blackwell storm was 35 nautical miles with partial damage extending two to five miles beyond, and the length of the path for the Udall storm was 30 nautical miles with partial damage extending an additional 10

nautical miles.

Analysis of the Data

Although this thesis is primarily concerned with results obtained by use of the High Frequency Direction Finder, the data must be supplemented with results obtained with radar in order to present the complete picture of the method used for identification and tracking of severe weather activity. For that reason data from the radar as well as the High Frequency Direction Finder are presented in the following analysis.

Because of the great amount of time required to count strokes from the High Frequency Direction Finder film record of this storm, it is possible to present only a part of these data in this thesis. It can be seen from the portion of the film record shown in Figures 27 and 28 that activity was very heavy and that an accurate count of lightning strokes is difficult. The resolution obtained with the film speed used, about 1-3/4 inches per second, is inadequate for extremely high stroke rates. Nevertheless, a count was made which is considered sufficiently reliable and accurate for this purpose since trends in the data are what is considered of primary importance. The azimuth of each stroke that was long enough to establish a direction was determined to the nearest two-degree segment of arc. All counts shown in this thesis were made

by Tornado Laboratory personnel and not by the writer. The total number of strokes occurring during several seconds of time at intervals of about 15 minutes were obtained. From these evaluations the average stroke rate per second per two-degree azimuth sector was calculated.

At about 2125 CST, just before the tornado struck Blackwell, the gain and scope intensity of the High Frequency Direction Finder were lowered in an attempt to provide a better film record. It was found, however, on developing the film that the gain and intensity had been cut too much. In order to make the graphs appear similar to those of the earlier periods, a total count of 5 seconds was used rather than an average stroke rate per second as previously described.

Figures 32 to 43 inclusive show the azimuth distribution of sferics count from 2008 CST to 2153 CST. During that time the Blackwell tornado was active. Figures 32 to 37 inclusive are plotted to an ordinate of strokes per five seconds. As explained before the gain and intensity of the High Frequency Direction Finder were reduced at 2129 CST. Unless otherwise specified the stroke rate is the average of three second intervals. In some cases the value of average stroke rate shown is the average over 10, 15, 20 or 30 seconds. Where comparisons were available, the averages over longer periods of time made no appreciable difference in the analysis of the data.

Azimuth Incidence Distribution of Sferic Activity Sampled by High Frequency Direction Finder 25 May, 1955. Beginning with 2008 Hours.

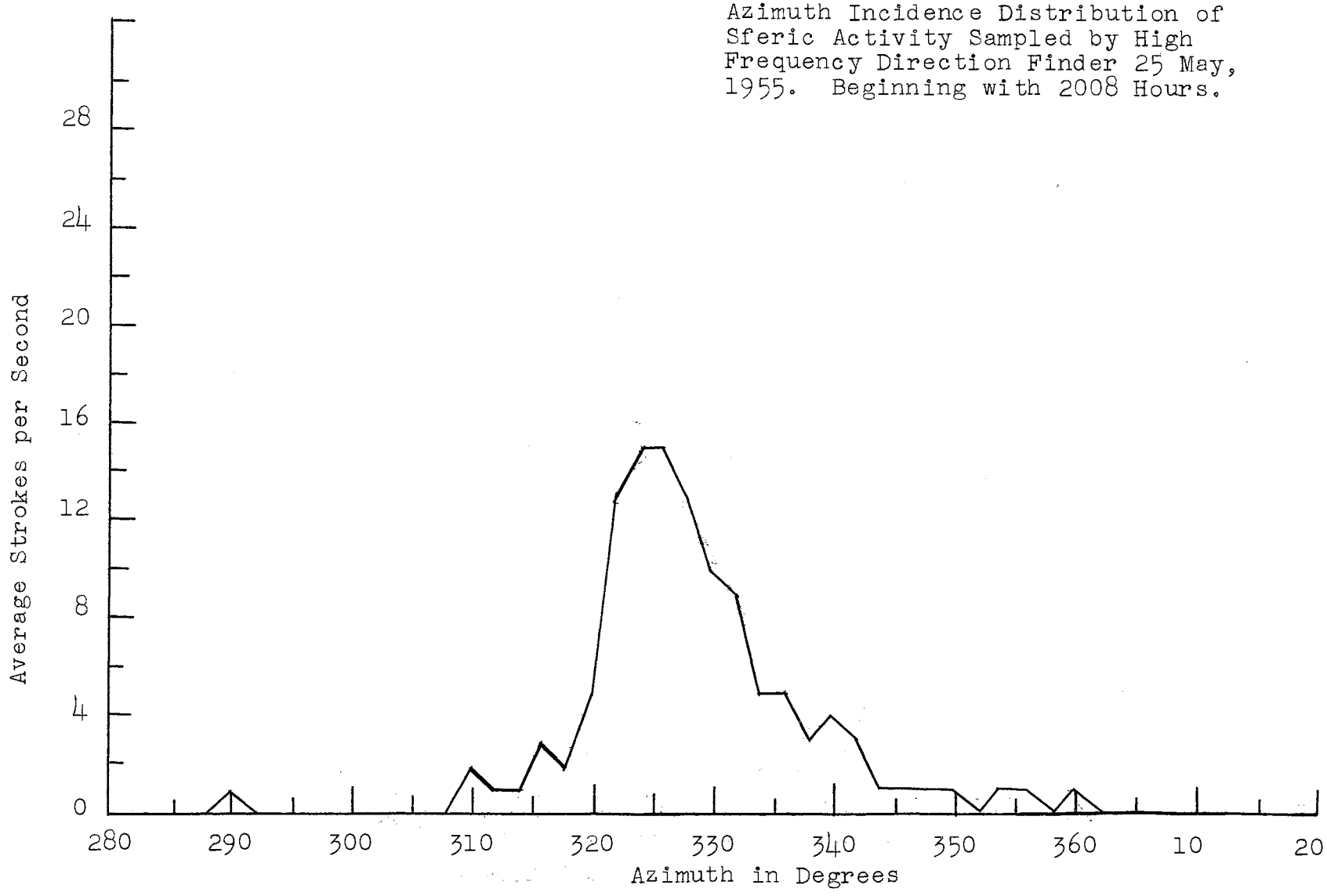

Figure 32.

Azimuth Incidence Distribution of Sferic Activity Sampled by High Frequency Direction Finder 25 May, 1955. Beginning with 2024 Hours.

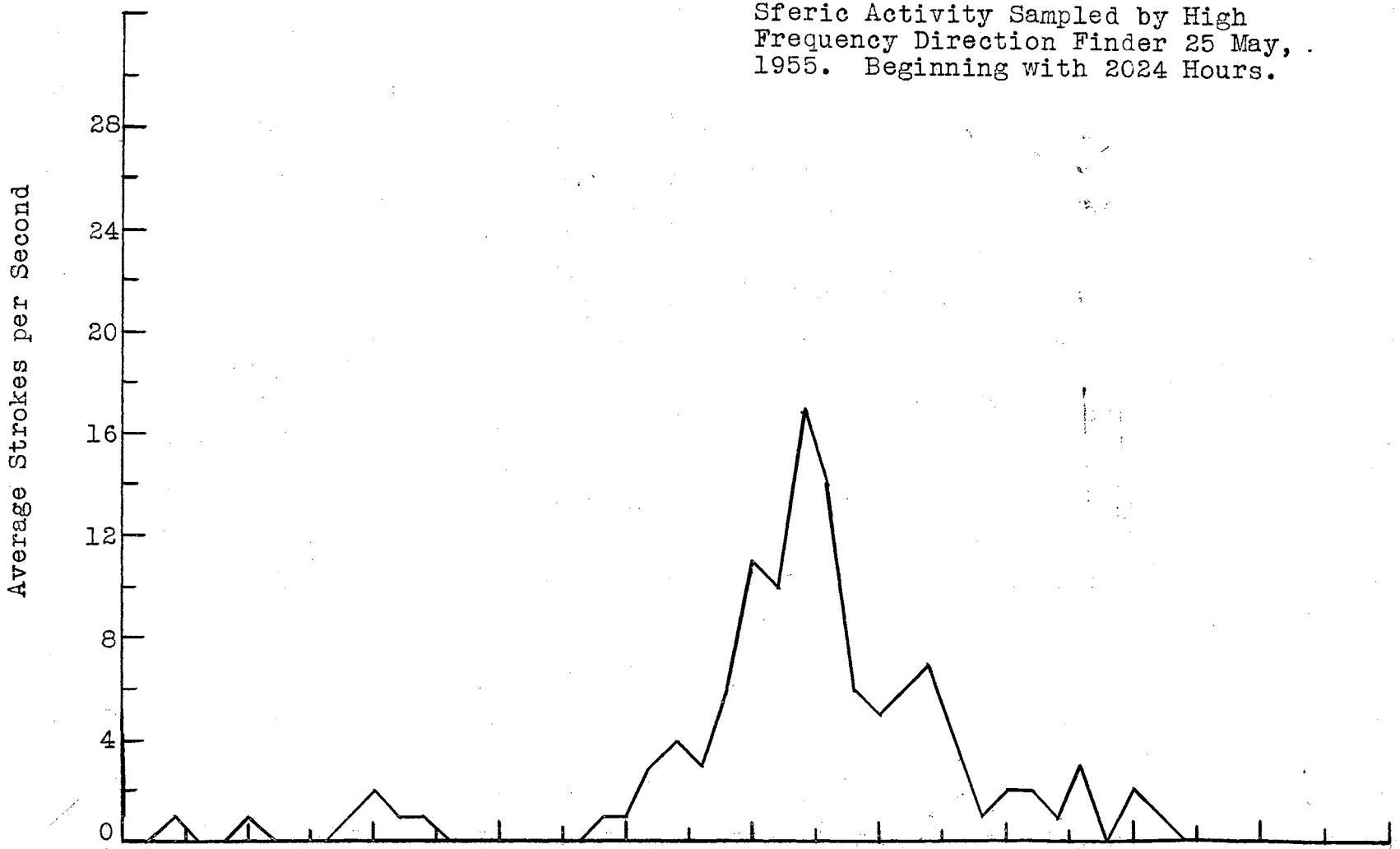

Figure 33

Azimuth Incidence Distribution of Sferic Activity Sampled by High Frequency Direction Finder 25 May, 1955. Beginning with 2038 Hours.

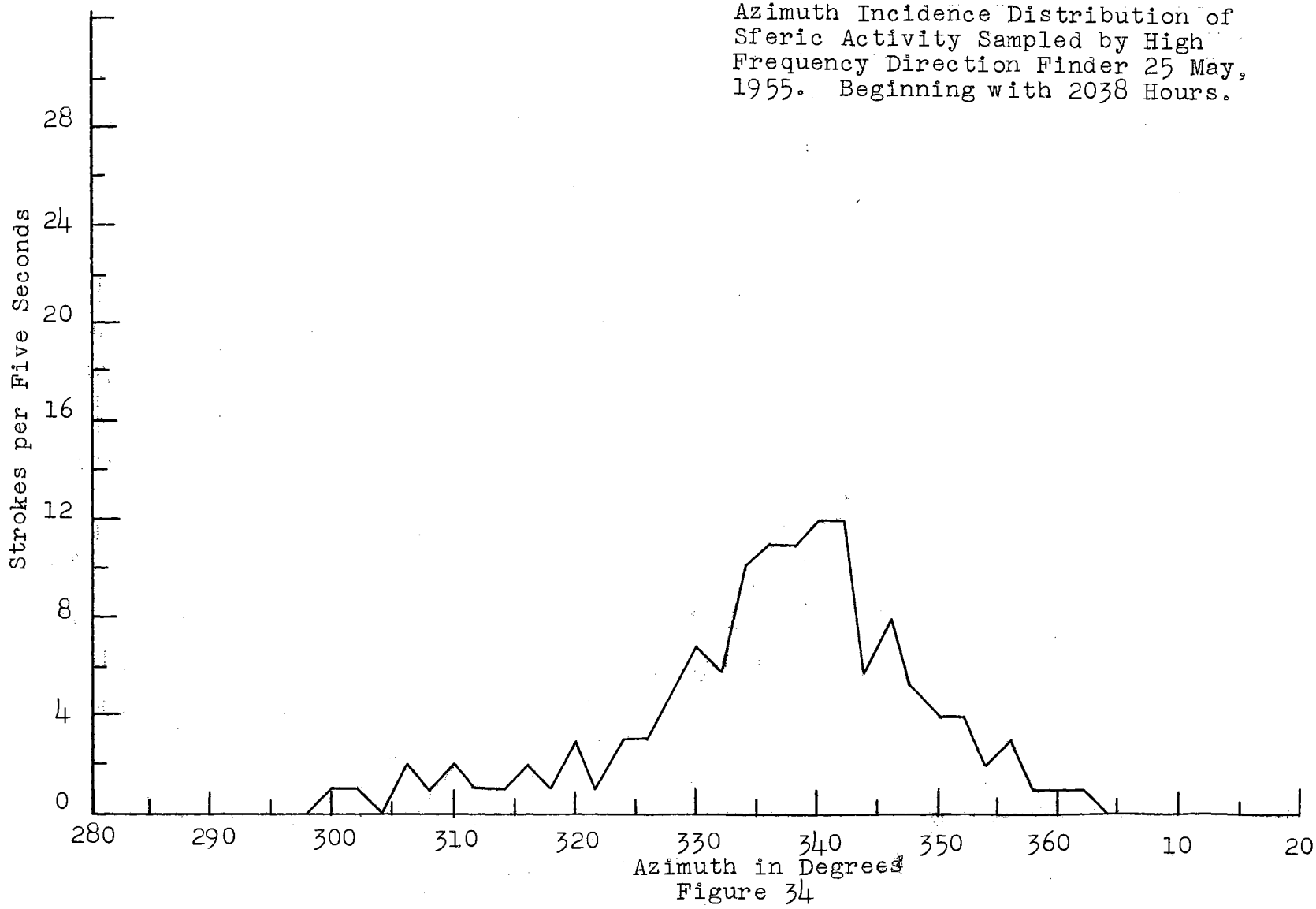

Figure 34

Azimuth Incidence Distribution of Sferic Activity Sampled by High Frequency Direction Finder 25 May, 1955. Beginning with 2053 Hours.

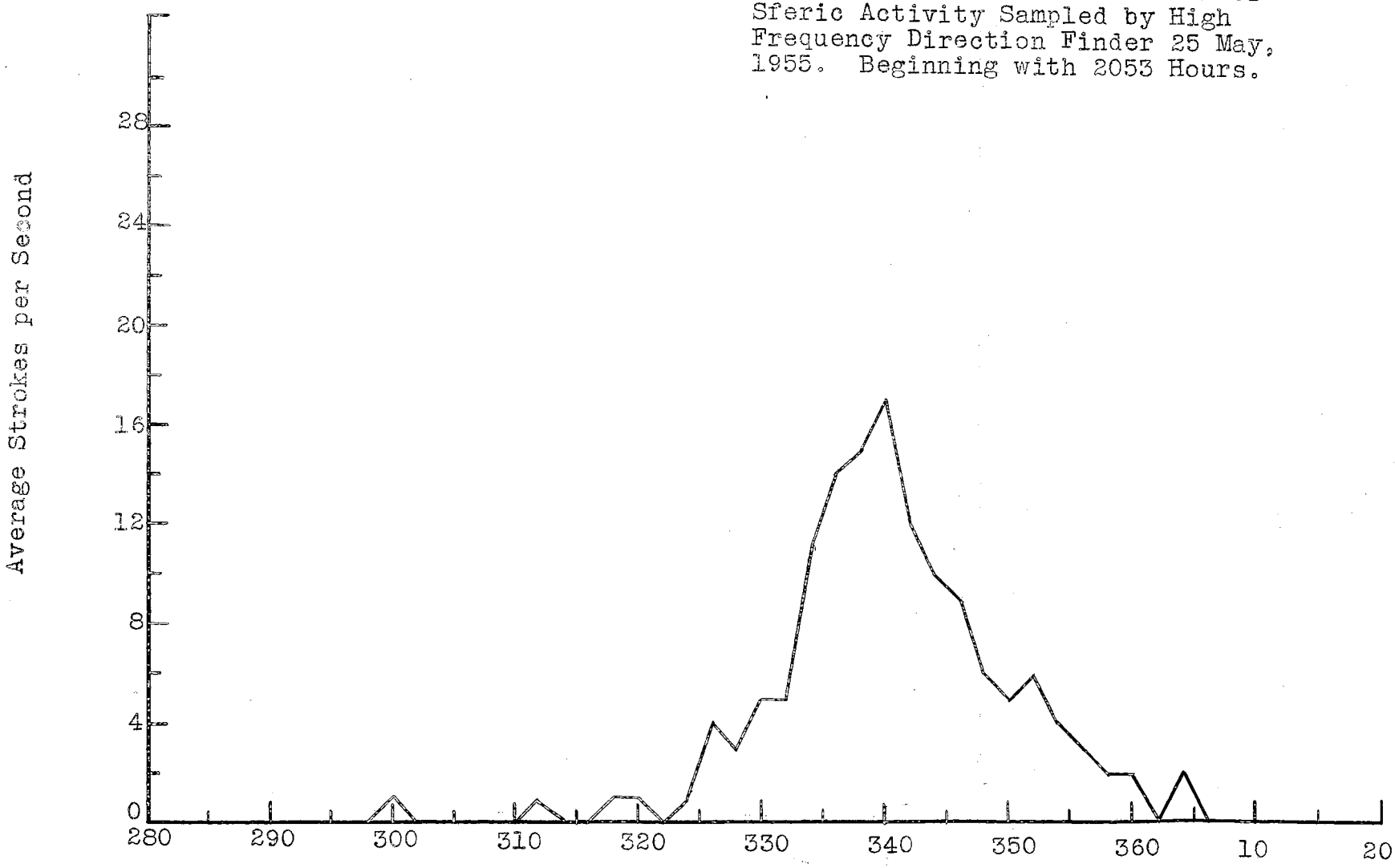

Figure 35

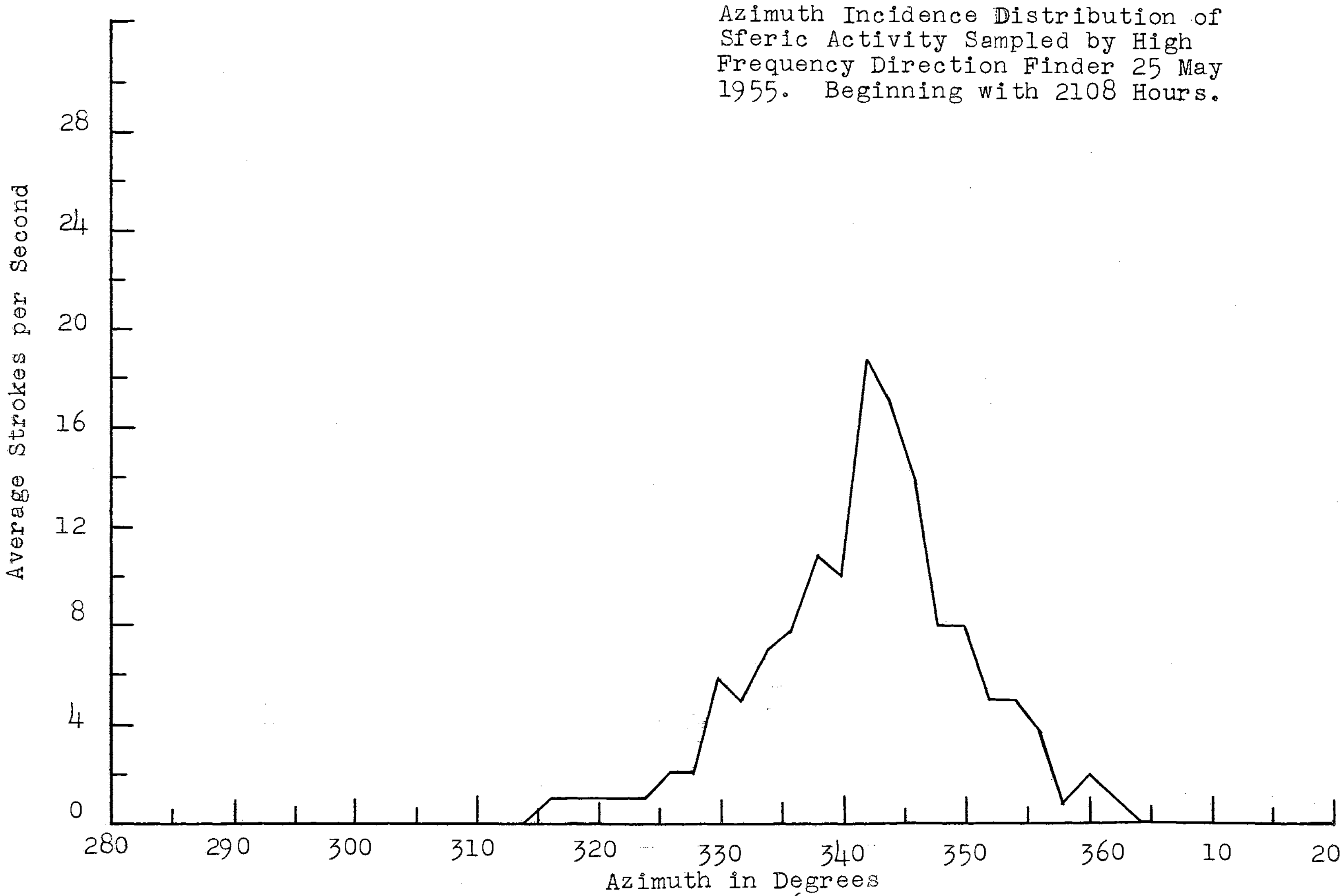
Azimuth Incidence Distribution of Sferic Activity Sampled by High Frequency Direction Finder 25 May 1955. Beginning with 2108 Hours.
Average Strokes per Second
28
24
20
16
12
8
4
0
280
290
300
310
320
330
340
350
360
10
20
Azimuth in Degrees

Figure 36

Azimuth Incidence Distribution of Sferic Activity Sampled by High Frequency Direction Finder, 25 May, 1955. Beginning with 2123 Hours.

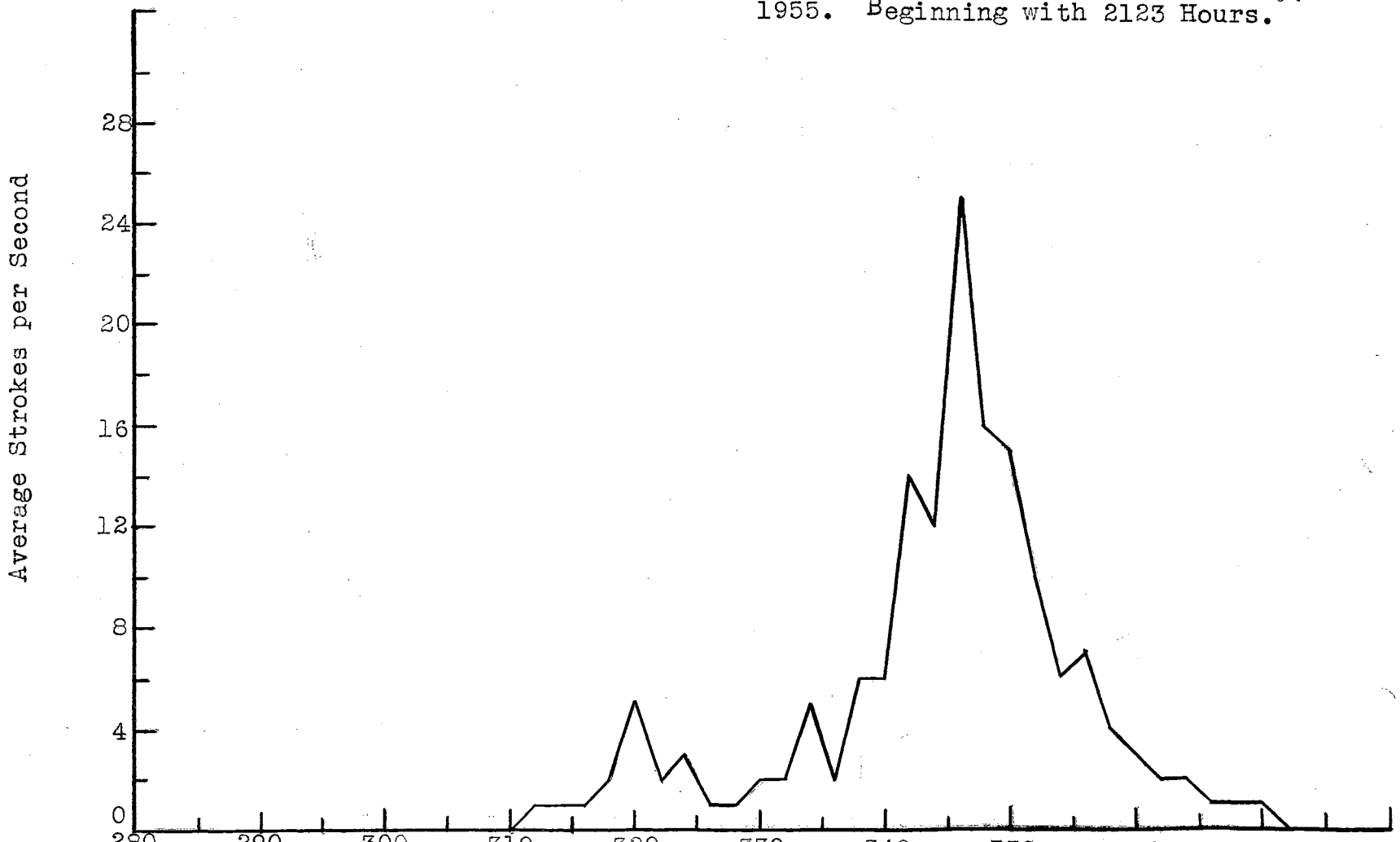

Figure 37

Azimuth Incidence Distribution of Sferic Activity Sampled by High Frequency Direction Finder 25 May, 1955. Beginning with 2129 Hours, Average of 15 Second Interval.

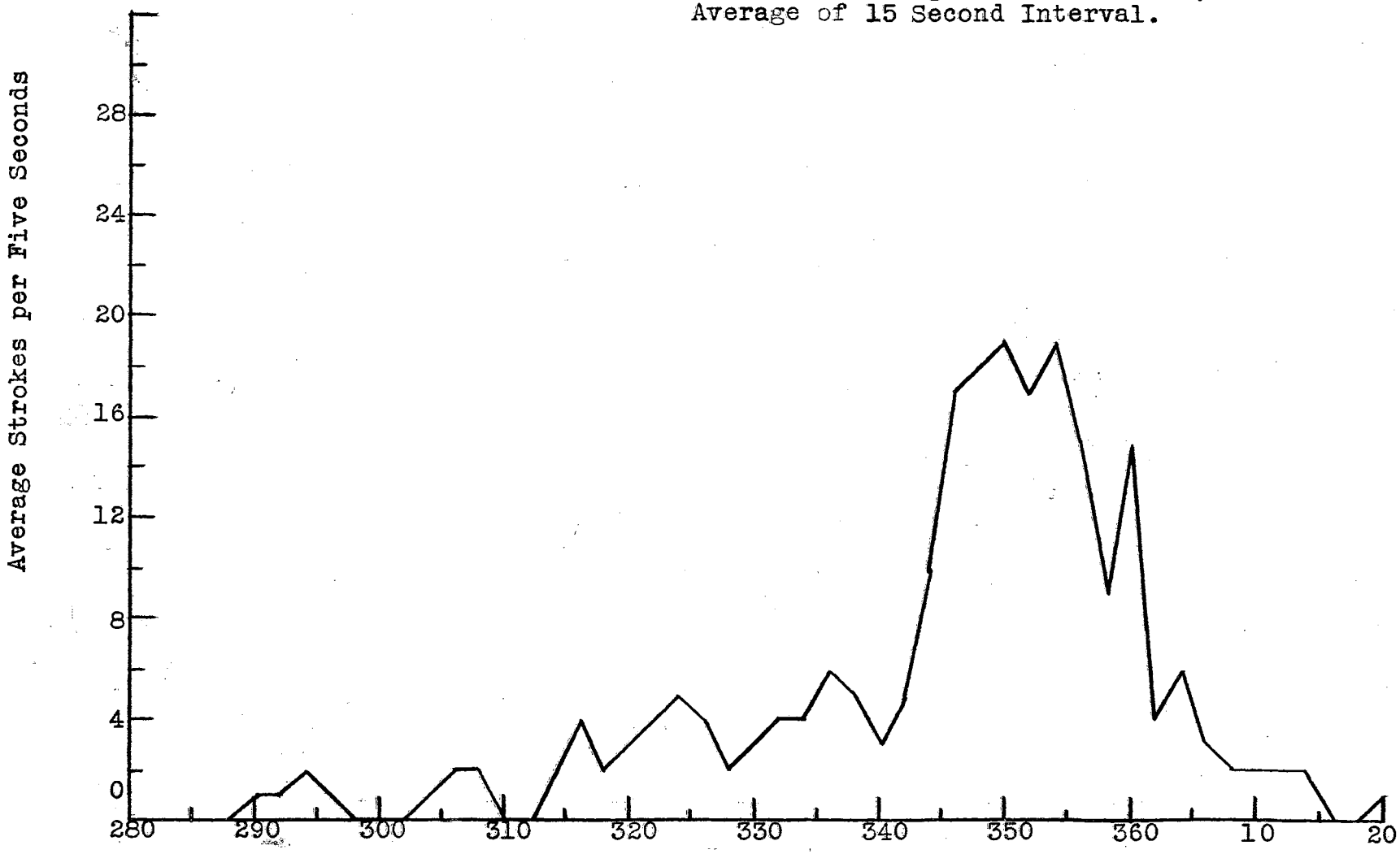

Figure 38

Azimuth Incidence Distribution of Sferic Activity Sampled by High Frequency Direction Finder 25 May, 1955. Beginning with 2133 Hours, Average of 30 Second Interval.

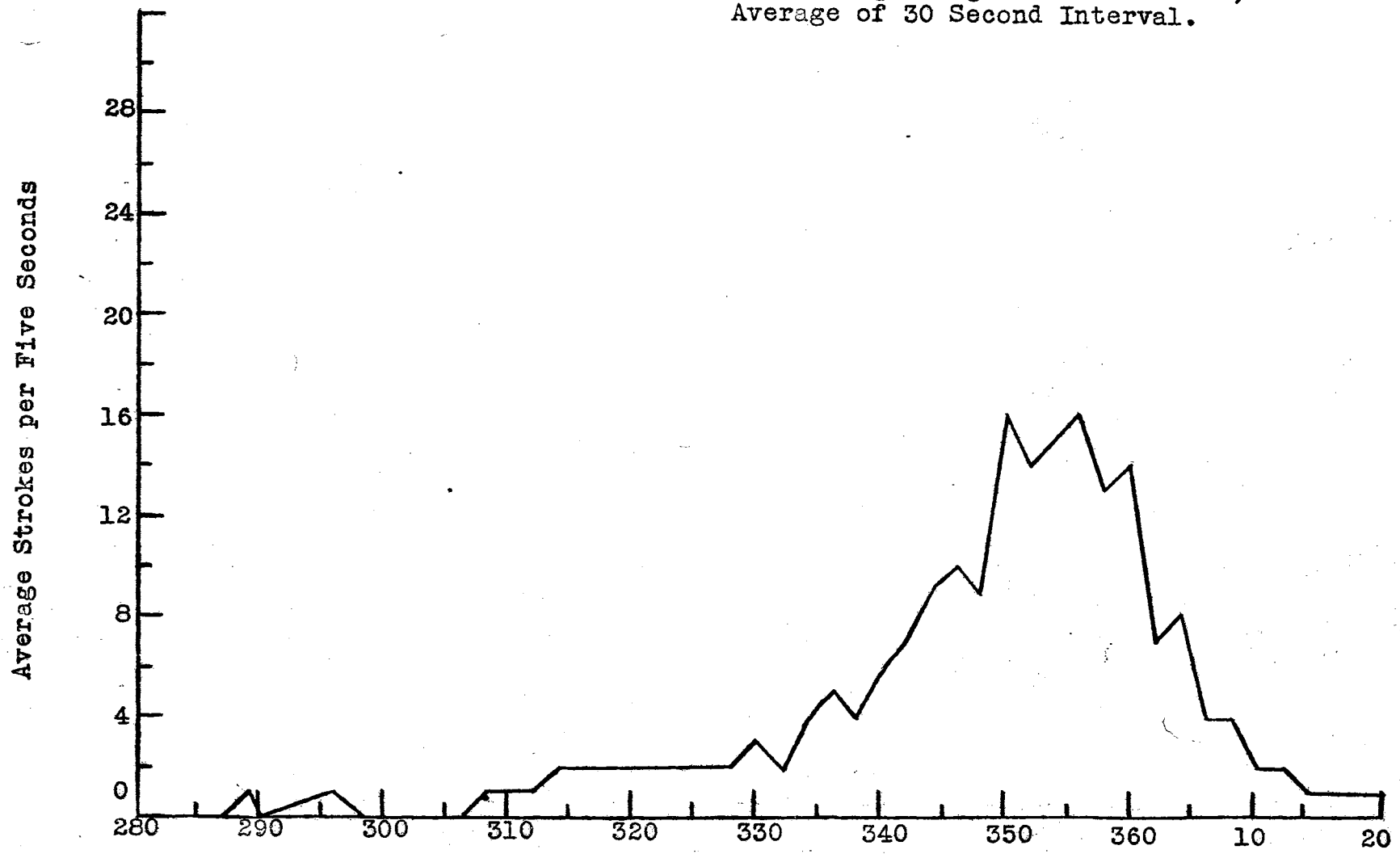

Figure 39

Azimuth Incidence Distribution of Sferic Activity Sampled by High Frequency Direction Finder, 25 May, 1955. Beginning with 2138 Hours.

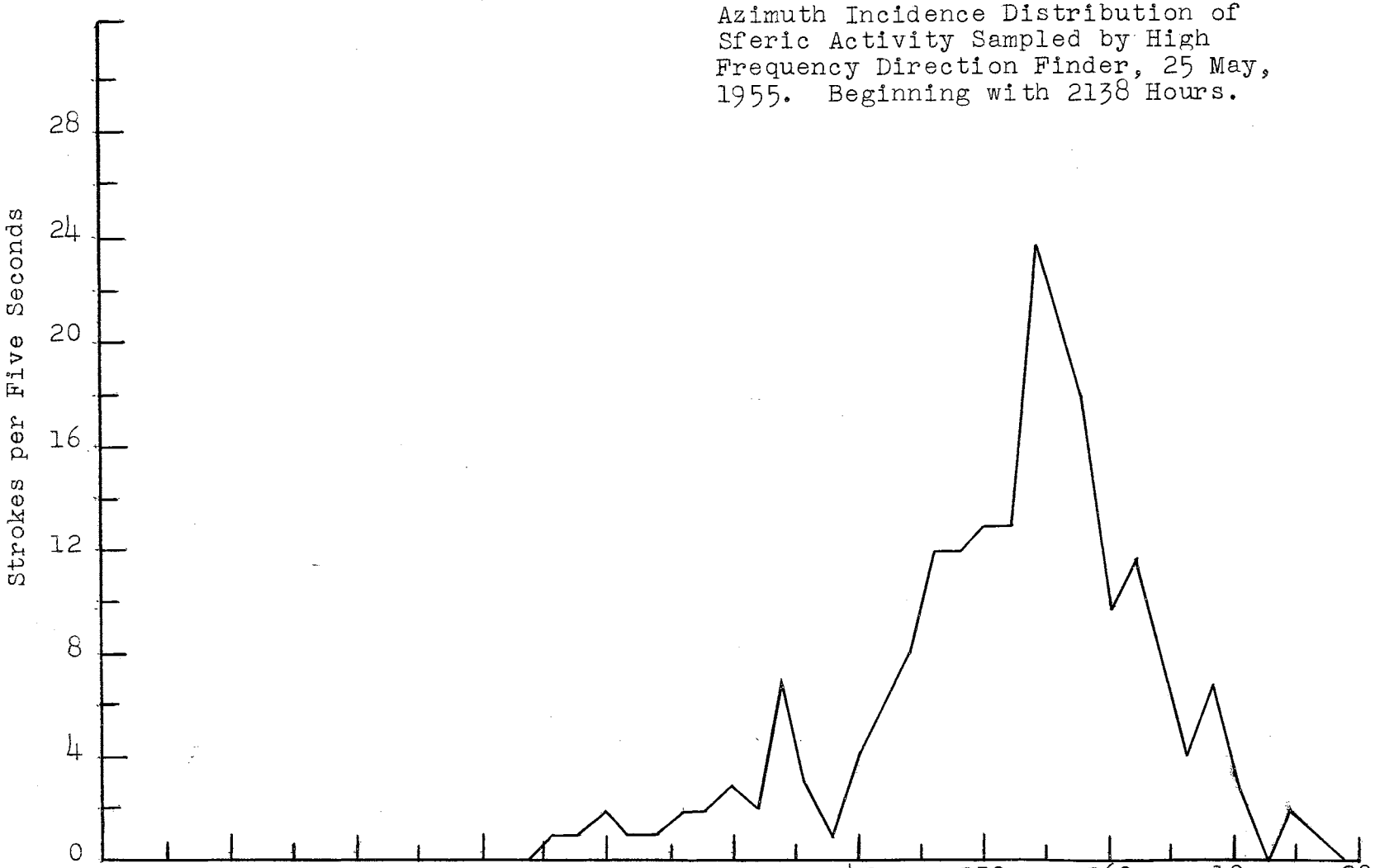

Figure 40

Azimuth Incidence Distribution of Sferic Activity Sampled by High Frequency Direction Finder 25 May, 1955. Beginning with 2143 Hours, Average of 20 Second Interval.

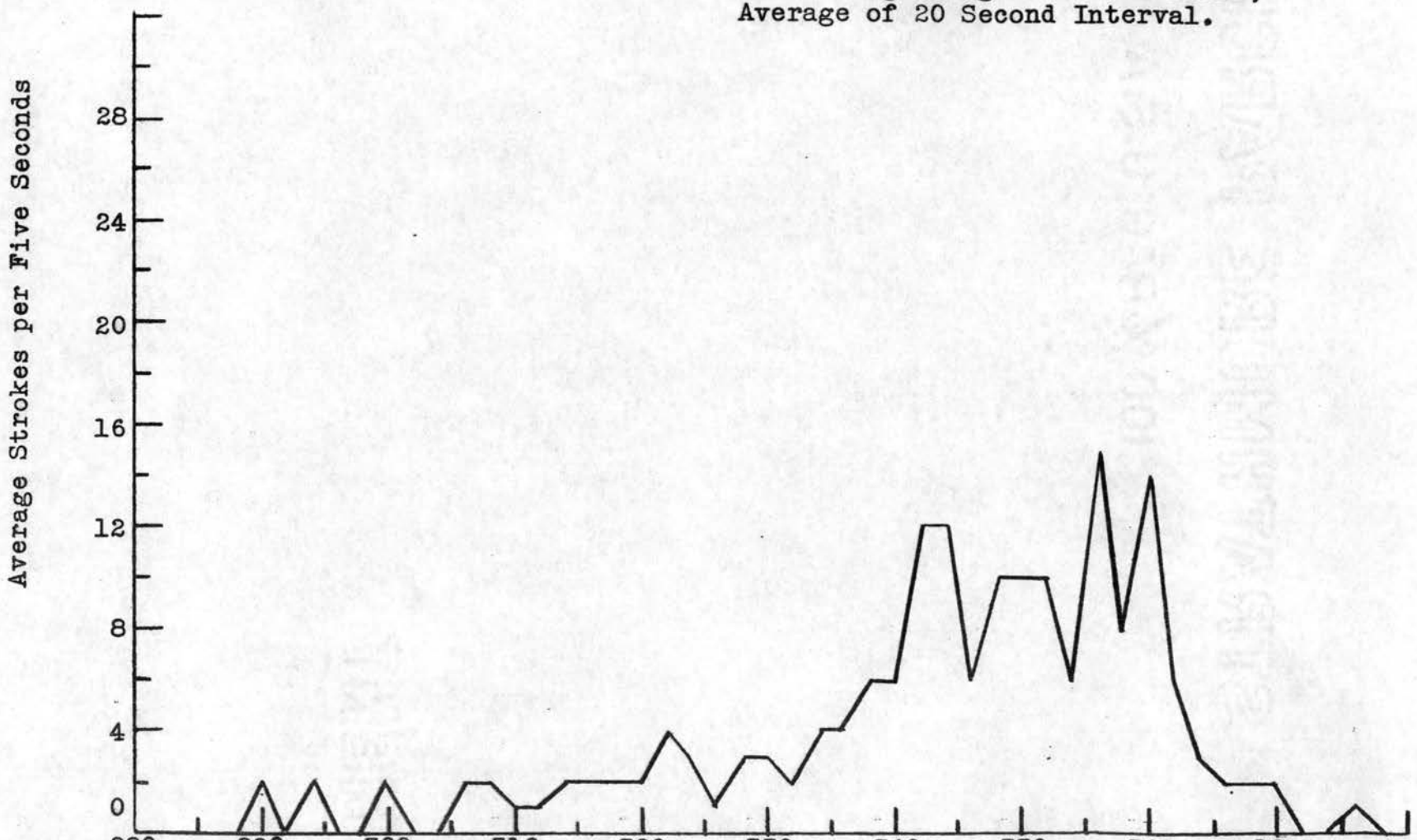

Figure 41

Azimuth Incidence Distribution of Sferic Activity Sampled by High Frequency Direction Finder 25 May, 1955. Beginning with 2148 Hours, Average of 10 Second Interval.

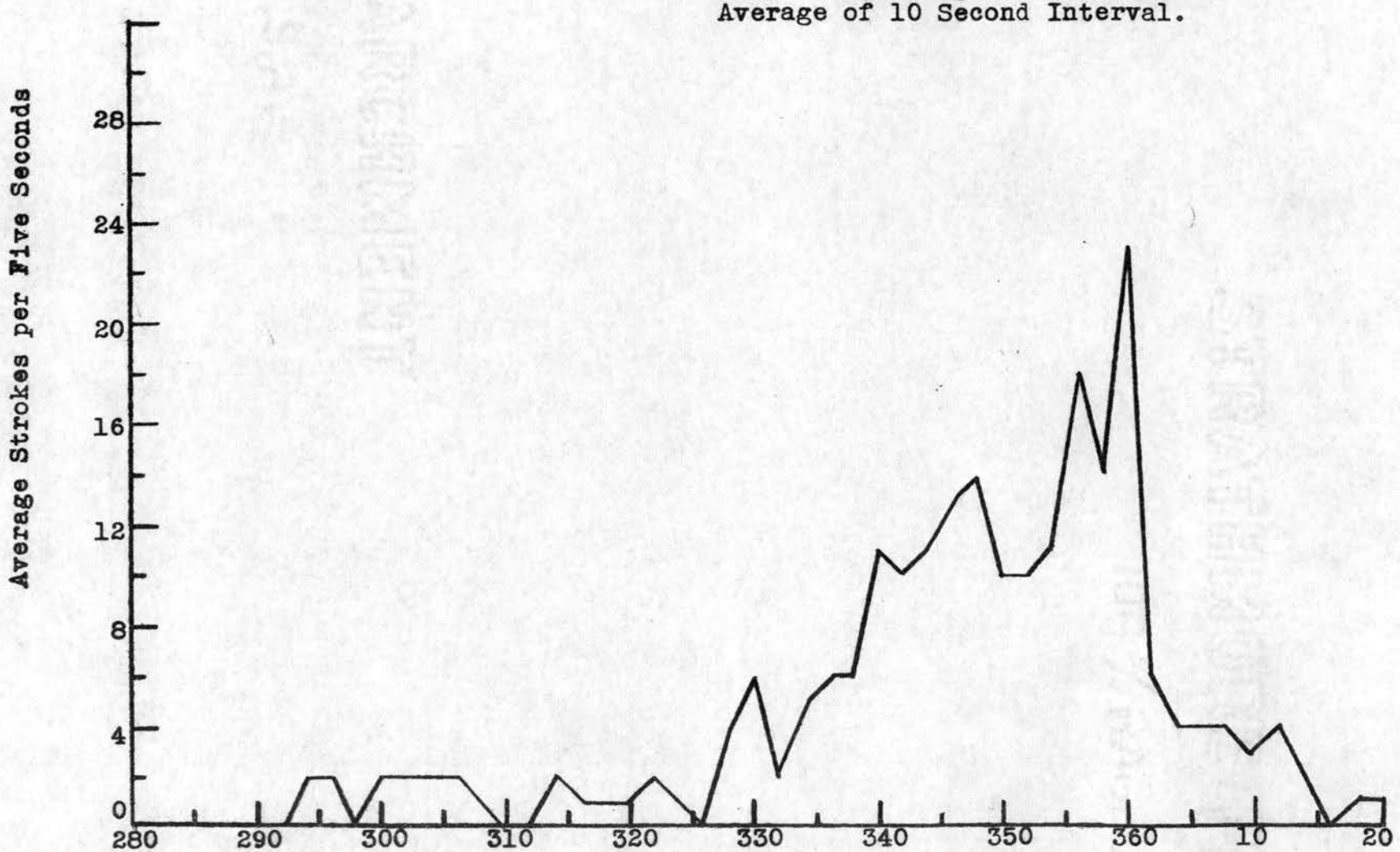

Figure 42

Azimuth Incidence Distribution of Sferic Activity Sampled by High Frequency Direction Finder 25 May, 1955. Beginning with 2153 Hours, Average of 10 Second Interval.

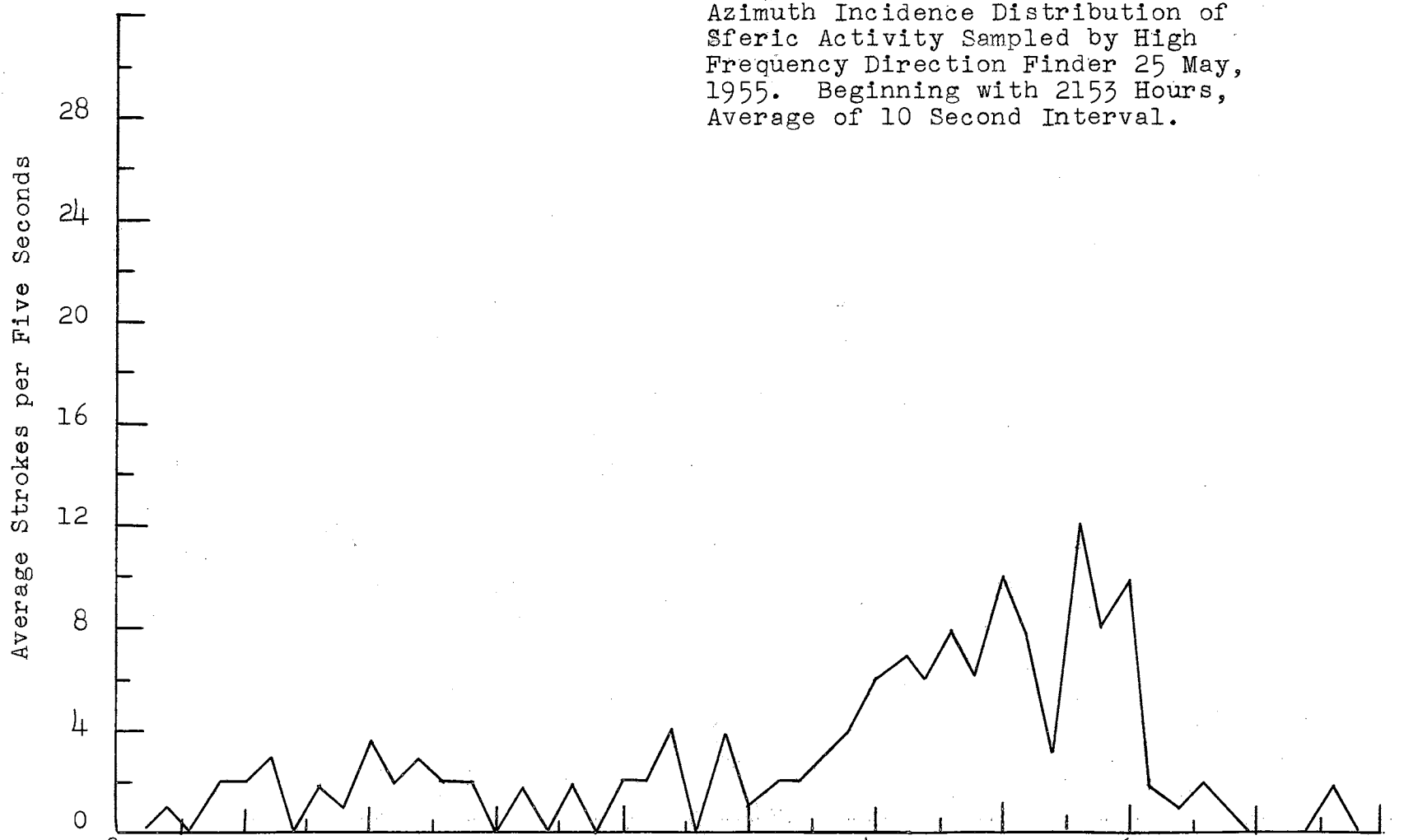

Figure 43

A study of the azimuth distribution of sferics shown in Figures 32 to 43 inclusive shows a gradual increase in the magnitude of the peak of the average curves as the azimuth of peak activity increases until the time the tornado struck Blackwell at 2130 CST. From Figure 31 it may be seen that the tornado was traveling north during that time which would increase the azimuth angle. It may be concluded from the increase in sferics count as the peak shifted northward that the intensity of the tornado increased as it approached Blackwell. After the tornado struck Blackwell there was a gradual decrease in the peak value of the sferics count as the tornado continued to move northward. This trend continued until the tornado was dissipated in southern Kansas. However, as the Blackwell tornado was dissipating, a second tornado was forming about five miles east. This tornado, which eventually destroyed Udall, Kansas, followed a course parallel to the now dissipating Blackwell tornado. In Figure 43 the azimuth distribution of sferics appears to be a double peaked curve which probably indicates that both tornadoes were active at that time.

In Figure 44 is shown a time distribution of sferics at azimuth 342° from the Tornado Laboratory. This azimuth was picked for study because it is the direction of Tonkawa. The tornado was reported as having passed within one mile of Tonkawa at 2115 CST. Figure 44 shows that

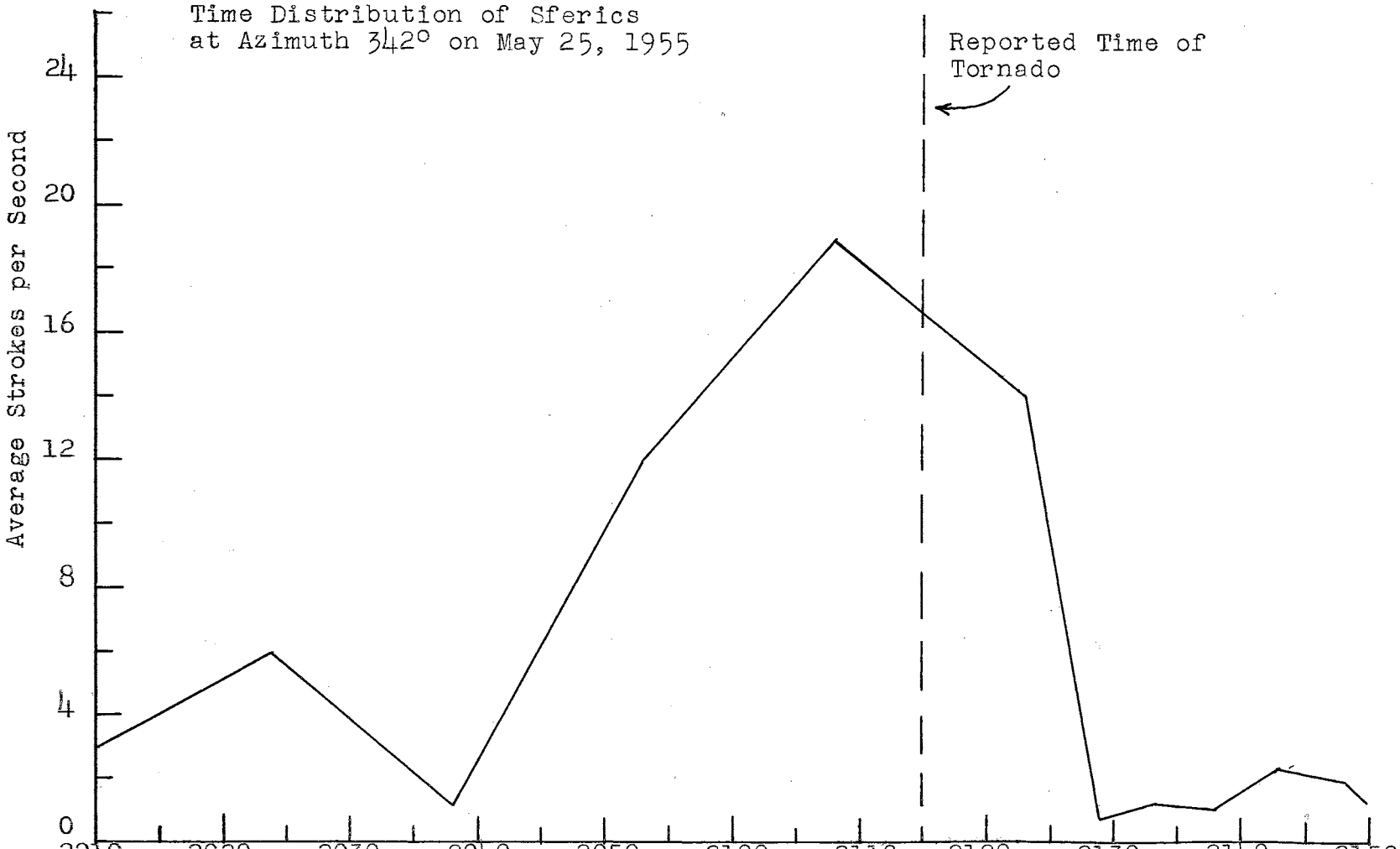
Time Distribution of Sferics
at Azimuth 342° on May 25, 1955
Reported Time of
Tornado
Average Strokes per Second
24
20
16
12
8
4
0
2010
2020
2030
2040
2050
2100
2110
2120
2130
2140
2150
Time

Figure 44

there was a gradual buildup in sferic activity as the tornado approached with the maximum occurring just prior to the actual time of the tornado. Within a few minutes after the tornado had passed there was a rather sharp decline in sferic activity.

Figure 45 shows the same analysis for an azimuth of 346° which is the direction of Blackwell. The same trend is observed here although not so conclusively because of the change in scale due to the reduction in Direction Finder gain and intensity. Figures 44 and 45 indicate that it should be possible to send out warnings to towns and cities which are in a direction in which the sferic count is rapidly building up. By means of the radar echoes it would be possible to determine the distance to the fast buildup and thus to locate accurately the danger zone.

Figures 46, 47 and 48 show photographs of the radar screen at three different times just before and during the active life of the tornado. Each range marker is ten nautical miles. Figure 46 was taken about thirty minutes prior to the formation of the tornado. The large echo near the center is the one from which the tornado eventually formed. Figure 47 was taken about the time the tornado was forming and Figure 48 was taken while the tornado was on the ground near Blackwell. The large echo at 40 miles from the station is from the cloud which supported the tornado. The azimuth distribution of sferics count is also

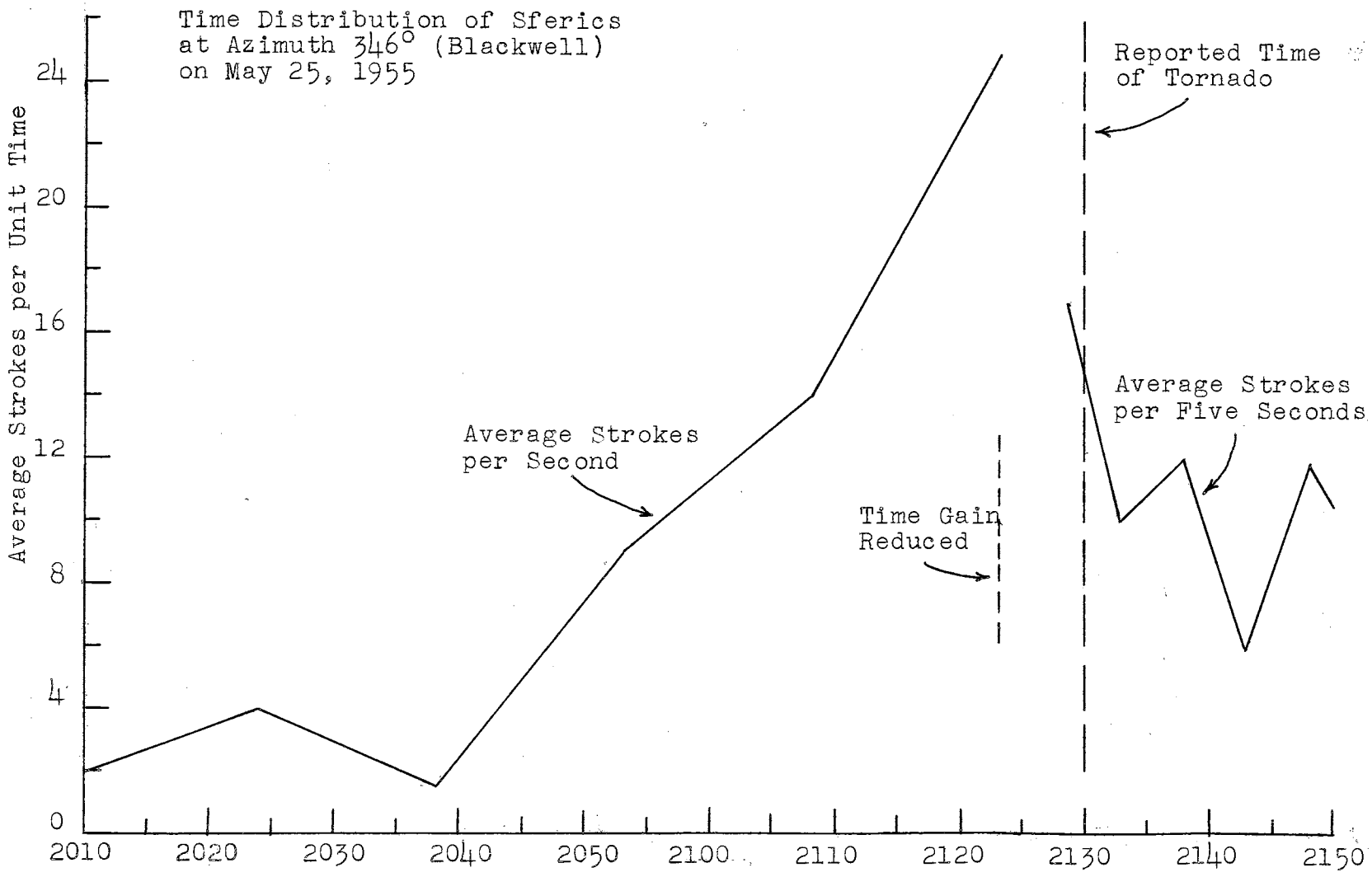
Time Distribution of Sferics
at Azimuth 346° (Blackwell)
on May 25, 1955
Reported Time
of Tornado
Average Strokes
per Five Seconds
Average Strokes
per Second
Time Gain
Reduced
Average Strokes per Unit Time
0
4
8
12
16
20
24
2010
2020
2030
2040
2050
2100
2110
2120
2130
2140
2150
Time

Figure 45

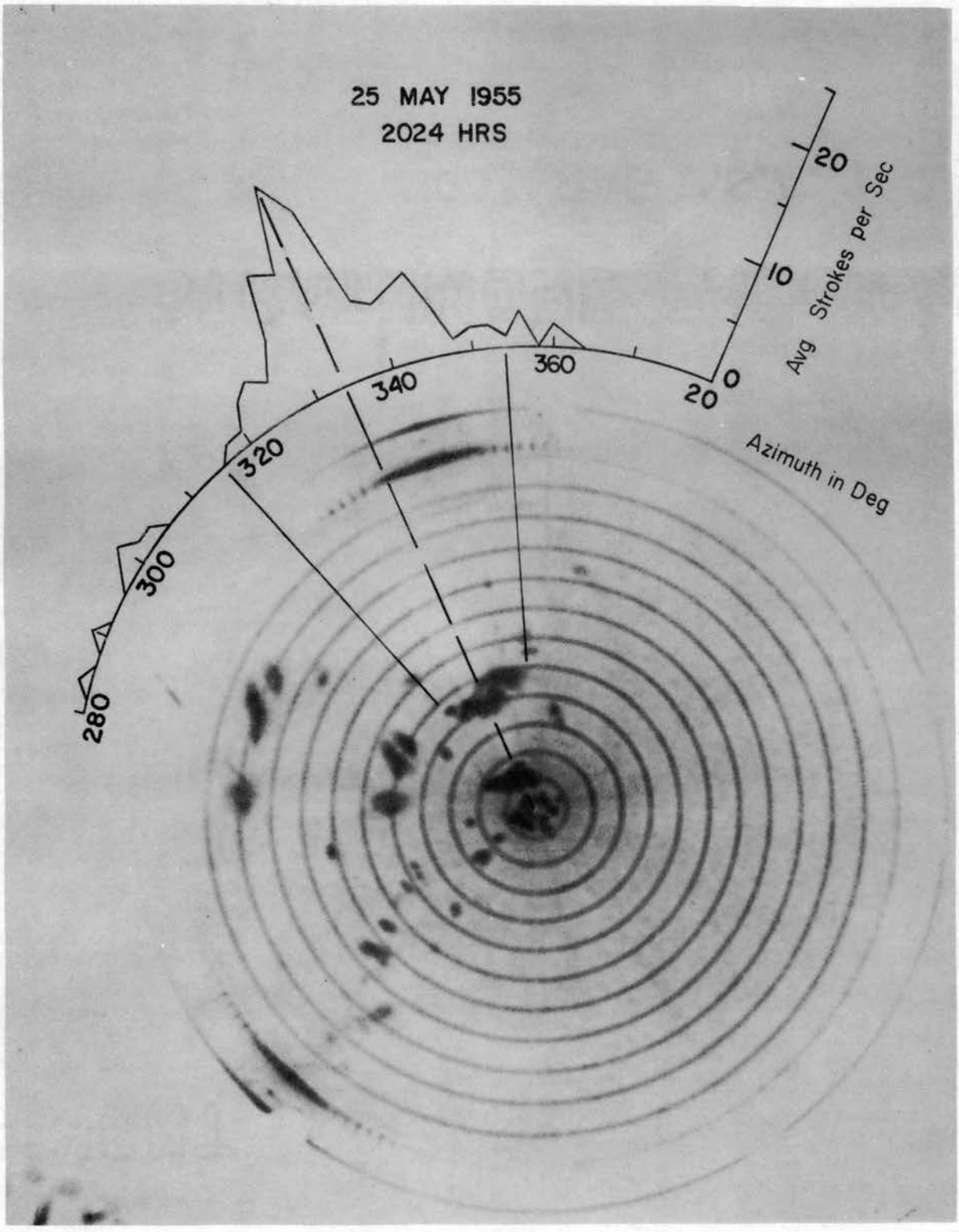

Figure 46. Correlation of Radar Sferic Records, 2024 CST.

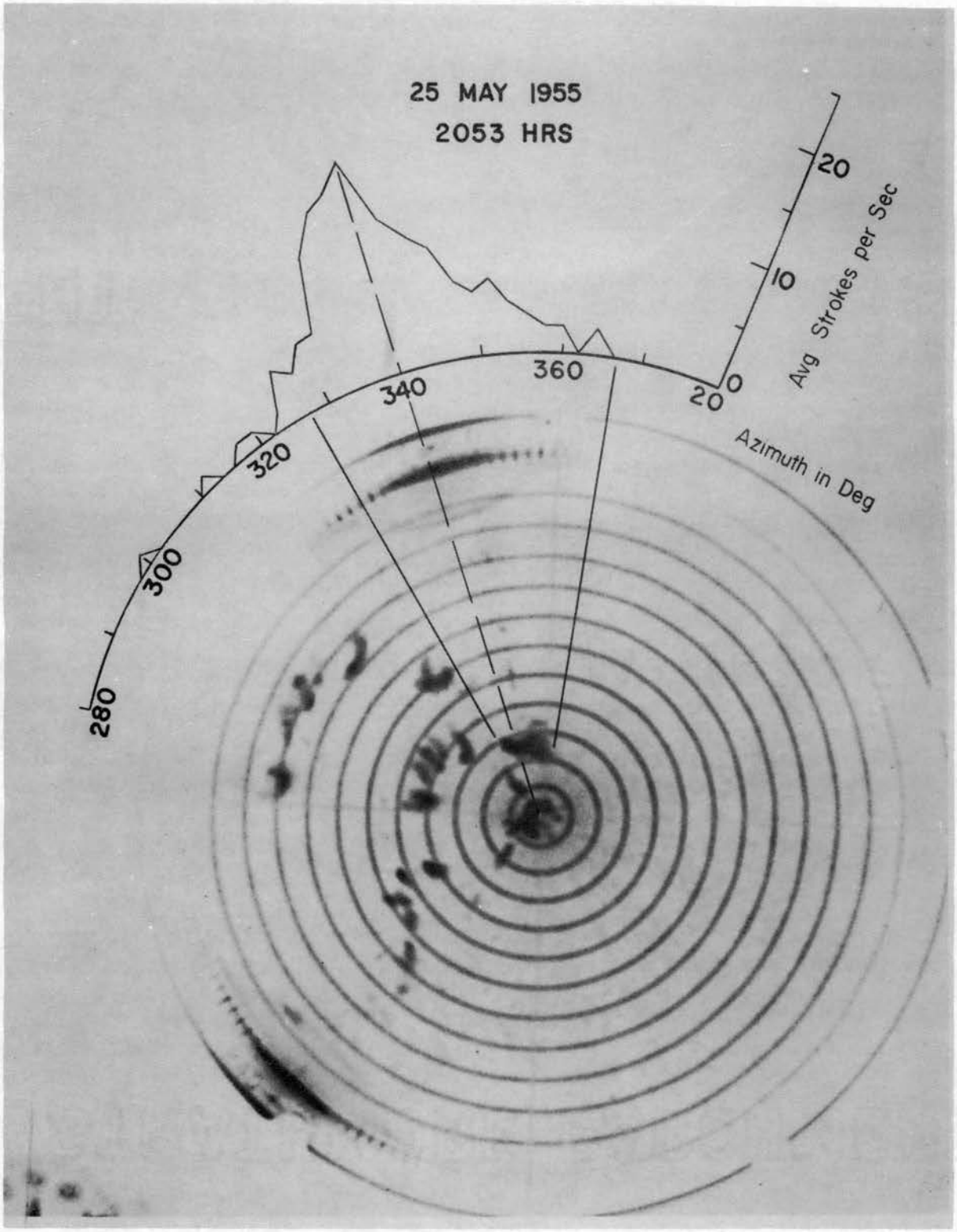

Figure 47. Correlation of Radar Sferic Records, 2053 CST.

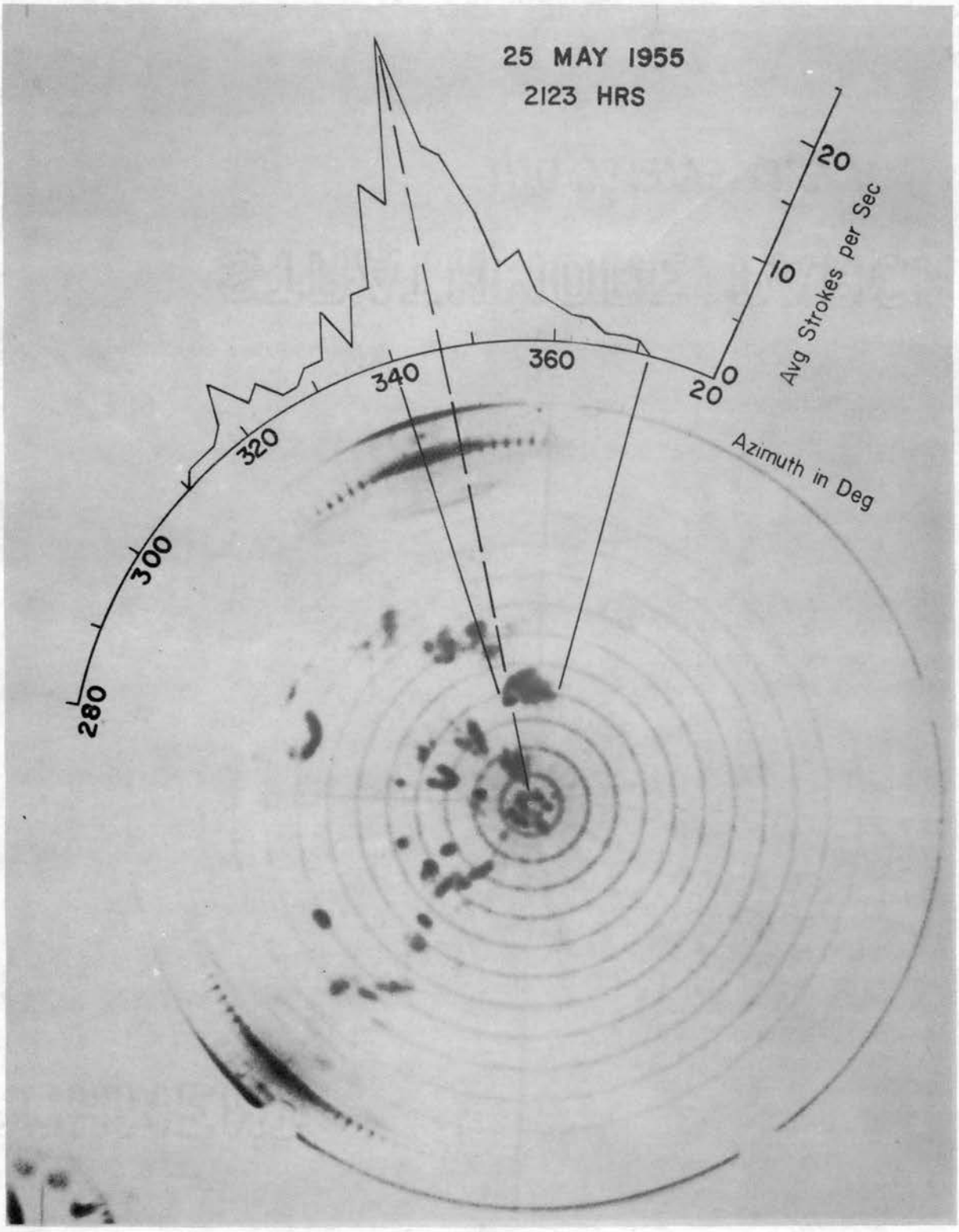

Figure 48. Correlation of Radar Sferic Records, 2123 CST.

plotted in Figures 46, 47 and 48. It may be noted in Figure 48 that the azimuth of maximum sferic count passes through a bulge on the side of the radar echo. There is evidence to support the belief that this peculiarly shaped bulge is indicative of, and actually associated with, the tornado[2]. Figures 49 to 60 inclusive show the azimuth distribution of sferics for the time from 2158 CST to 2258 CST. During that time the Udall tornado was active. In fact, at 2158 CST, the time of Figure 49, both tornadoes were probably active as evidenced by the rather broad peak in the sferics distribution plot. From 2158 CST until 2253 CST, after the tornado struck Udall, the peak of sferics activity was essentially constant. At least there seems to be no definite trend. It was only after 2253 CST that the sferic activity began to die out.

Since the Udall tornado was traveling almost due north and away from the Tornado Laboratory it is difficult to obtain a time distribution of sferics which is meaningful. In Figure 61 is shown an attempt to make such a display. There is a slight peak in sferics activity at about the time the tornado struck near Oxford, Kansas, but the background count is very high due to the fact that the tornado was at all times very close to the two degree

---

[2]Charles M. Turrentine, "A Radar-Sferic Analysis of the Tornadoes of May 25, 1955", Unpublished Master Thesis, Oklahoma A & M College, (1956), p. 27.

Azimuth Incidence Distribution of Sferic Activity Sampled by High Frequency Direction Finder 25 May, 1955. Beginning with 2158 Hours, Average of 10 Second Interval.

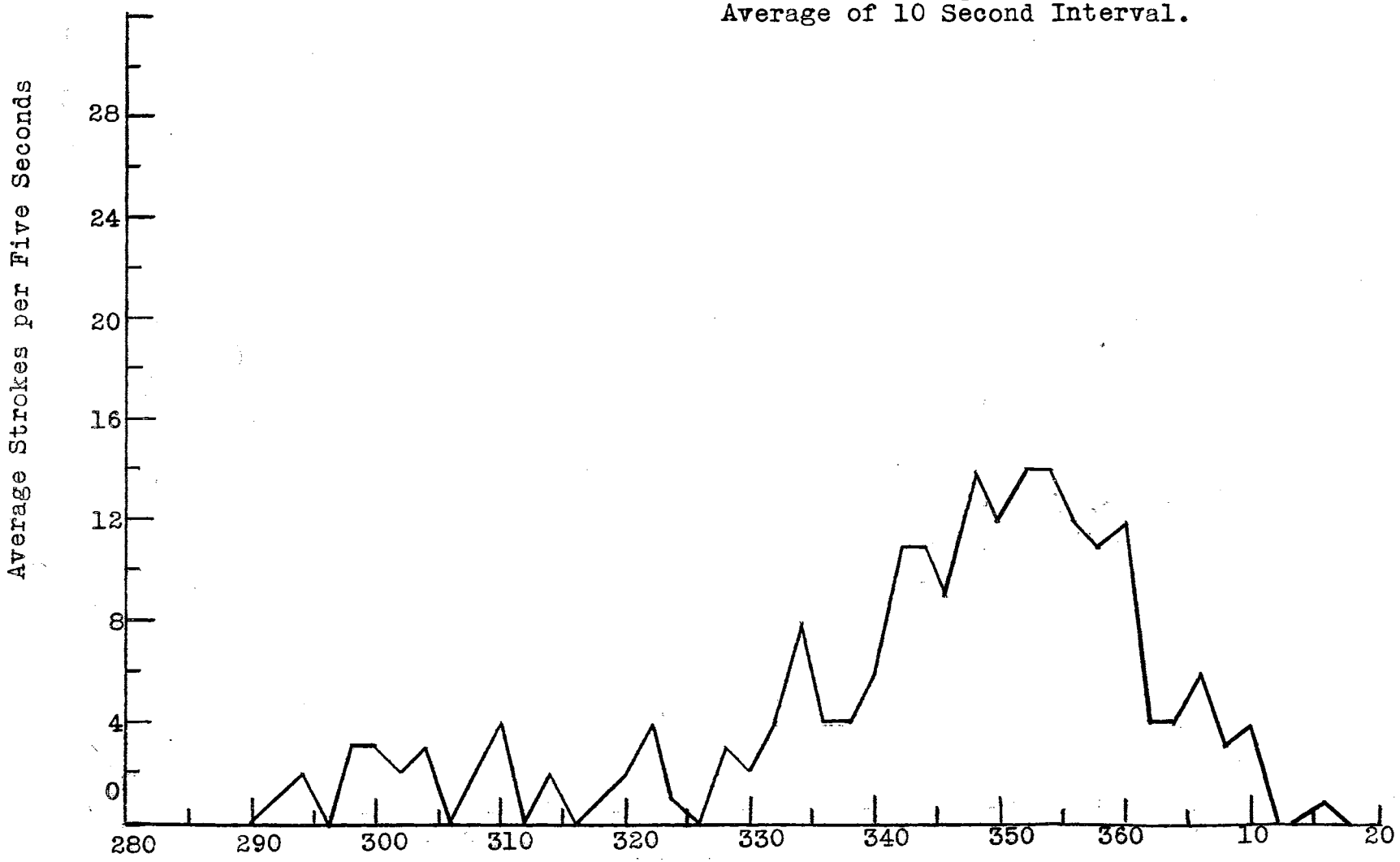

Figure 49

Azimuth Incidence Distribution of Sferic Activity Sampled by High Frequency Direction Finder 25 May, 1955. Beginning with 2202 Hours, Average of 10 Second Interval.

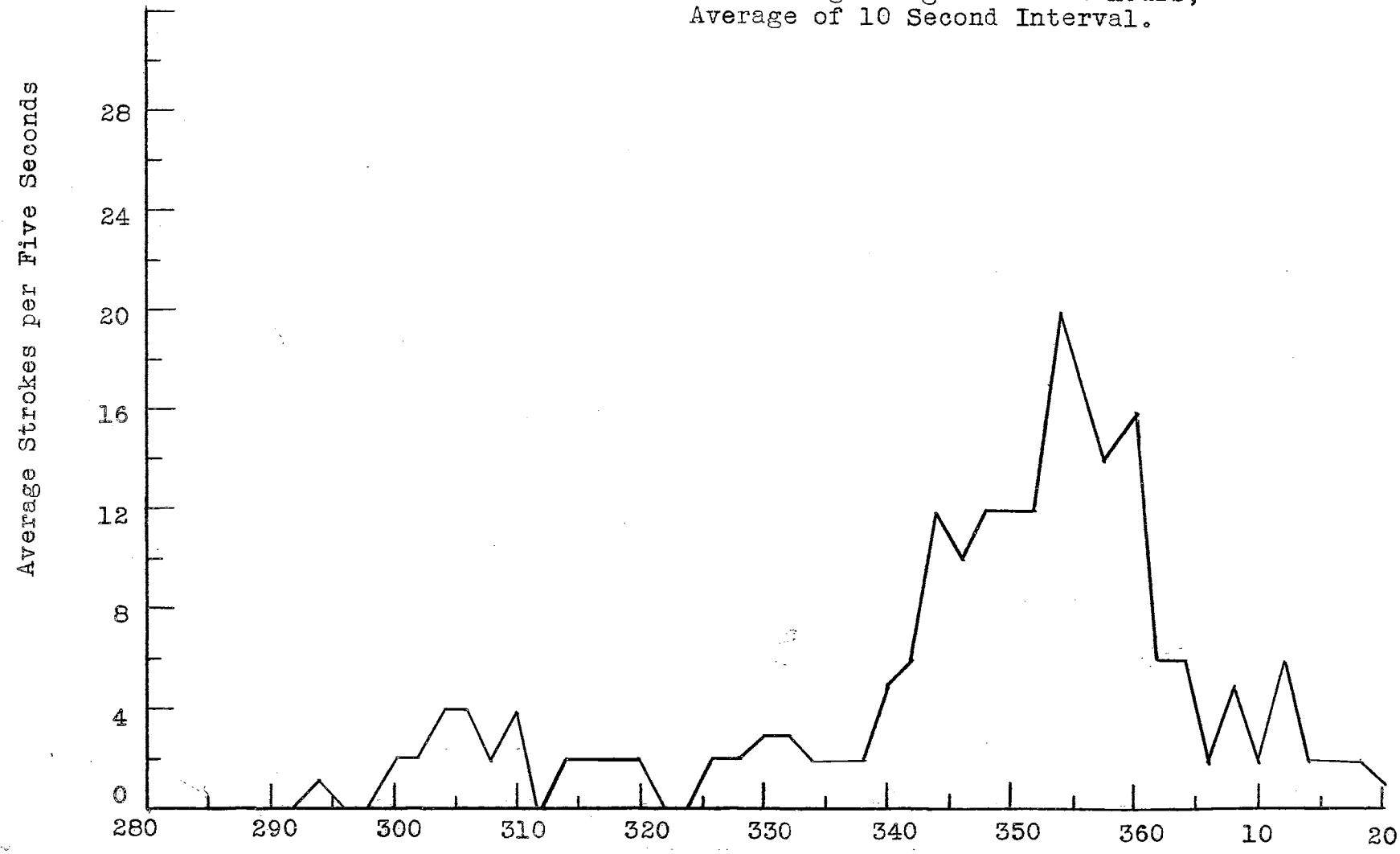

Figure 50

Azimuth Incidence Distribution of Sferic Activity Sampled by High Frequency Direction Finder 25 May, 1955. Beginning with 2208 Hours, Average of 10 Second Interval.

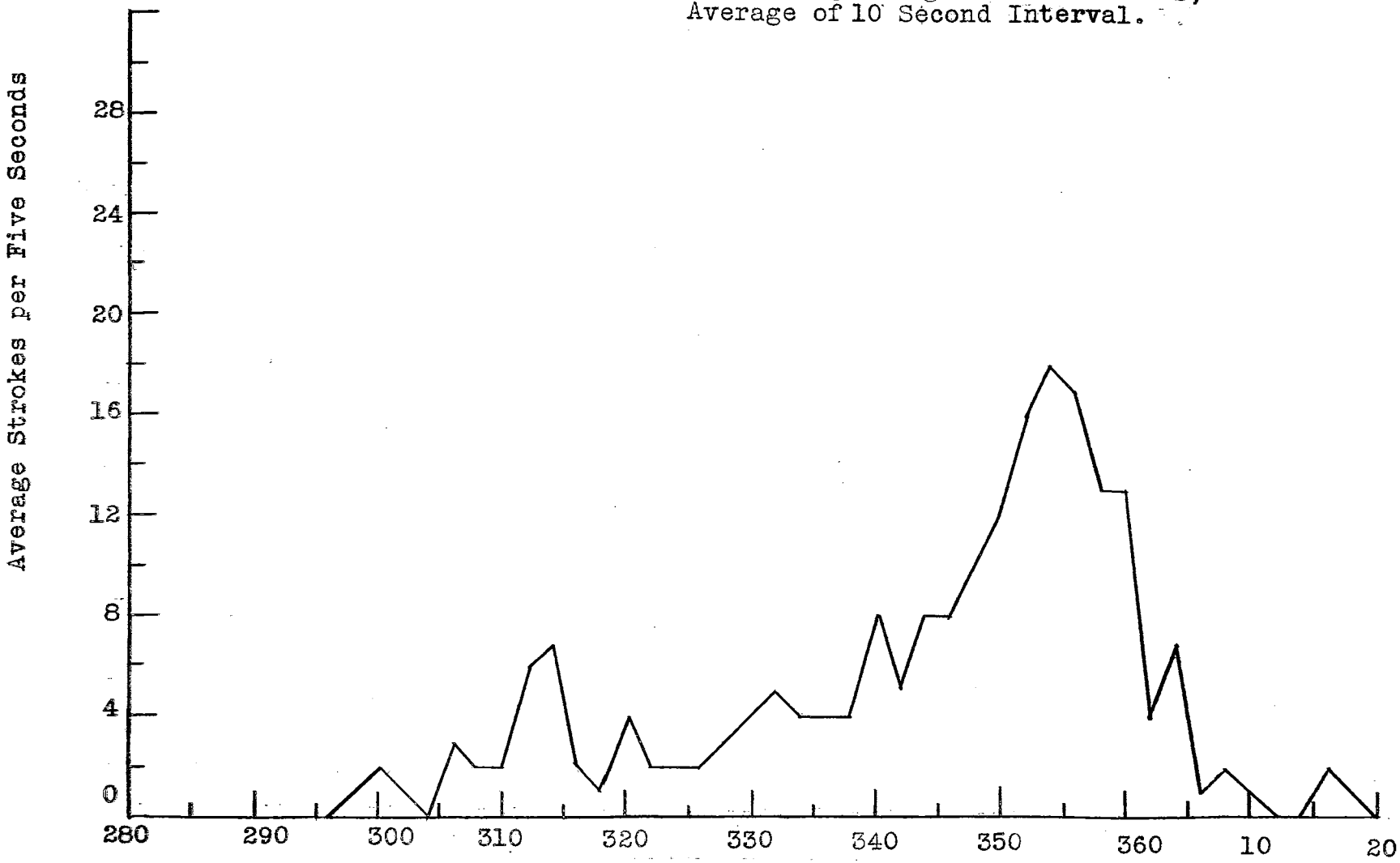

Figure 51

Azimuth Incidence Distribution of Sferic Activity Sampled by High Frequency Direction Finder 25 May, 1955. Beginning with 2218 Hours, Average of 10 Second Interval.

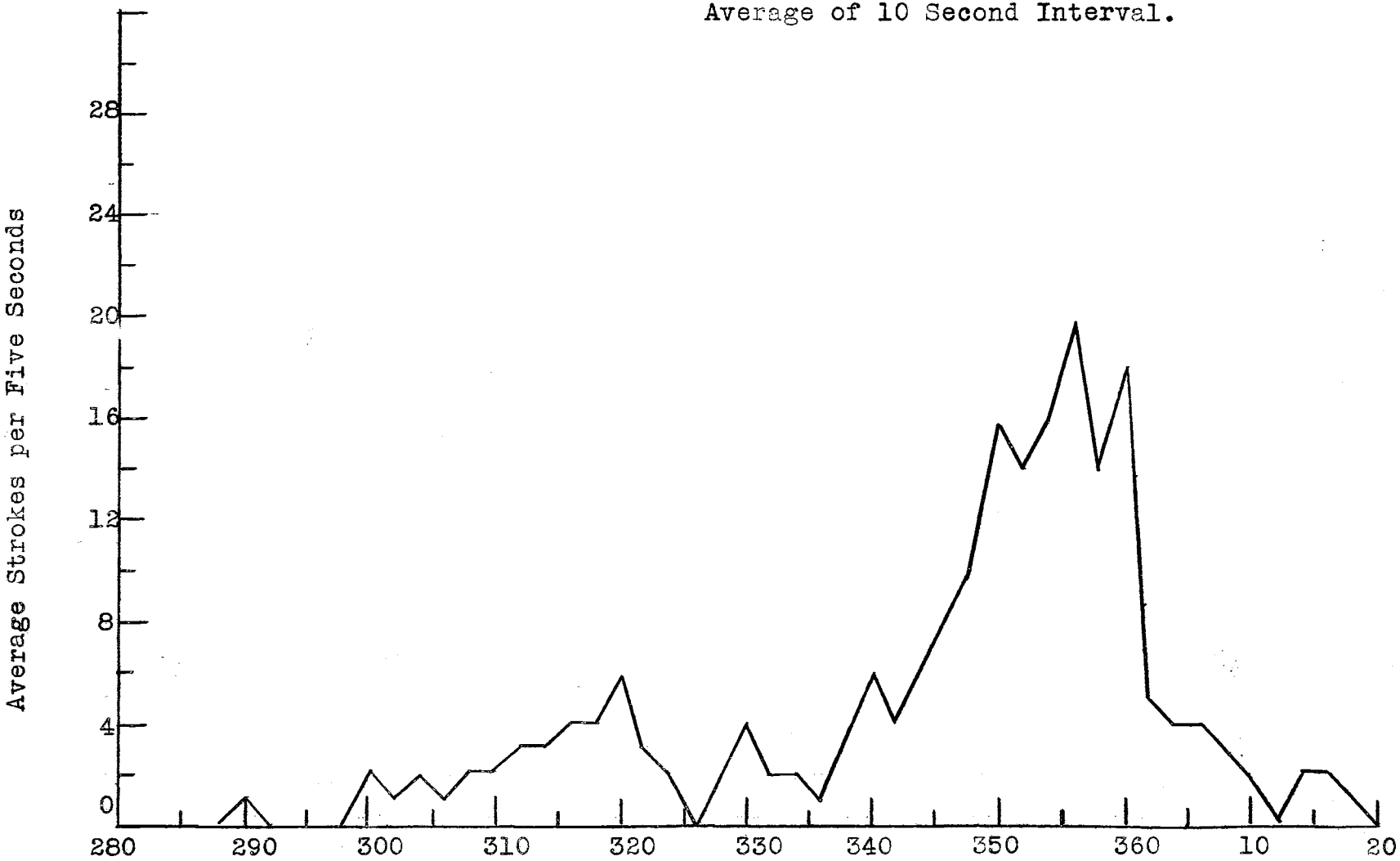

Figure 52

Azimuth Incidence Distribution of Sferic Activity Sampled by High Frequency Direction Finder 25 May, 1955. Beginning with 2223 Hours, Average of 10 Second Interval.

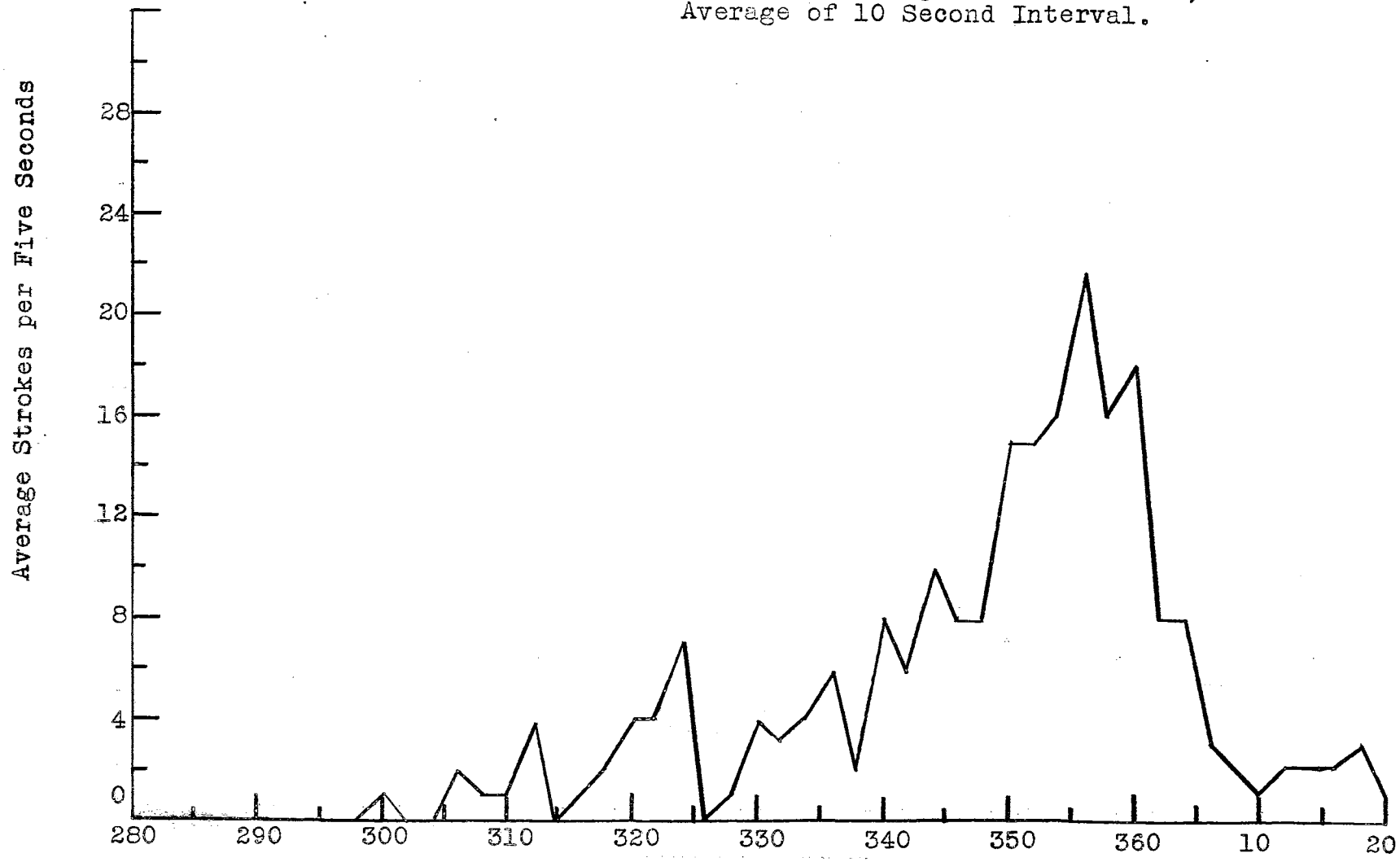

Figure 53

Azimuth Incidence Distribution of Sferic Activity Sampled by High Frequency Direction Finder 25 May, 1955. Beginning with 2228 Hours, Average of 10 Second Interval.

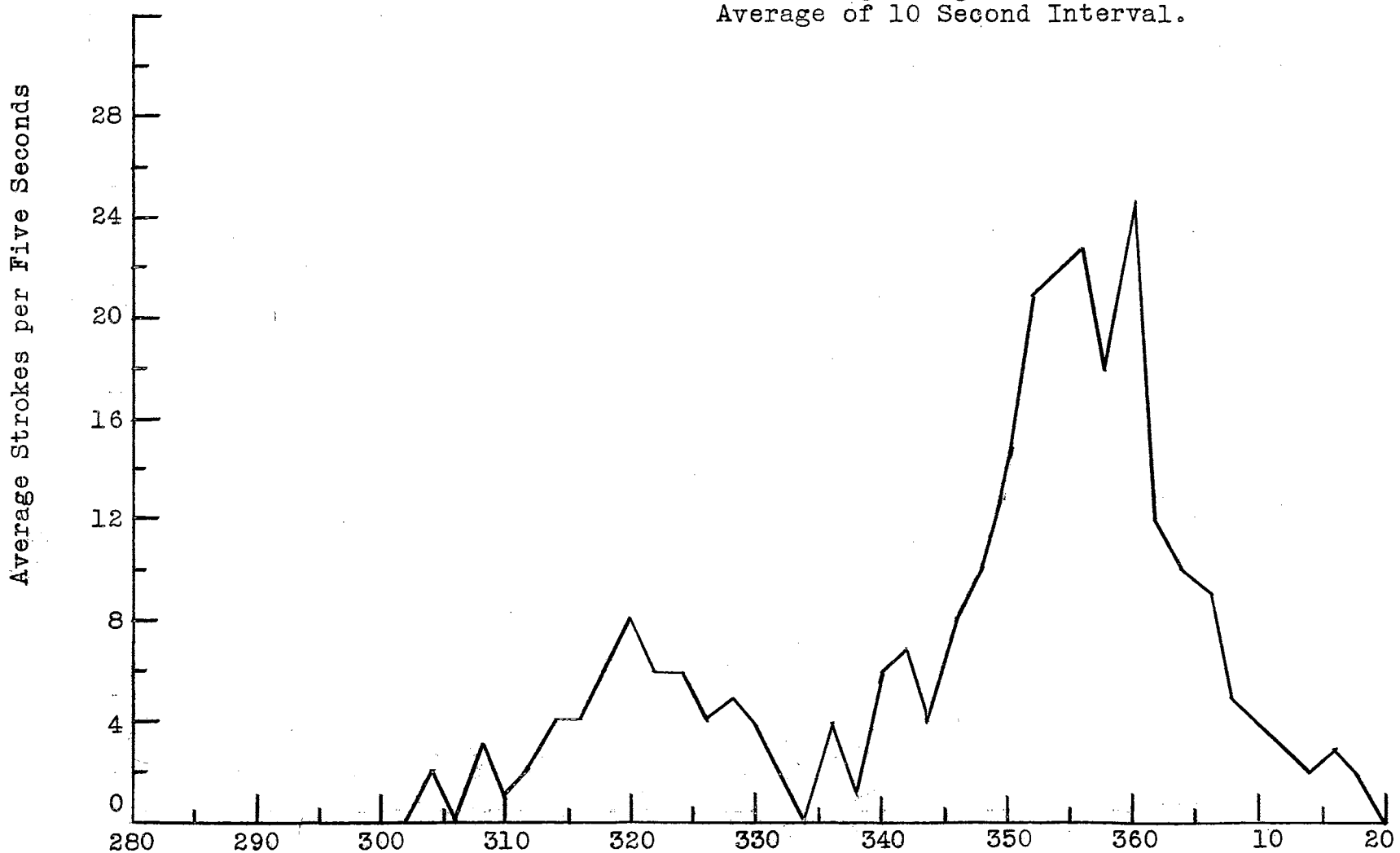

Figure 54

Azimuth Incidence Distribution of Sferic Activity Sampled by High Frequency Direction Finder 25 May, 1955. Beginning with 2233 Hours, Average of 10 Second Interval.

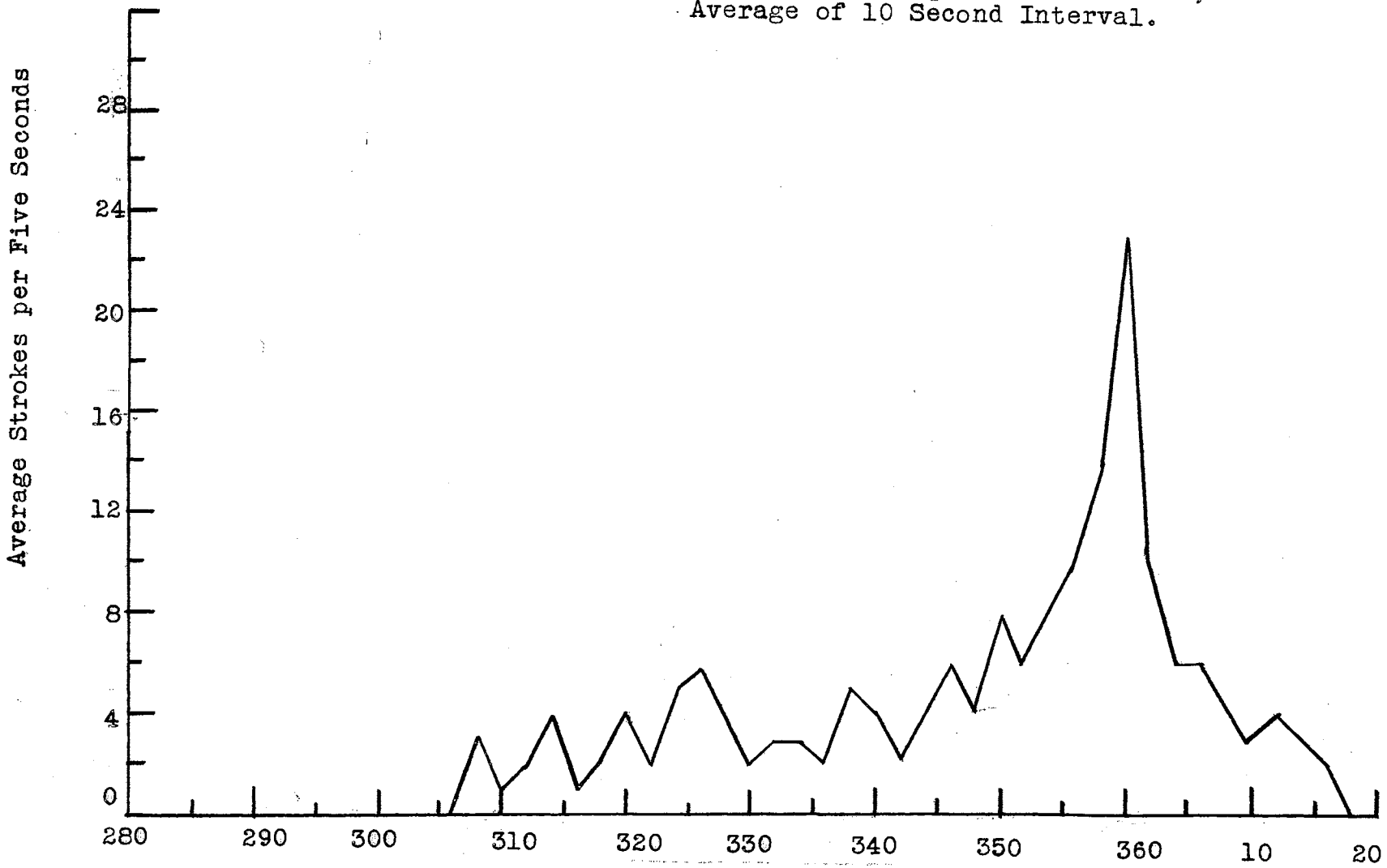

Figure 55

Azimuth Incidence Distribution of Sferic Activity Sampled by High Frequency Direction Finder 25 May, 1955. Beginning with 2238 Hours, Average of 10 Second Interval.

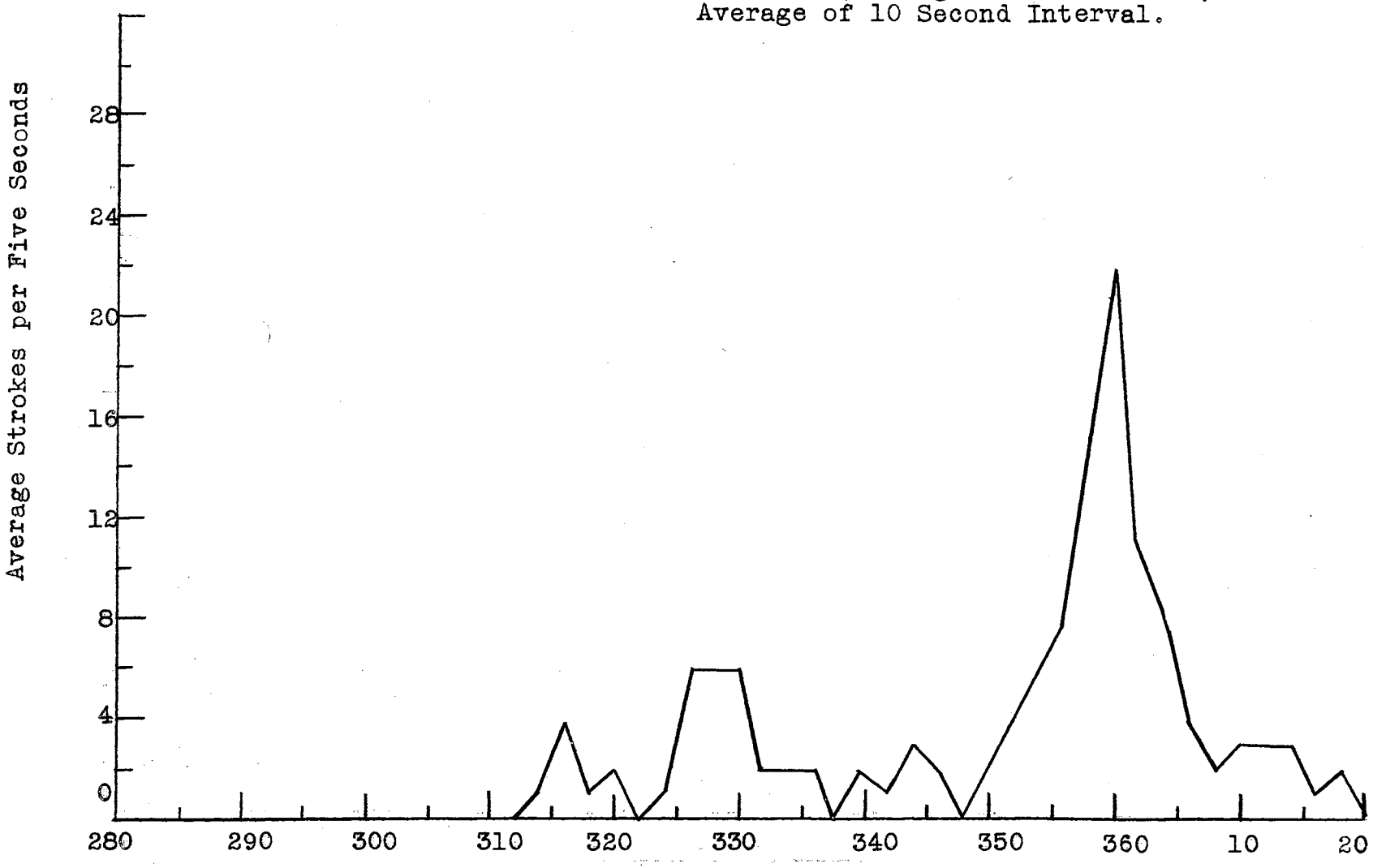

Figure 56

Azimuth Incidence Distribution of Sferic Activity Sampled by High Frequency Direction Finder 25 May, 1955. Beginning with 2243 Hours, Average of 10 Second Interval.

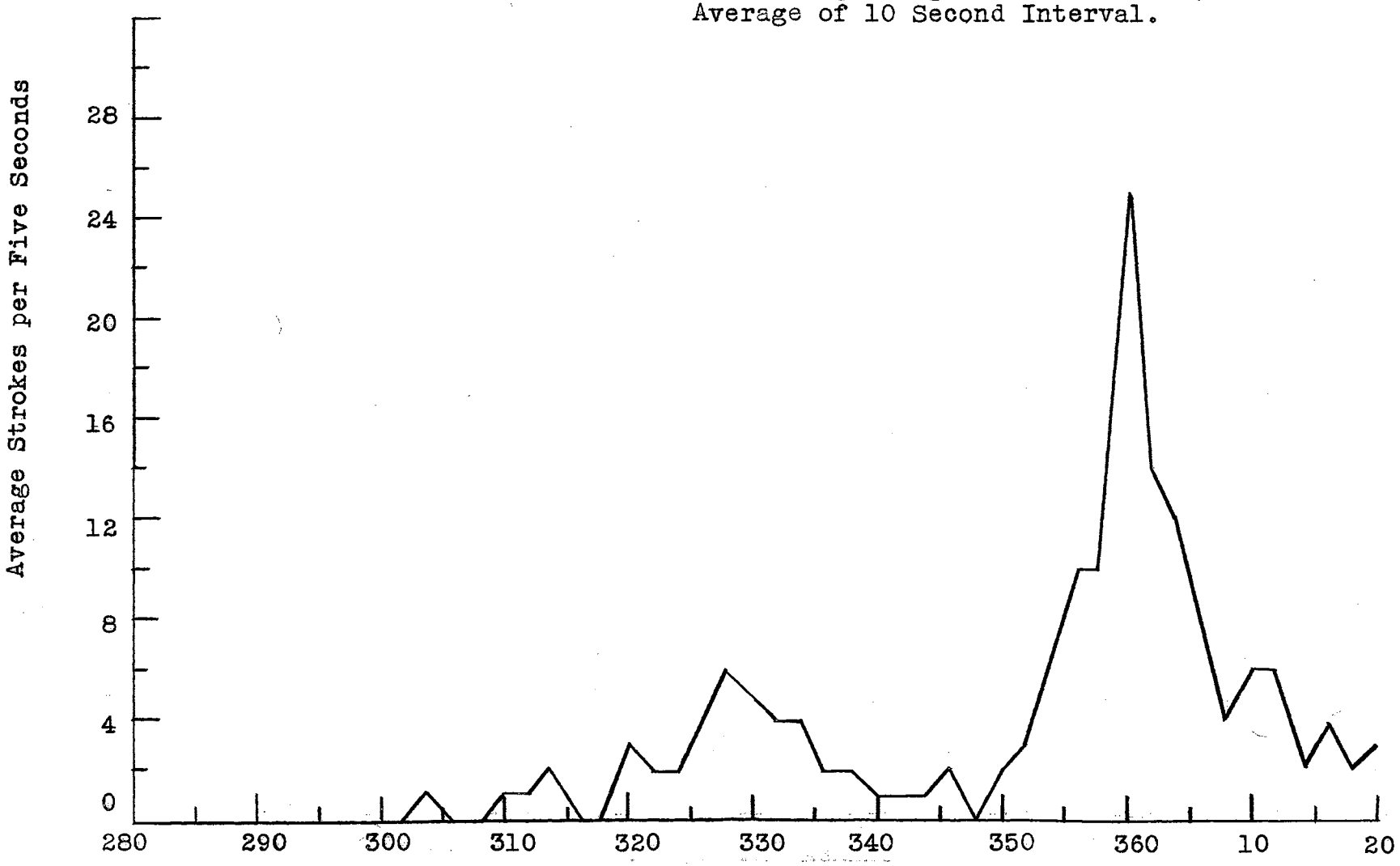

Figure 57

Azimuth Incidence Distribution of Sferic Activity Sampled by High Frequency Direction Finder 25 May, 1955. Beginning with 2248 Hours, Average of 10 Second Interval.

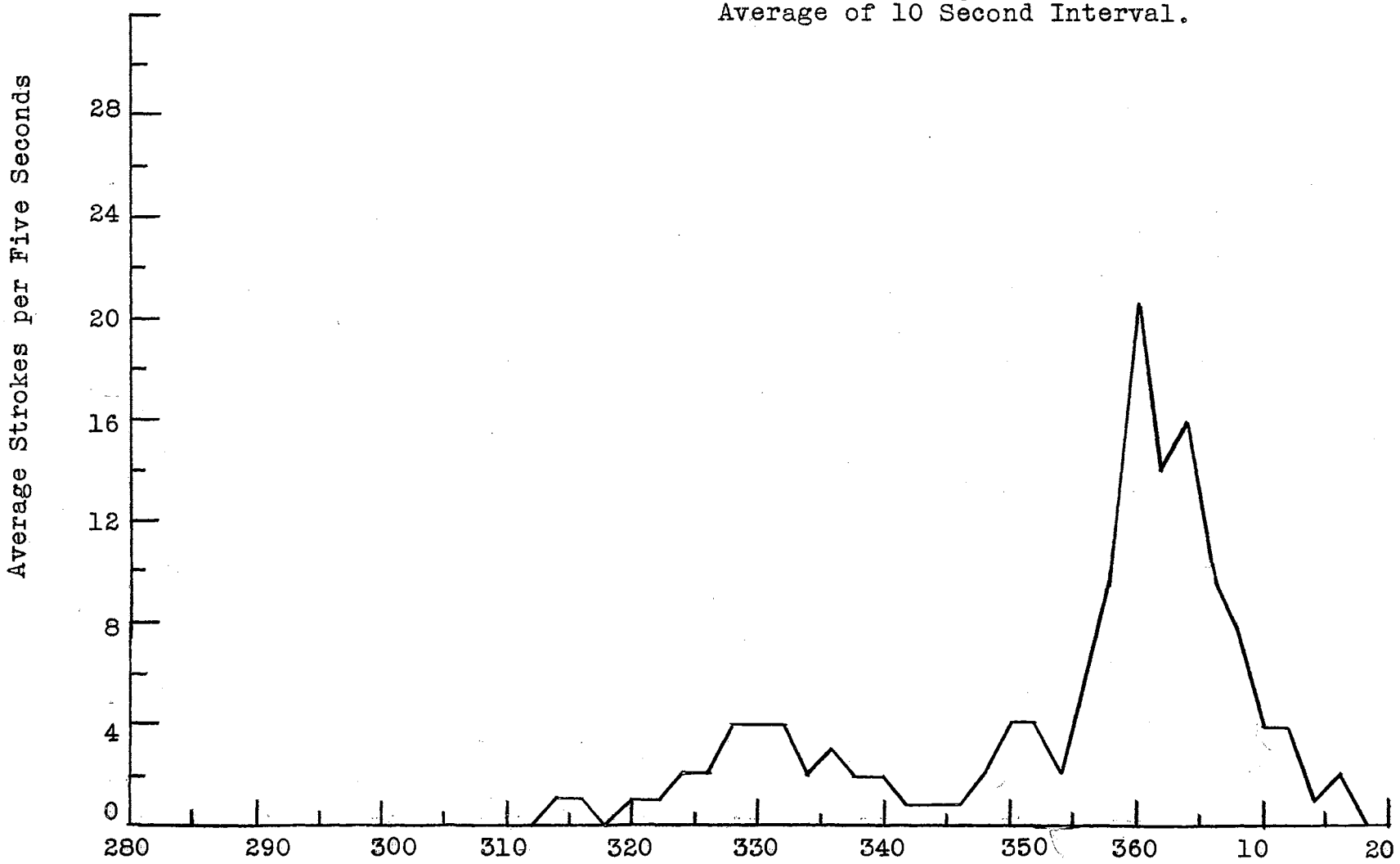

Figure 58

Azimuth Incidence Distribution of Sferic Activity Sampled by High Frequency Direction Finder 25 May, 1955. Beginning with 2253 Hours, Average of 10 Second Interval.

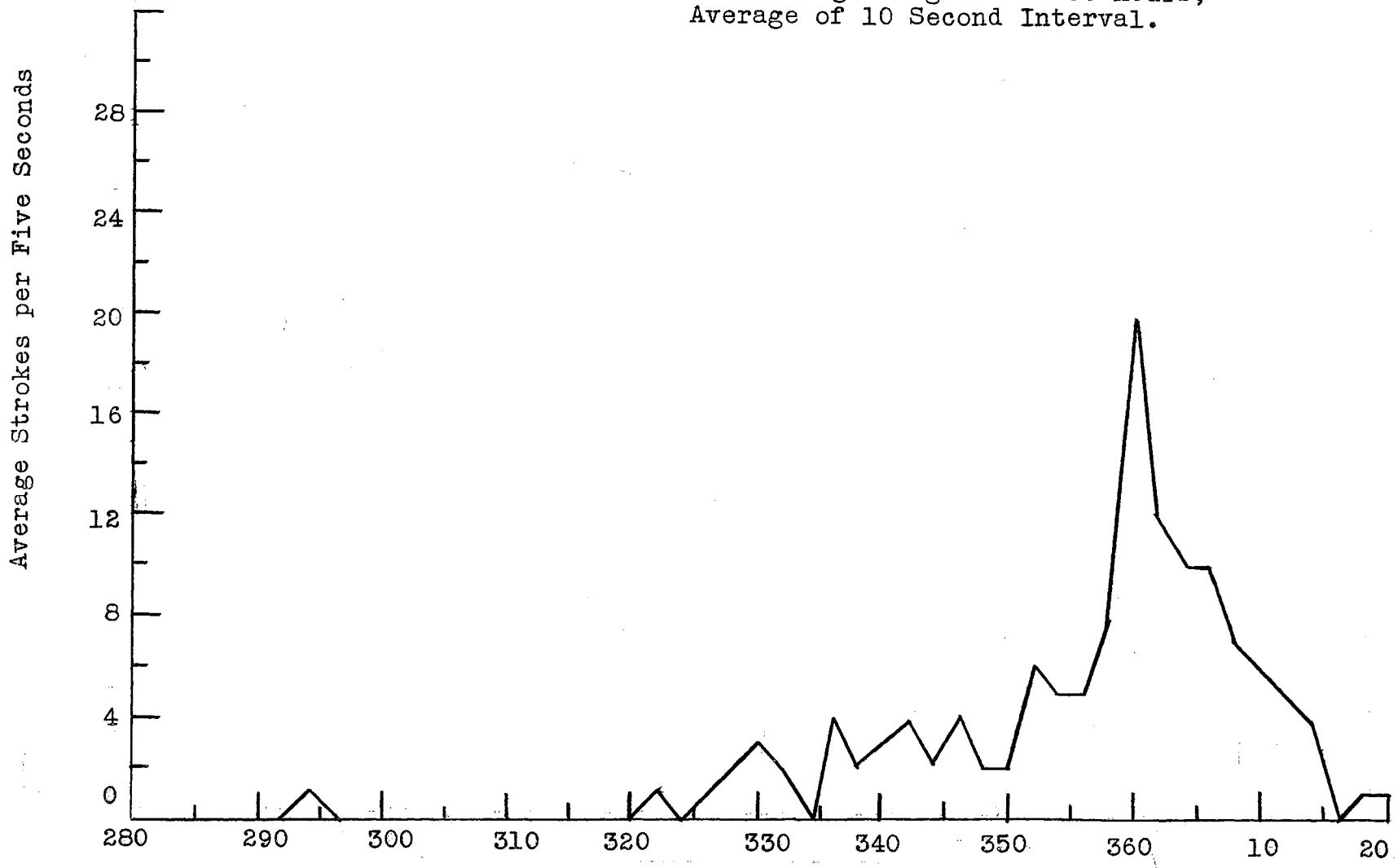

Figure 59

Azimuth Incidence Distribution of Sferic Activity Sampled by High Frequency Direction Finder 25 May, 1955. Beginning with 2258 Hours, Average of 10 Second Interval.

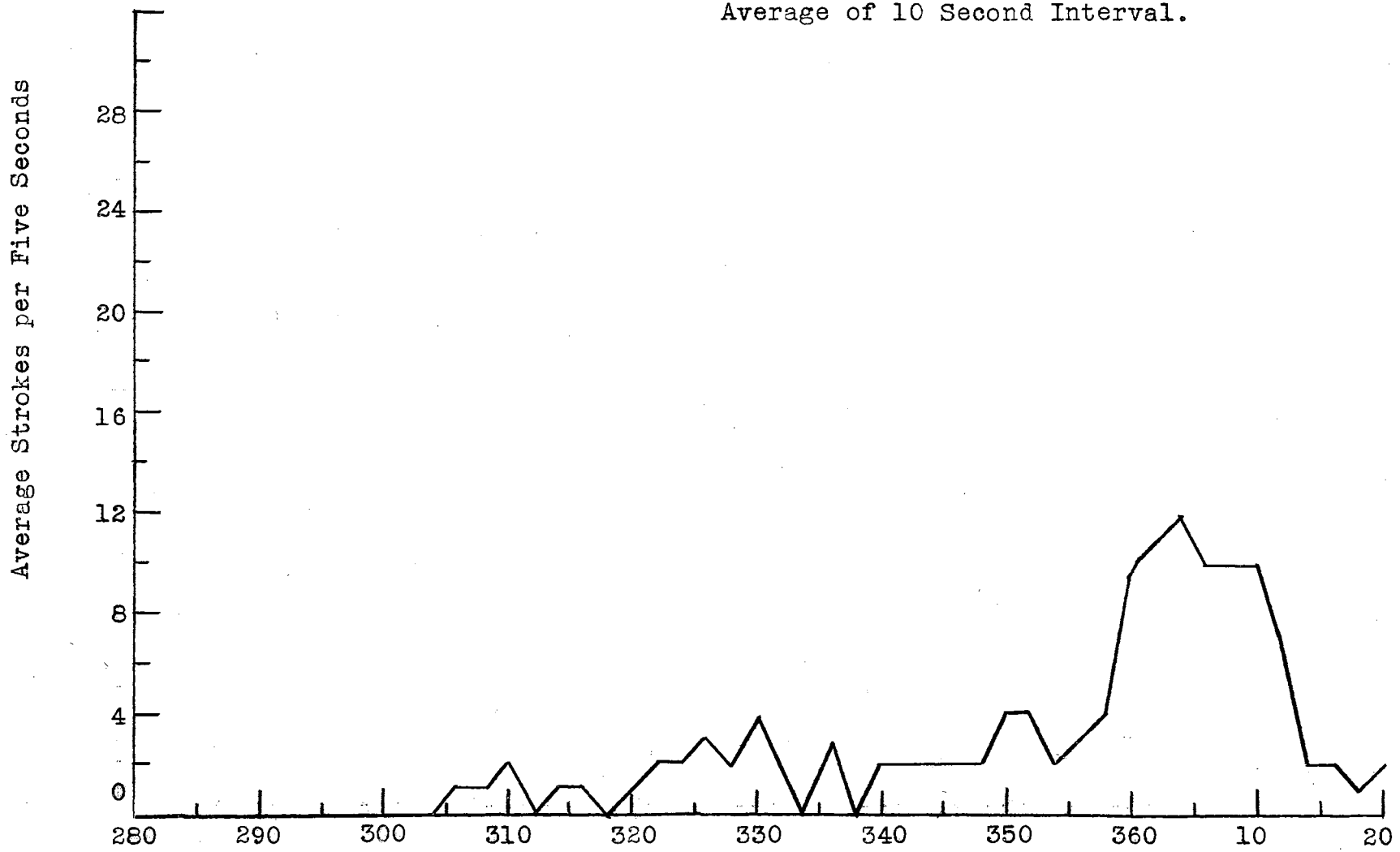

Figure 60

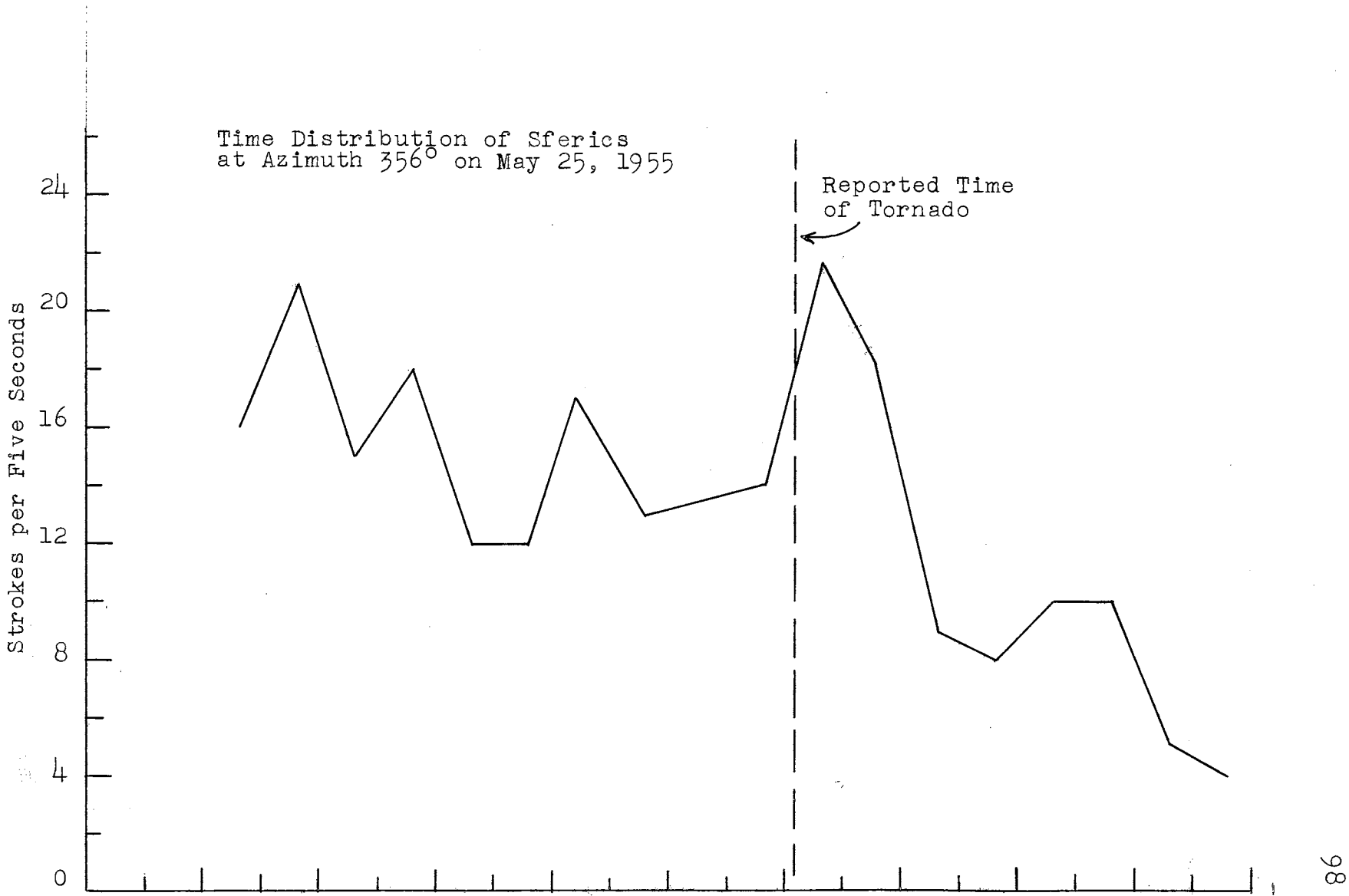
Time Distribution of Sferics
at Azimuth 356° on May 25, 1955
Reported Time
of Tornado
Strokes per Five Seconds
0
4
8
12
16
20
24
2130
2140
2150
2200
2210
2220
2230
2240
2250
2300
Time

Figure 61

sector in which the count was made. Figure 62 shows a similar time distribution of sferics for the azimuth of Udall. Results are essentially the same as in Figure 61 and for the same reason. There is a slightly pronounced peak at the time the tornado struck. The Udall tornado was out of radar range and no radar photographs are available for study.

Conclusions

From the data described here it may be concluded that the Blackwell and Udall tornadoes were typical of those that develop in the Great Plains region. The Blackwell tornado had a maximum sferics count of 24 strokes per second which is consistant with previous observations. Although the maximum sferics count of the Udall tornado was somewhat lower, the trend of the data was much the same as before. The change in gain of the Direction Finder could completely account for the lower count of the Udall tornado. The radar screen photographs of the Blackwell tornado are quite spectacular and worthy of further study. The Blackwell and Udall tornadoes presented an opportunity for the first real test of the High Frequency Direction Finder and it may be concluded the equipment performed quite satisfactorily.

The results from these tornadoes indicate that the radar-sferics method of tornado tracking and identifi-

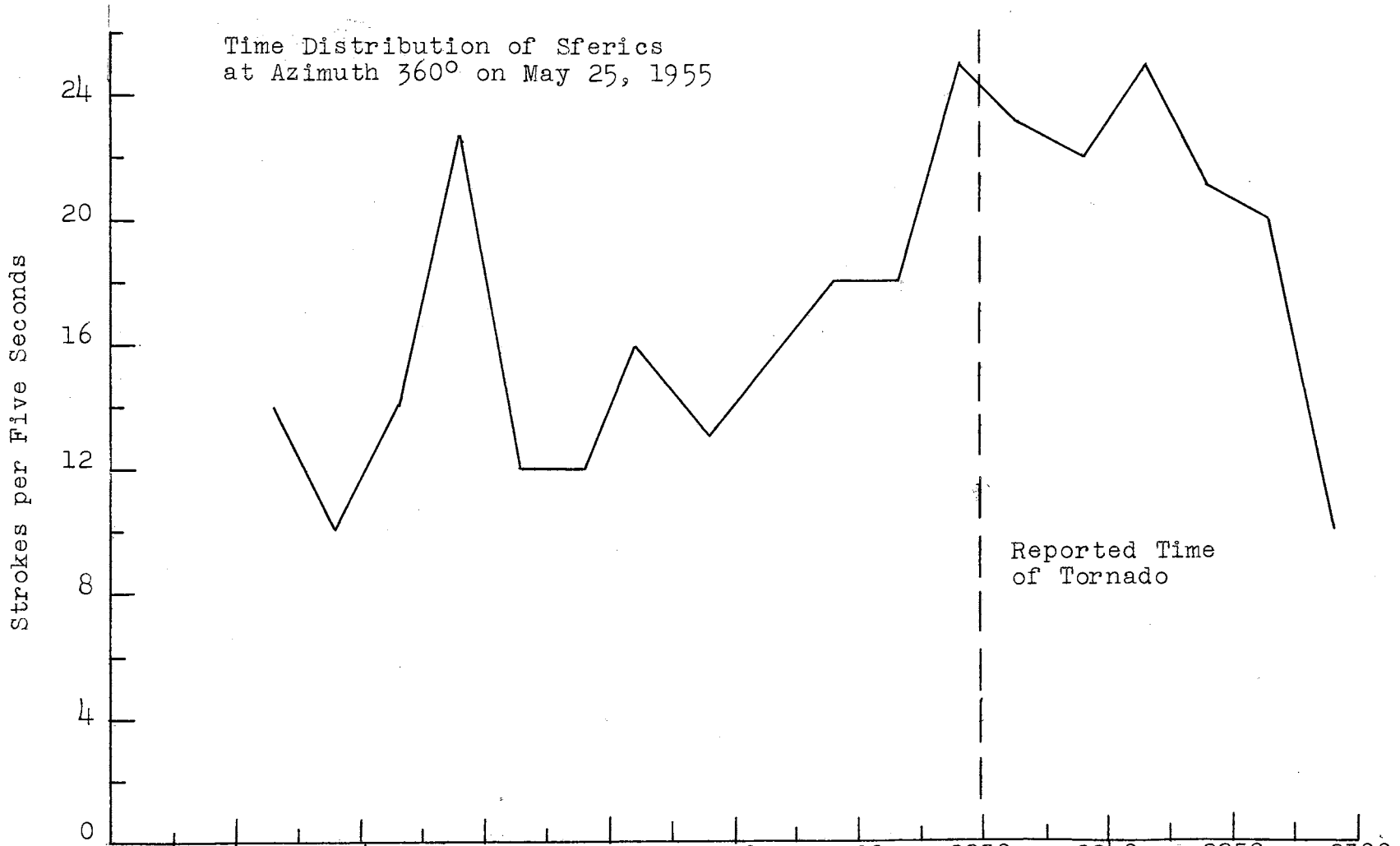
Time Distribution of Sferics
at Azimuth 360° on May 25, 1955
Strokes per Five Seconds
0
4
8
12
16
20
24
2130
2140
2150
2200
2210
2220
2230
2240
2250
2300
Time
Reported Time
of Tornado

Figure 62

cation is quite feasible. Differences between the actual paths of the tornadoes as determined by physical evidence and the paths of the tornadoes as determined by the radar-sferics method can be neglected in practical applications.

CHAPTER V

RESULTS FROM THE STORM OF MAY 27, 1955

Meteorological Conditions Associated with the Storm of May 27, 1955

During the late afternoon of May 27, a squall line developed along a front of Pacific air which was advancing rapidly to the east through Nebraska and Kansas[1]. By 1830 CST, a closed circulation was evident at the surface around the northern tip of the front in east-central Nebraska. The front extended from this area southwestward through central Kansas across the eastern edge of the Oklahoma Panhandle, the northern tip of the Texas Panhandle, and then almost due west across central New Mexico, Arizona, southern California and into a low center near latitude 45° N longitude 140° E in the northwest Pacific.

This front succeeded the front that moved through the area two days earlier and which was associated with the Blackwell and Udall tornadoes of May 25. On May 27, however, all of the thunderstorms that were observed on the radar were confined to the squall line. During its exist-

---

[1] "Research on Tornado Identification", Second Quarterly Progress Report, Signal Corps Research, Project No. 172B, (1955) p. 12.

ence, the line was apparently coincident with the surface position of the advancing front. Two severe thunderstorms and a number of medium and light thunderstorms formed along the squall line. The severe thunderstorms were easily identified by observing the indicator of the High Frequency Direction Finder. Three funnels were reported as sighted just east of Ponca City but the existence of a real tornado is doubtful, at least, according to the relatively slight damage in the area.

This squall line and the storm centers associated with it were plotted by using the radar to locate the squall line and the High Frequency Direction Finder to determine the position of the major storm centers.

Analysis of the Data

During the storm of May 27, 1955 the sferics received with the High Frequency Direction Finder were recorded on film and later analyzed to obtain the sferics count. From 2142 CST to 2347 CST, these analyses were made for periods of five seconds at approximately five-minute intervals. The average number of directional pips per second for each of the five-second periods was calculated for each two degree interval over the azimuth range that encompassed the active squall line. The results of these calculations are shown in Figures 63 to 89 inclusive.

The information presented in these graphs may be re-

Azimuth Incidence Distribution of Sferic Activity Sampled by High Frequency Direction Finder, 27 May, 1955. Beginning with 2142 Hours, Average of 5 Second Interval.

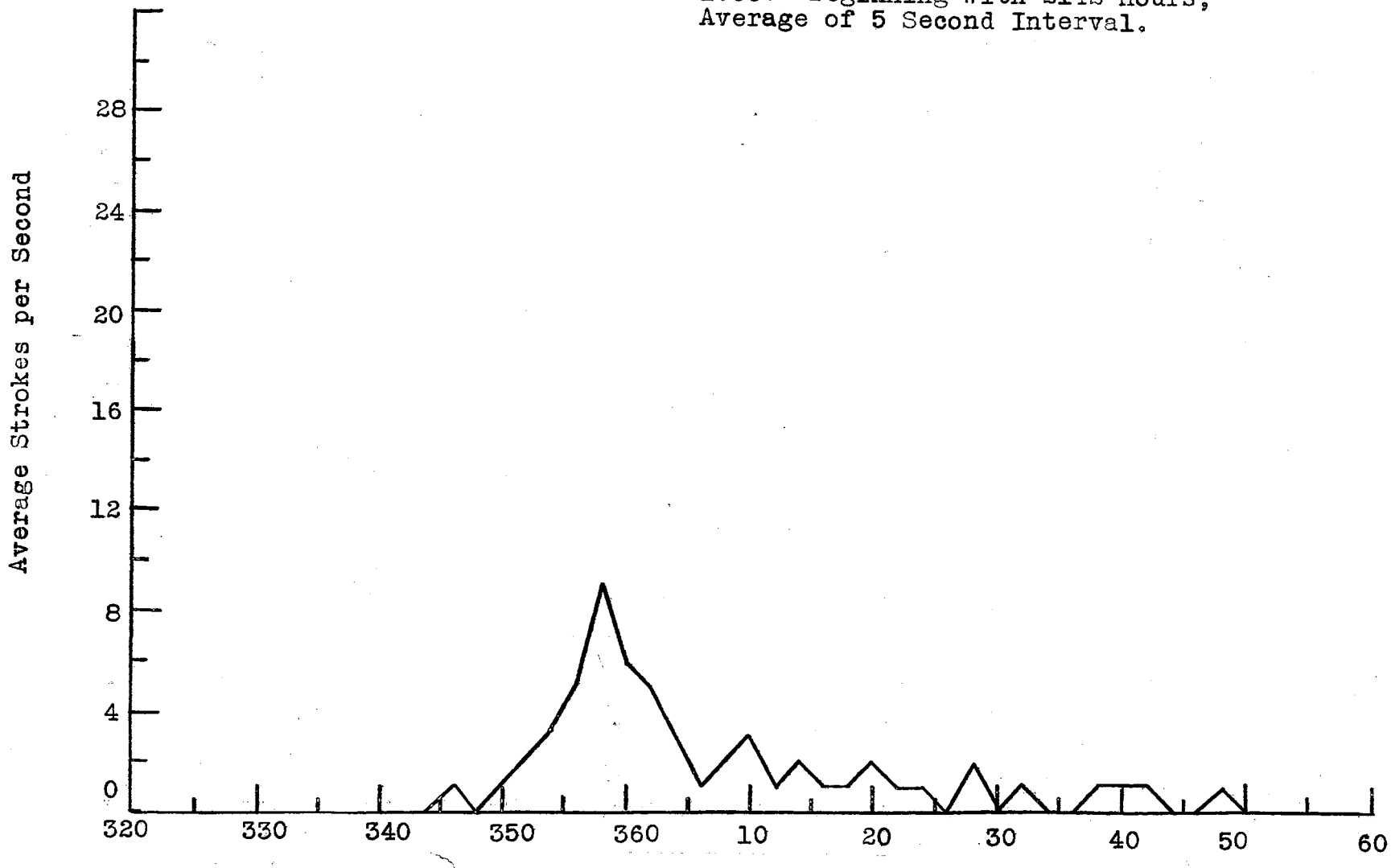

Figure 63

Azimuth Incidence Distribution of Sferic Activity Sampled by High Frequency Direction Finder, 27 May, 1955. Beginning with 2153 Hours, Average of 5 Second Interval.

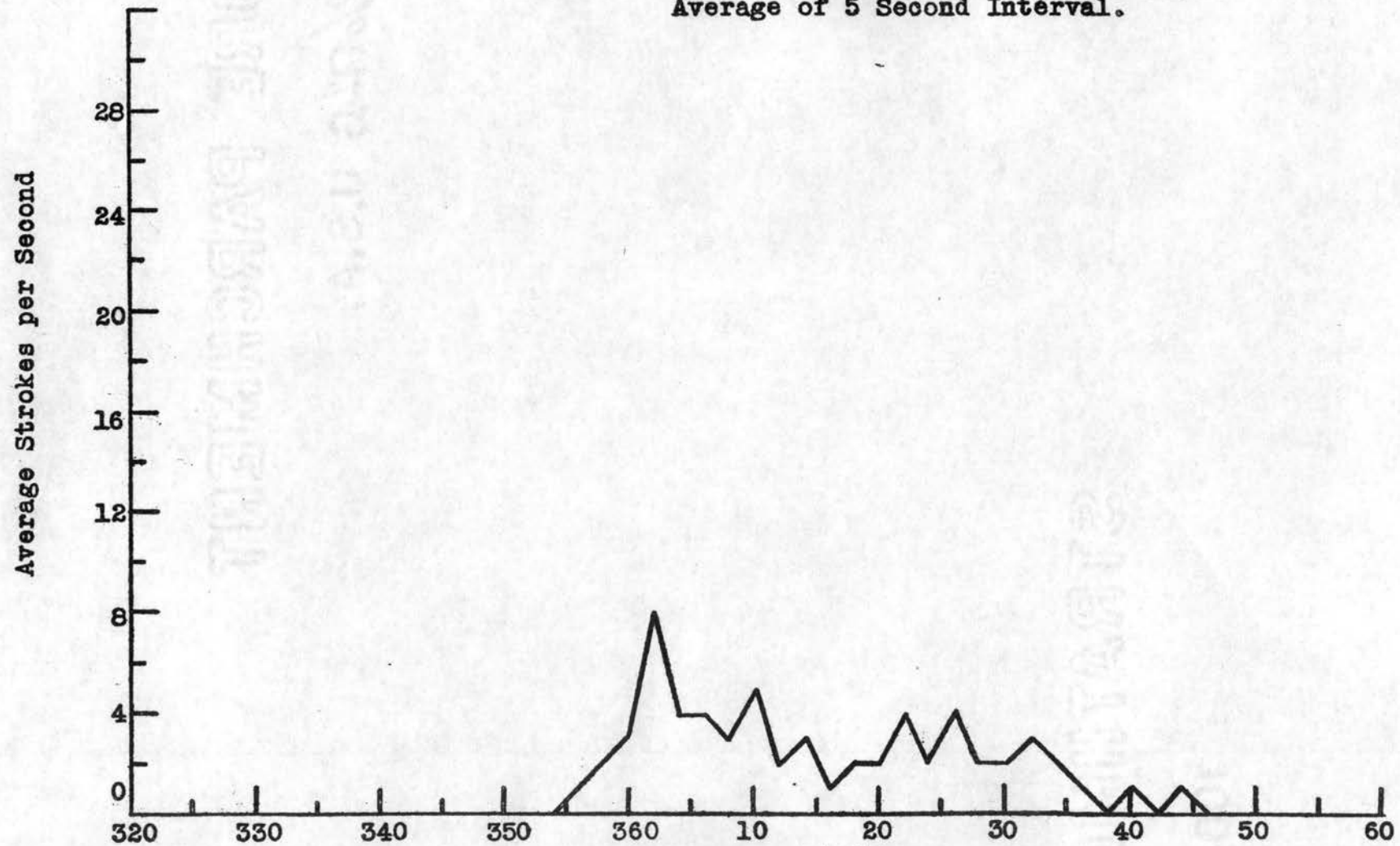

Figure 64

Azimuth Incidence Distribution of Sferic Activity Sampled by High Frequency Direction Finder, 27 May, 1955. Beginning with 2157 Hours, Average of 5 Second Interval.

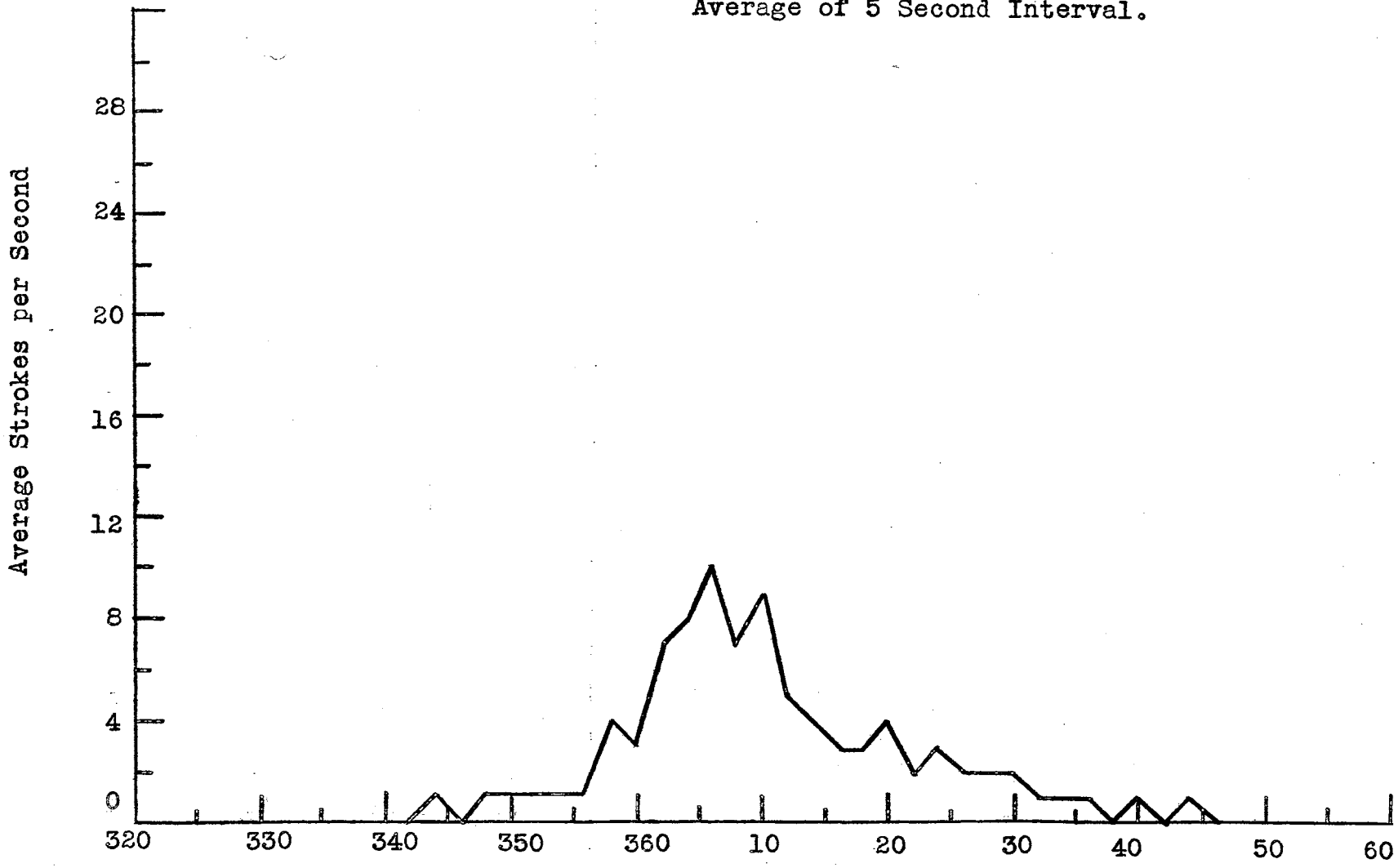

Figure 65

Azimuth Incidence Distribution of Sferic Activity Sampled by High Frequency Direction Finder, 27 May, 1955. Beginning with 2202 Hours, Average of 5 Second Interval.

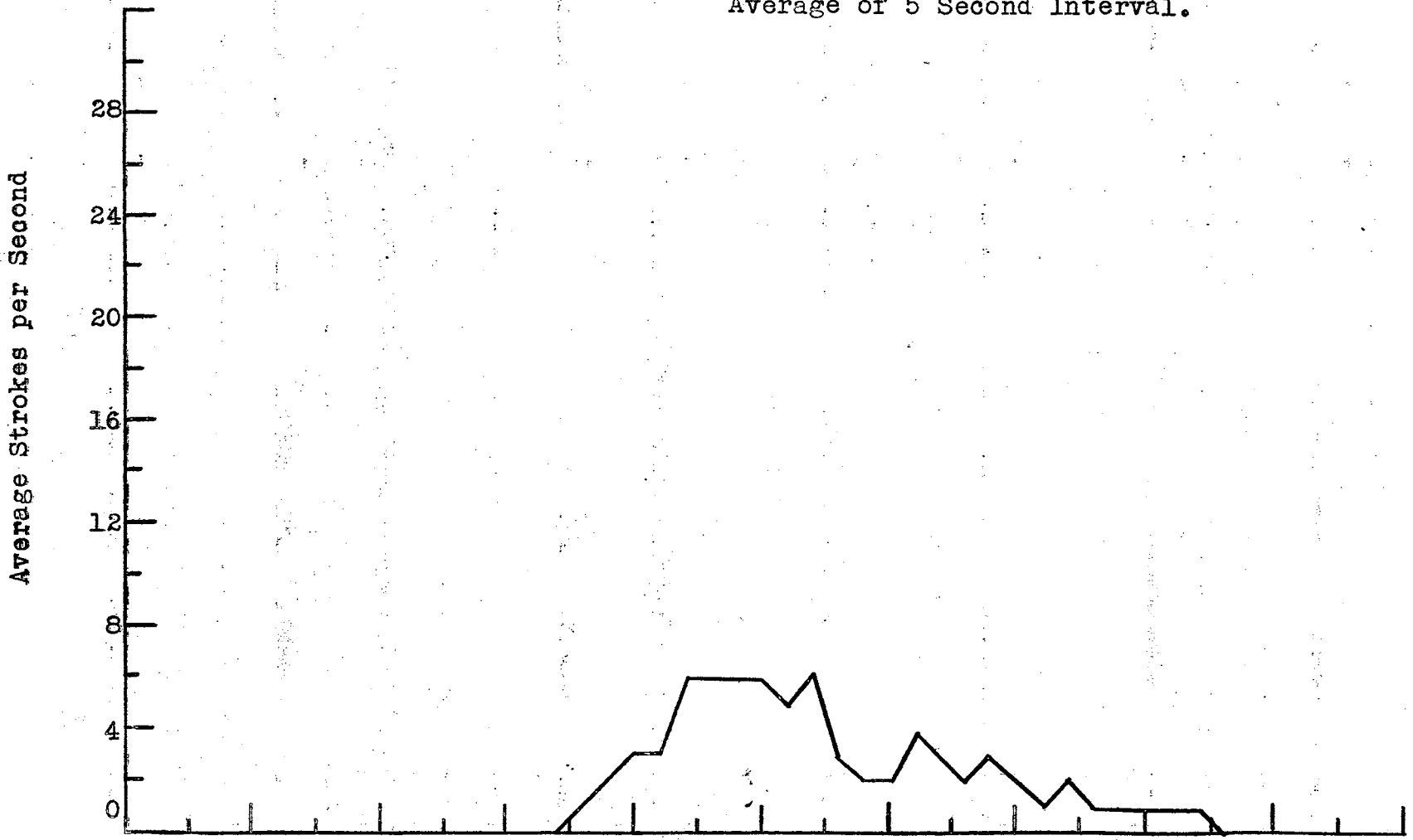

Figure 66

Azimuth Incidence Distribution of Sferic Activity Sampled by High Frequency Direction Finder, 27 May, 1955. Beginning with 2207 Hours, Average of 5 Second Interval.

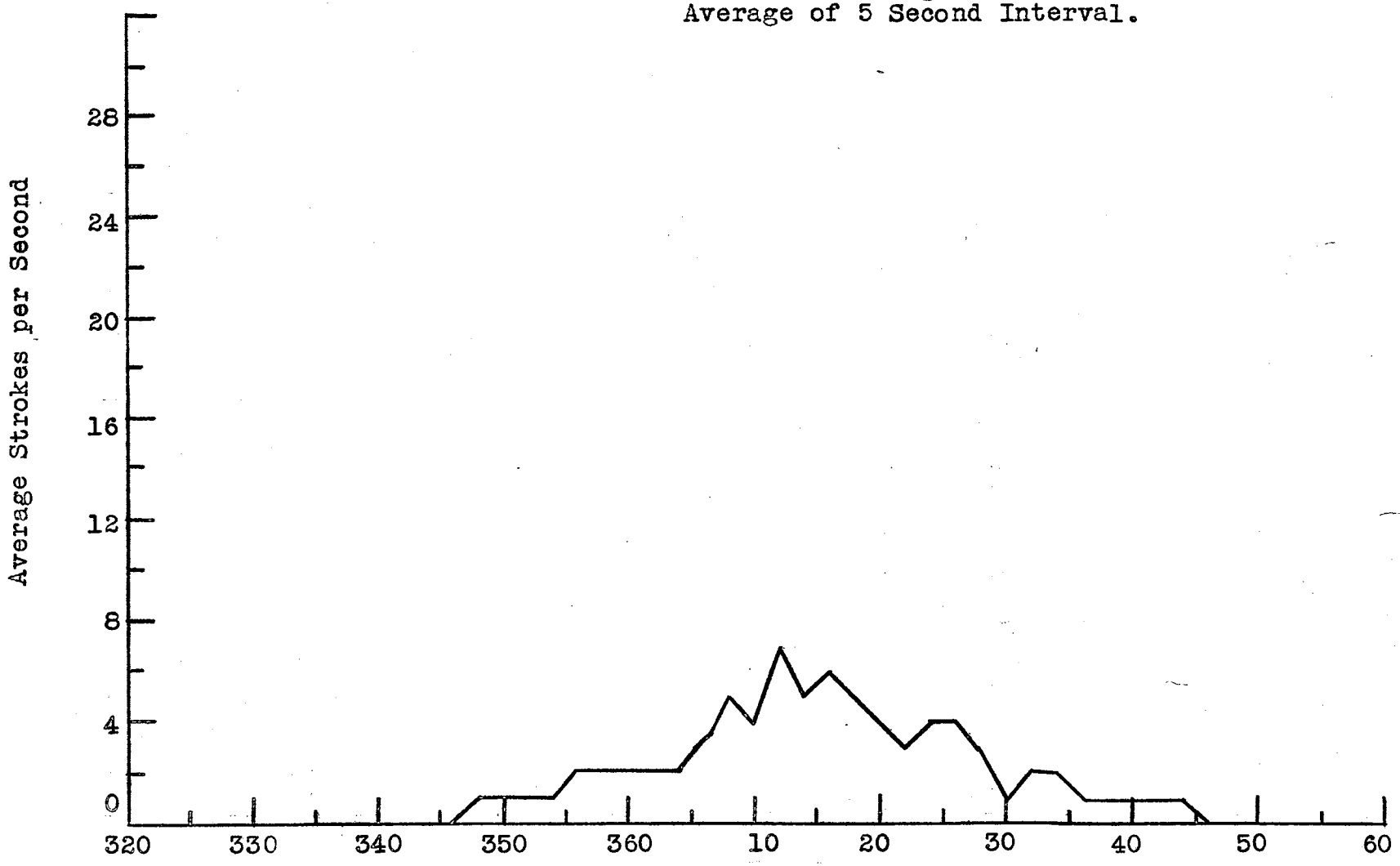

Figure 67

Azimuth Incidence Distribution of Sferic Activity Sampled by High Frequency Direction Finder, 27 May, 1955. Beginning with 2212 Hours, Average of 5 Second Interval.

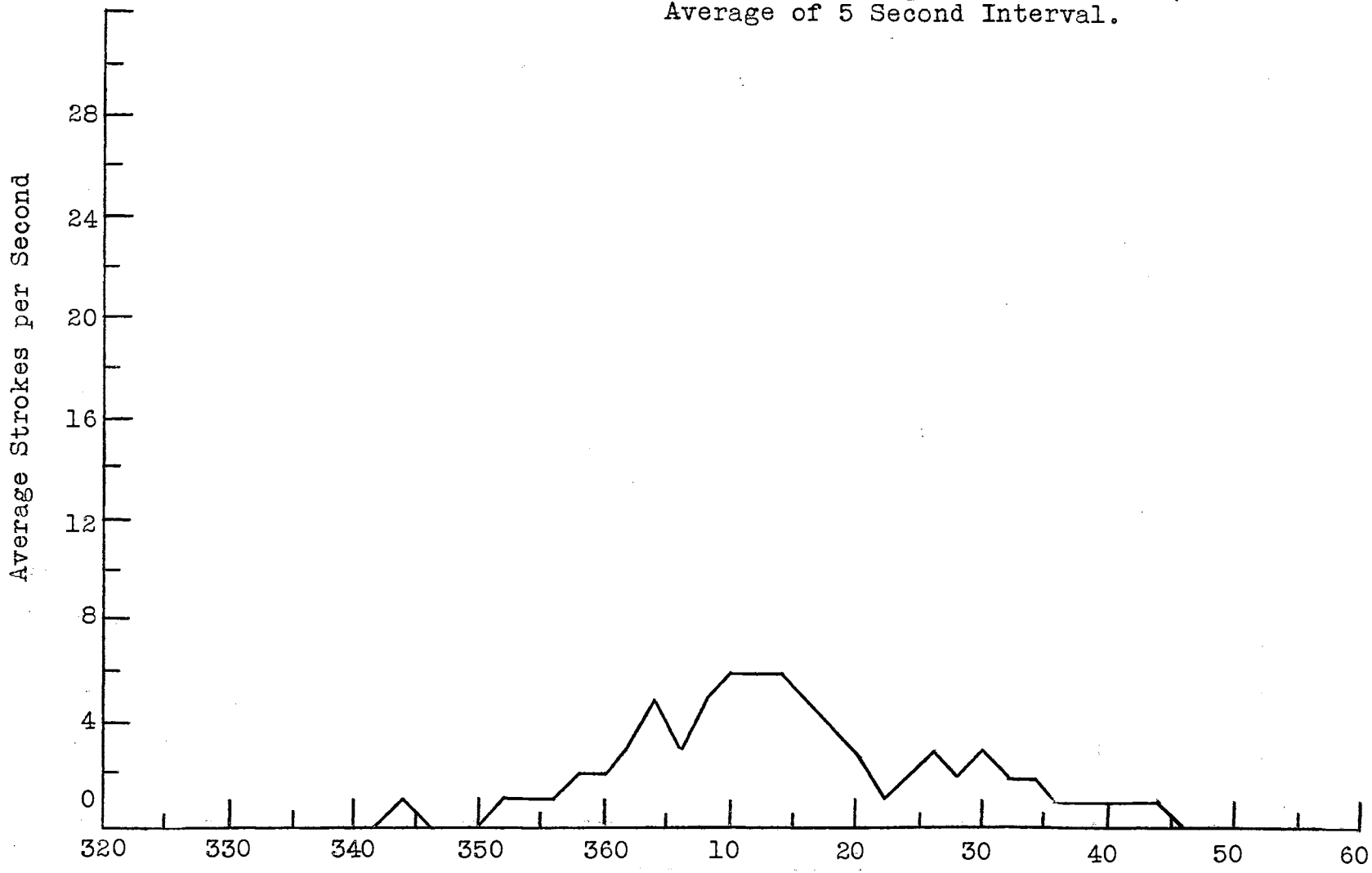

Figure 68

Azimuth Incidence Distribution of Sferic Activity Sampled by High Frequency Direction Finder, 27 May, 1955. Beginning with 2217 Hours, Average of 5 Second Interval.

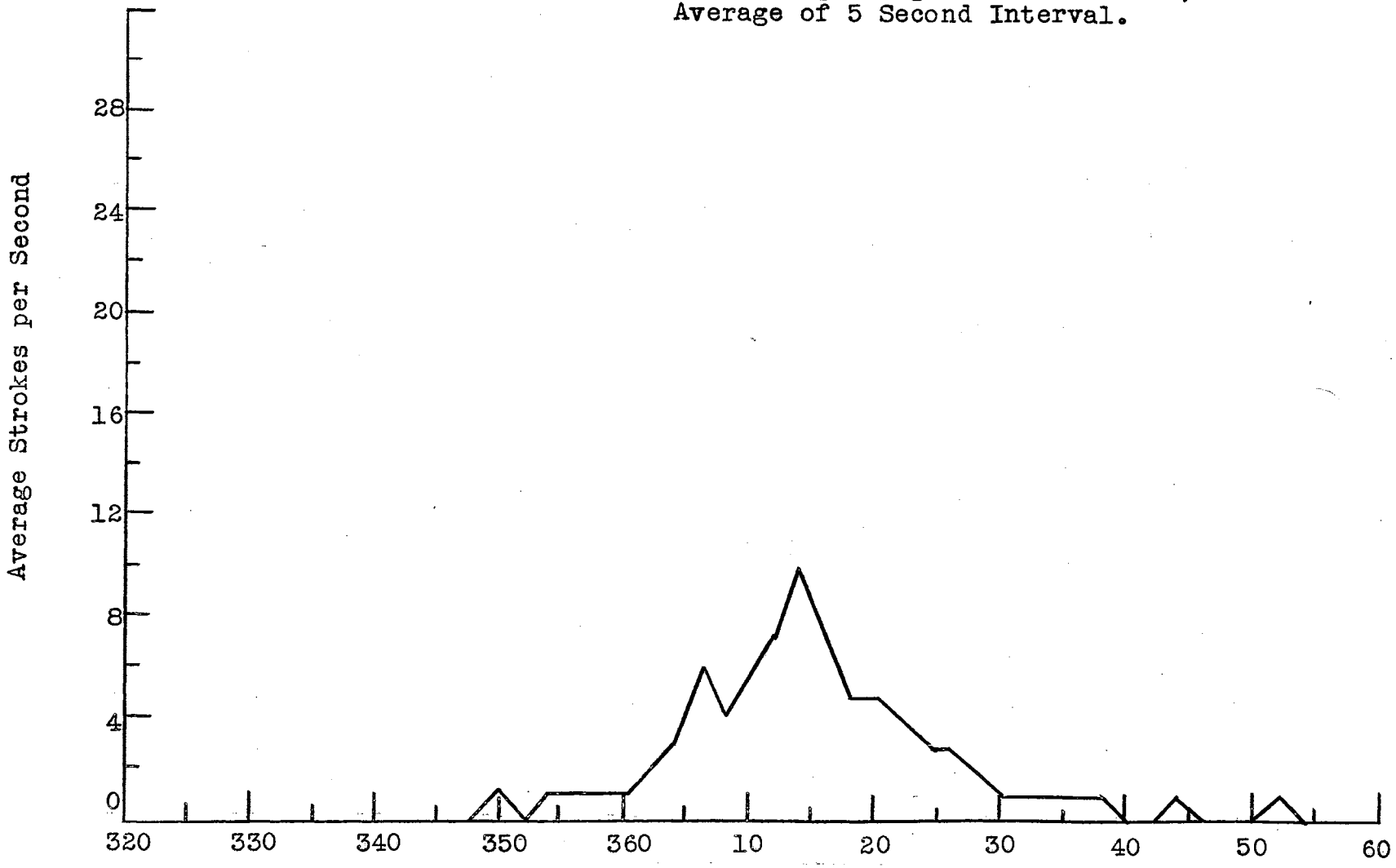

Figure 69

Azimuth Incidence Distribution of Sferic Activity Sampled by High Frequency Direction Finder, 27 May, 1955. Beginning with 2222 Hours, Average of 5 Second Interval.

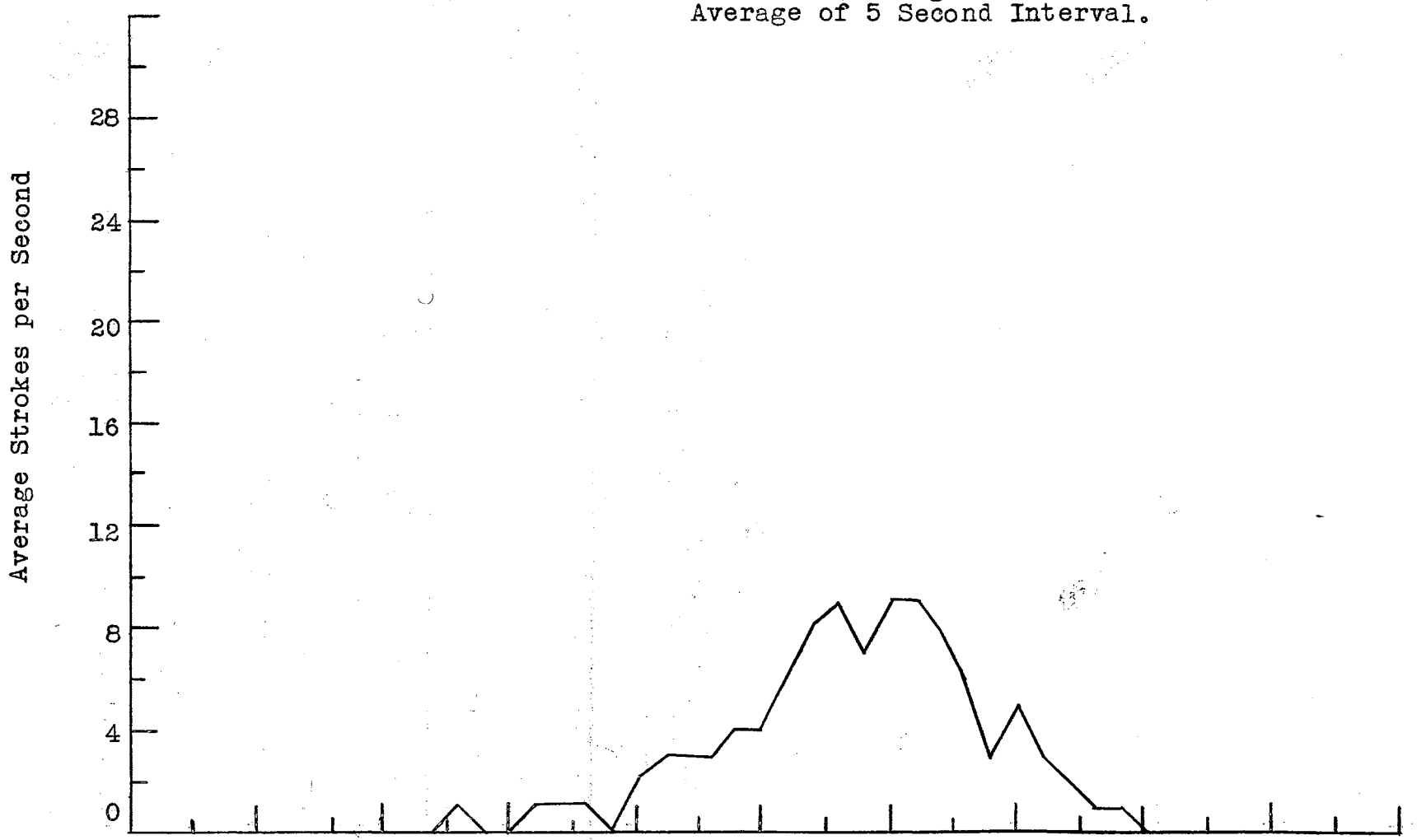

Figure 70

Azimuth Incidence Distribution of Sferic Activity Sampled by High Frequency Direction Finder, 27 May, 1955. Beginning with 2228 Hours, Average of 5 Second Interval.

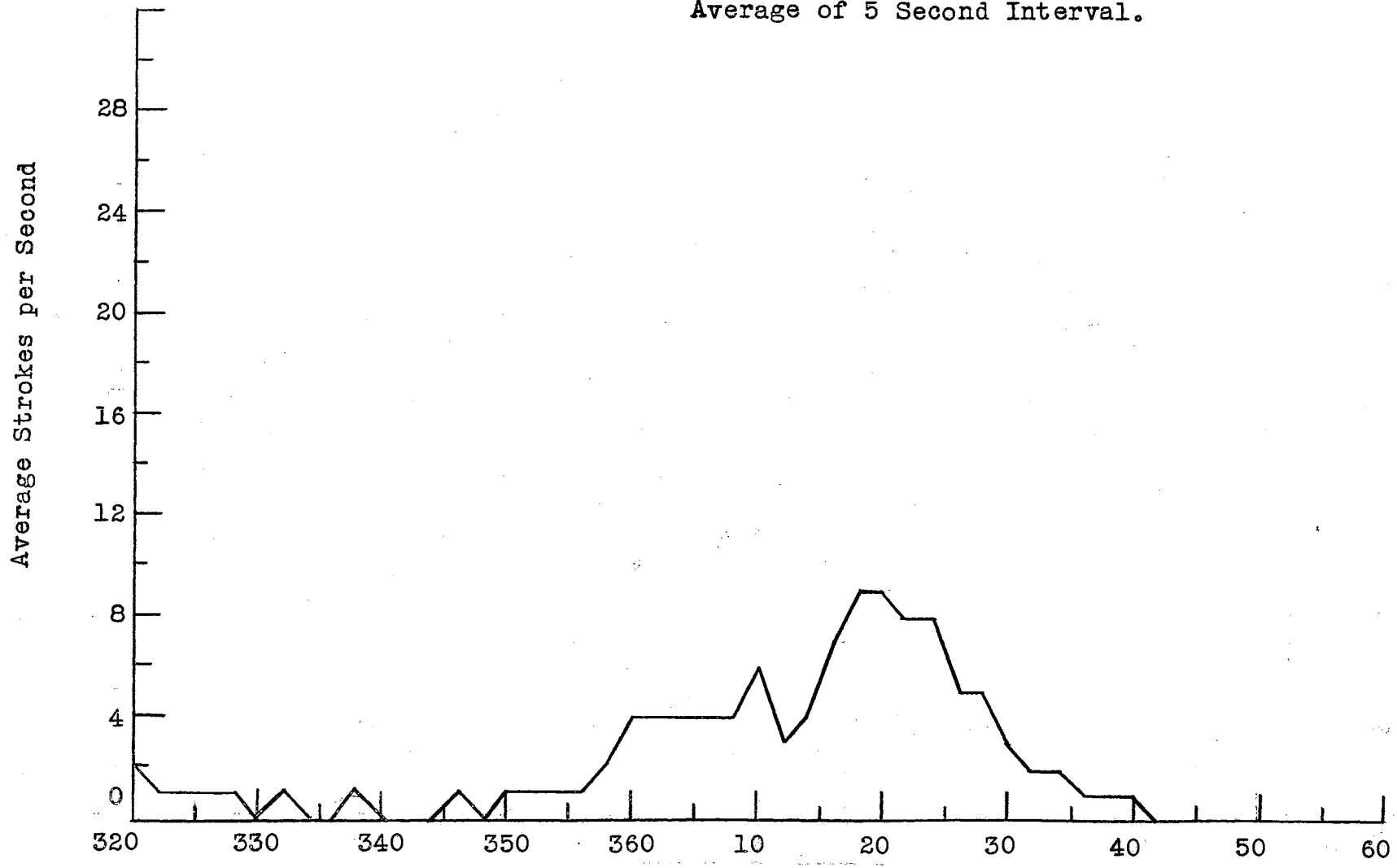

Figure 71

Azimuth Incidence Distribution of Sferic Activity Sampled by High Frequency Direction Finder, 27 May, 1955. Beginning with 2233 Hours, Average of 5 Second Interval.

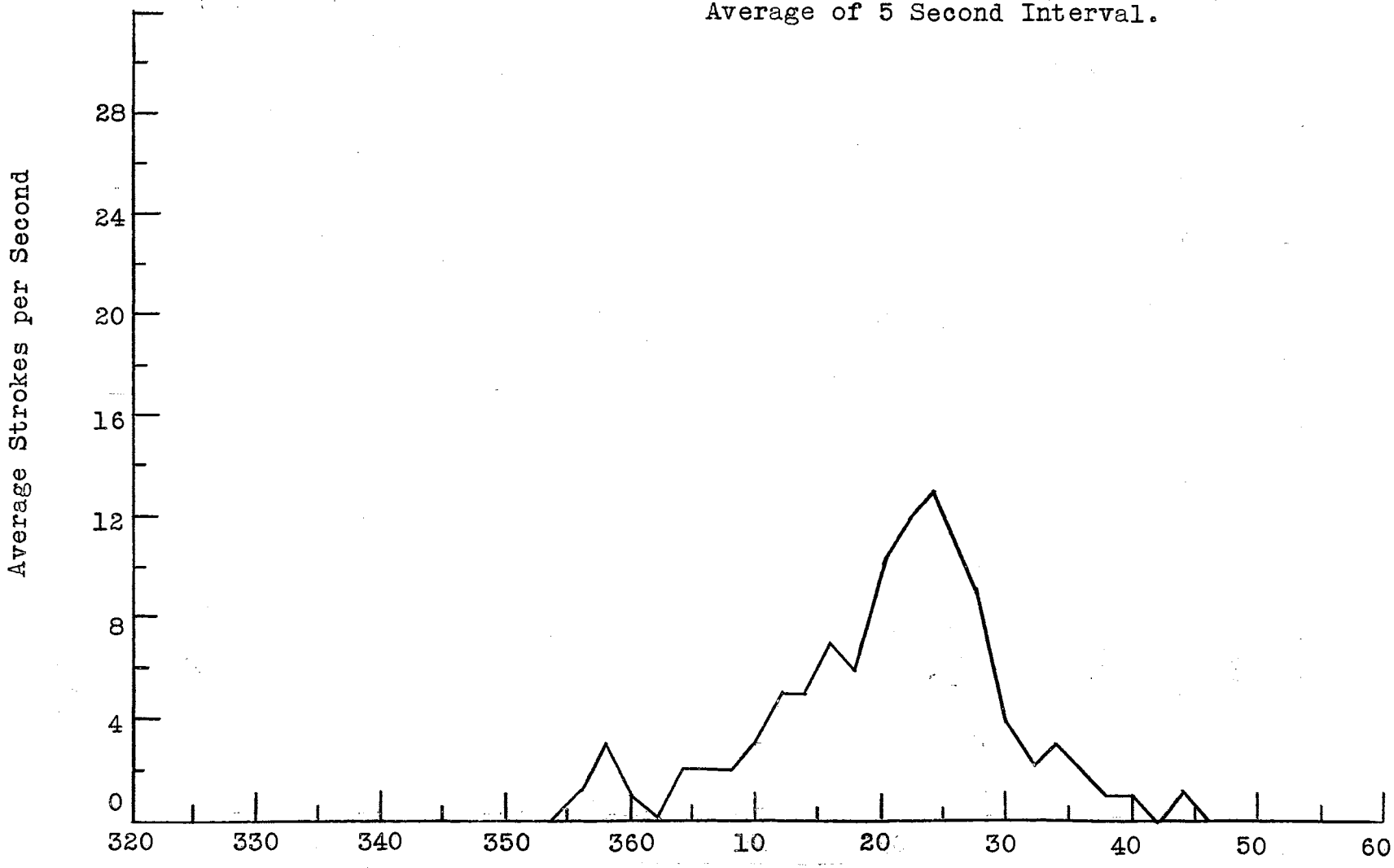

Figure 72

Azimuth Incidence Distribution of Sferic Activity Sampled by High Frequency Direction Finder, 27 May, 1955. Beginning with 2238 Hours, Average of 5 Second Interval.

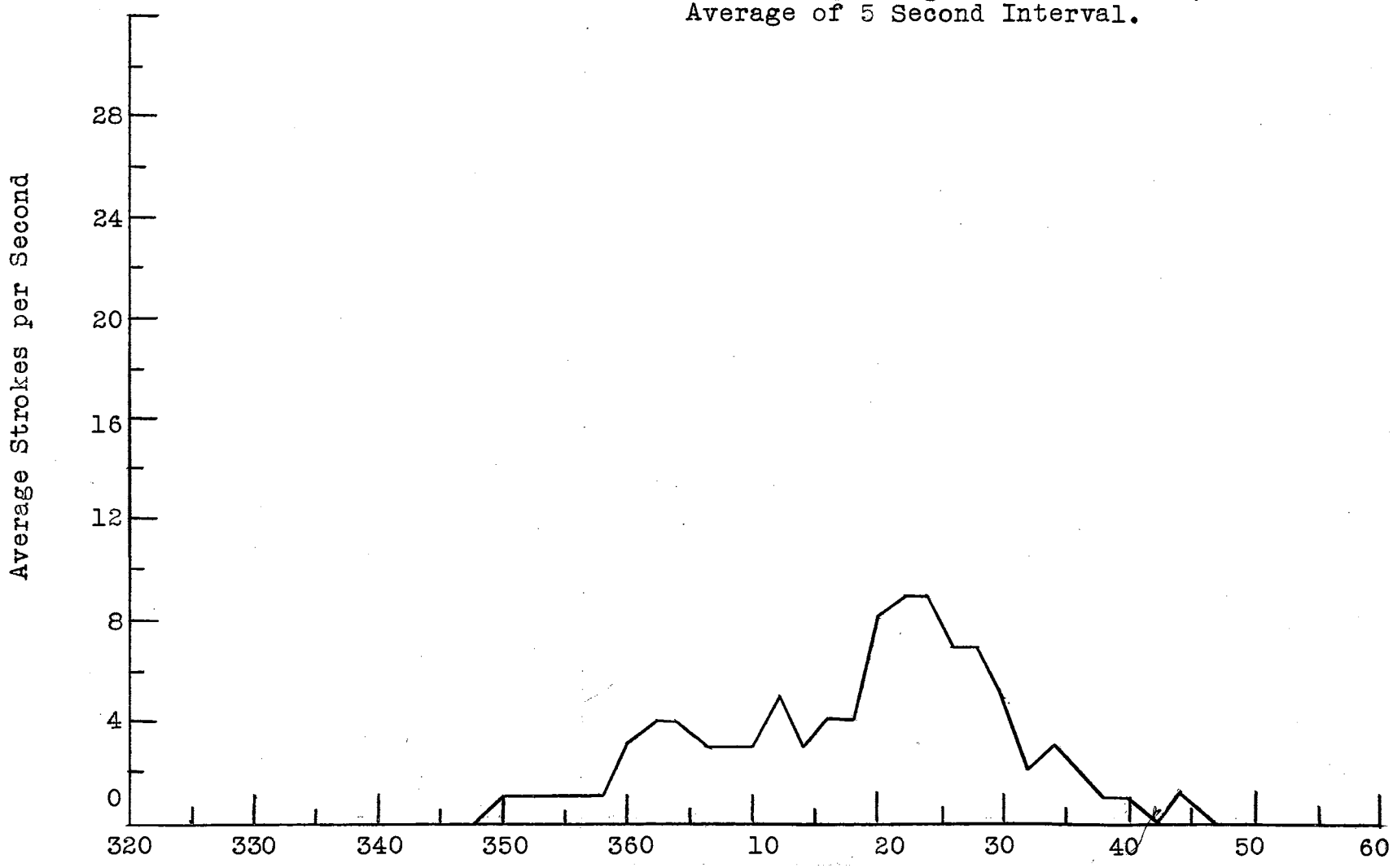

Figure 73

Azimuth Incidence Distribution of Sferic Activity Sampled by High Frequency Direction Finder, 27 May, 1955. Beginning with 2243 Hours, Average of 5 Second Interval.

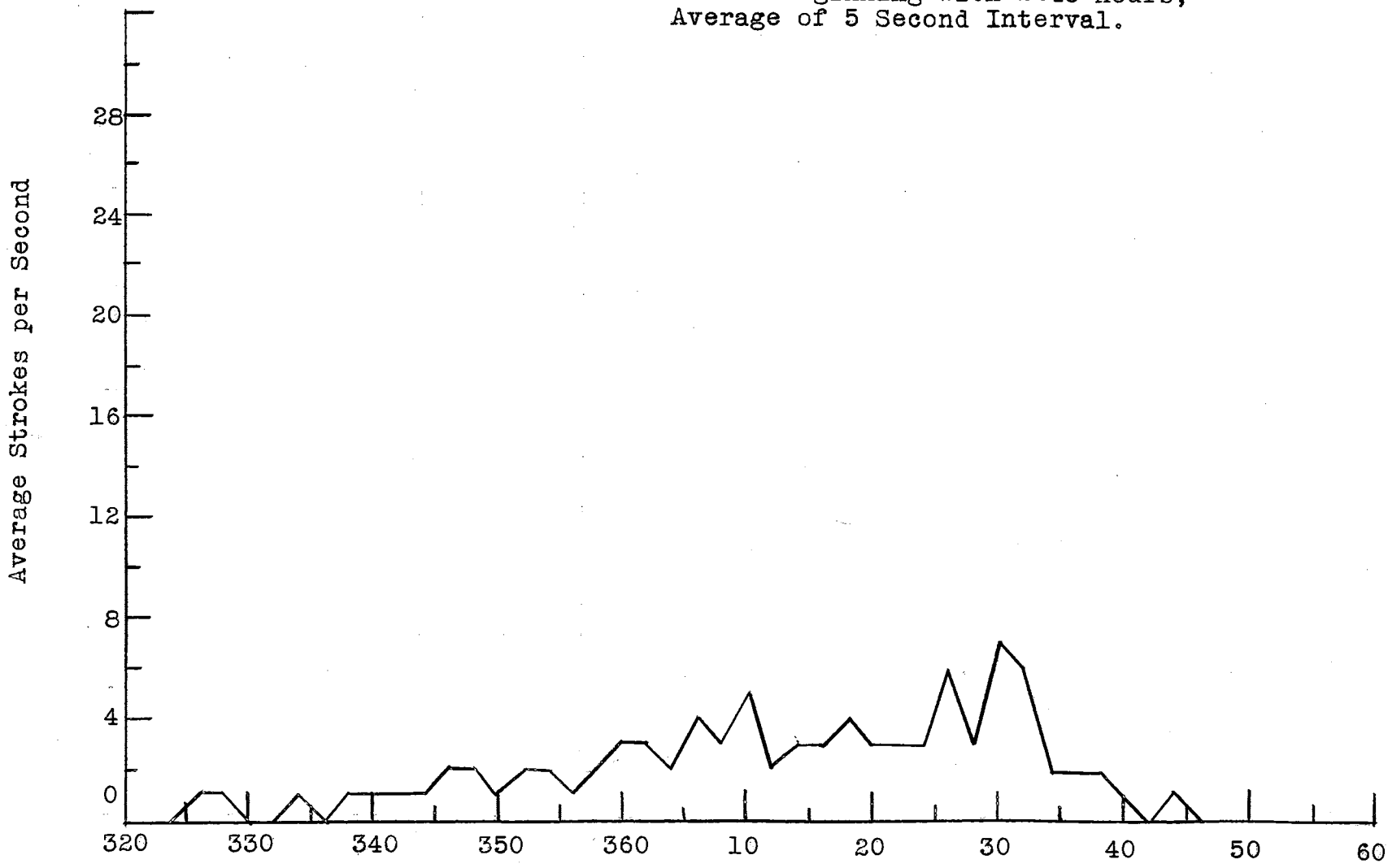

Figure 74

Azimuth Incidence Distribution of Sferic Activity Sampled by High Frequency Direction Finder, 27 May, 1955. Beginning with 2248 Hours, Average of 5 Second Interval.

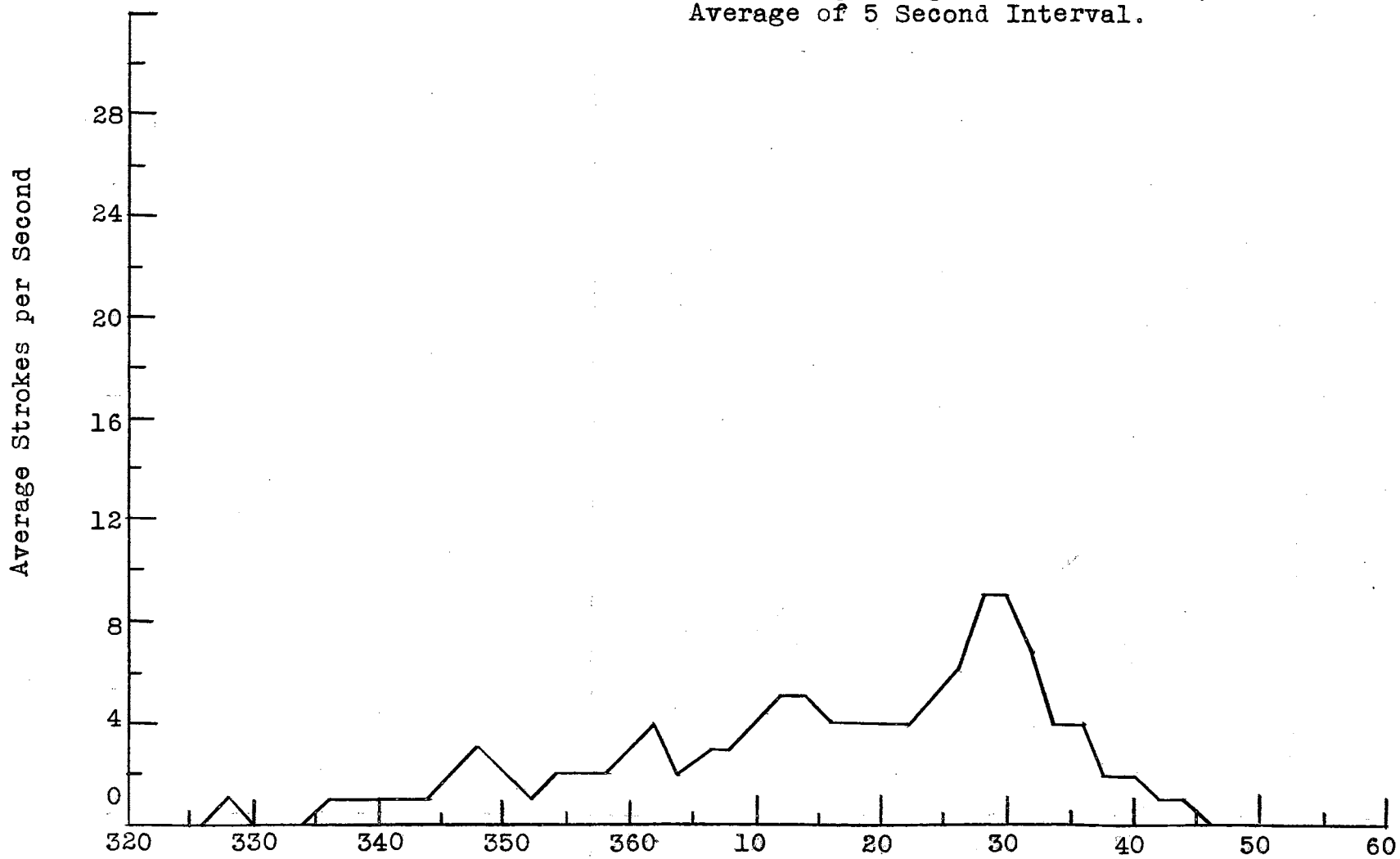

Figure 75

Azimuth Incidence Distribution of Sferic Activity Sampled by High Frequency Direction Finder, 27 May, 1955. Beginning with 2253 Hours, Average of 5 Second Interval.

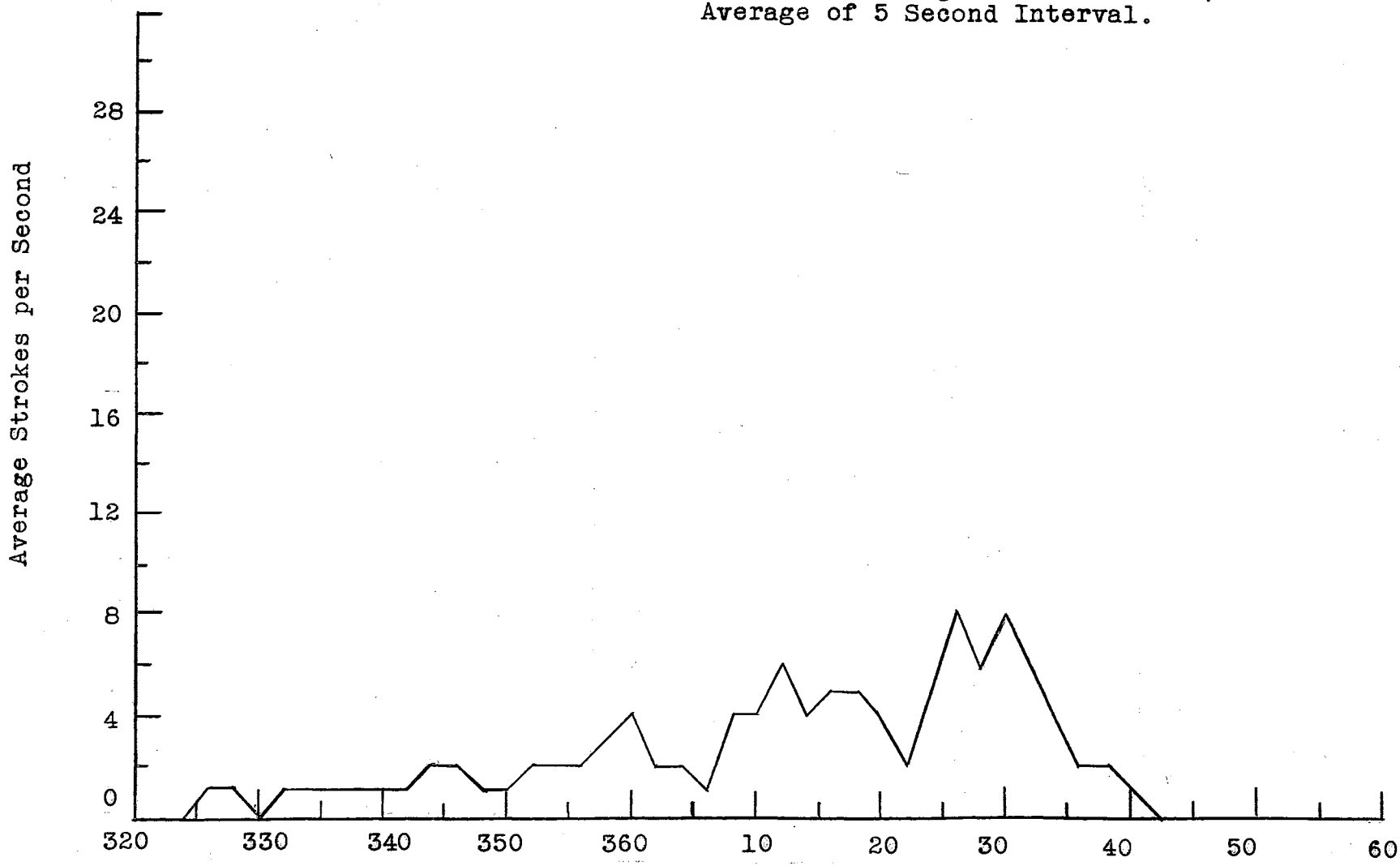

Figure 76

Azimuth Incidence Distribution of Sferic Activity Sampled by High Frequency Direction Finder 27 May, 1955. Beginning with 2257 Hours, Average of 5 Second Interval.

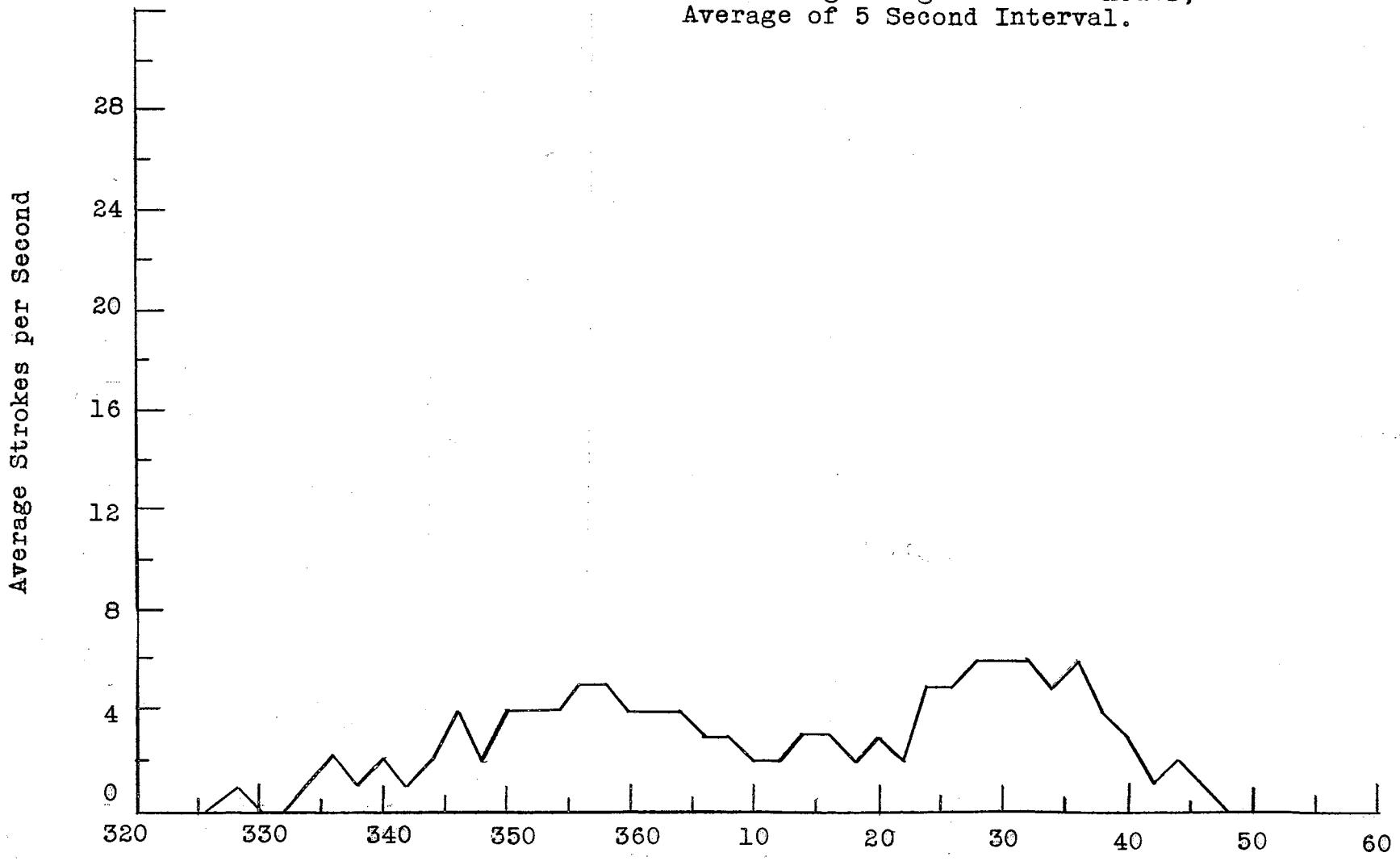

Figure 77

Azimuth Incidence Distribution of Sferic Activity Sampled by High Frequency Direction Finder, 27 May, 1955. Beginning with 2302 Hours, Average of 5 Second Interval.

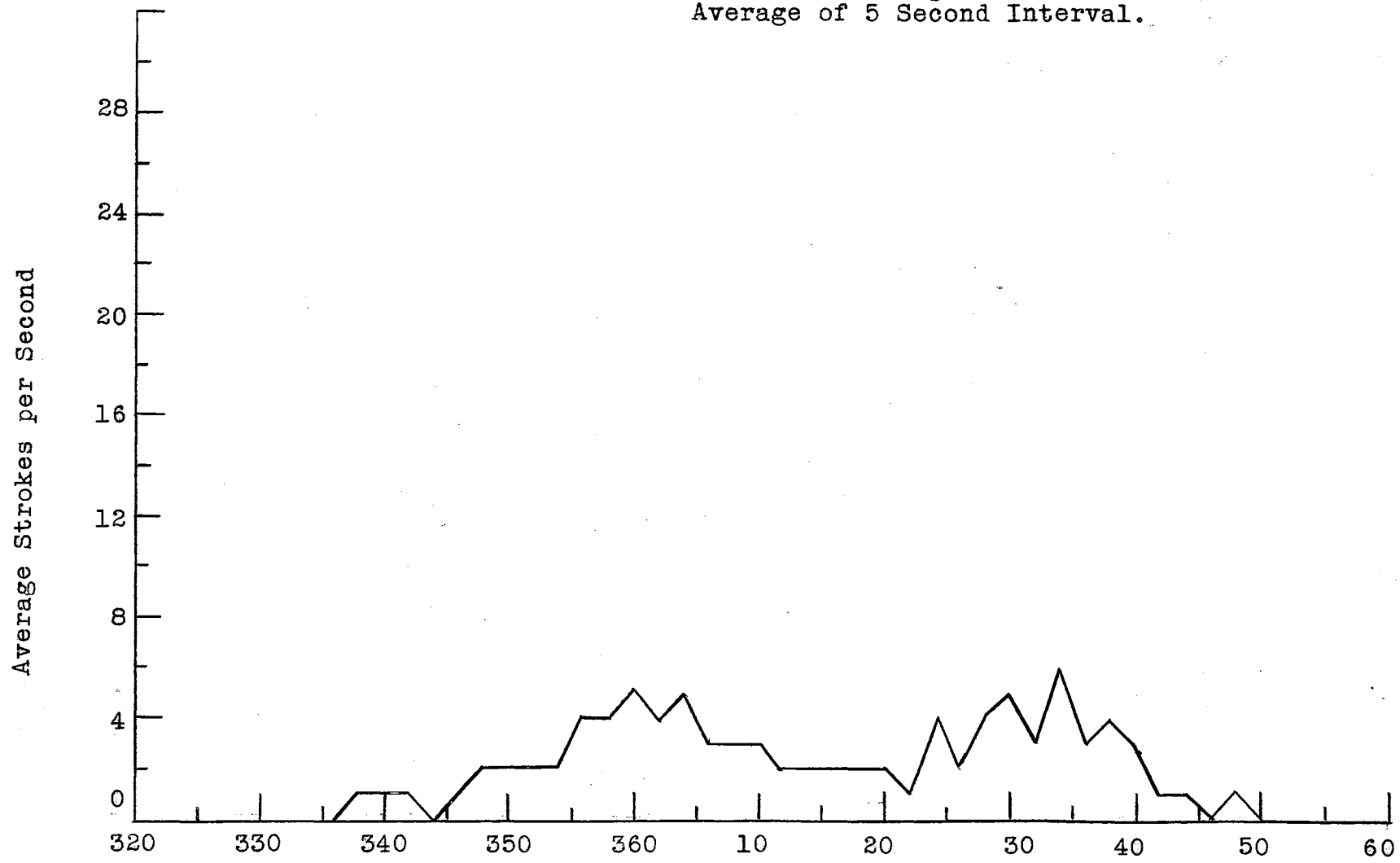

Figure 78

Azimuth Incidence Distribution of Sferic Activity Sampled by High Frequency Direction Finder, 27 May, 1955. Beginning with 2307 Hours, Average of 5 Second Interval.

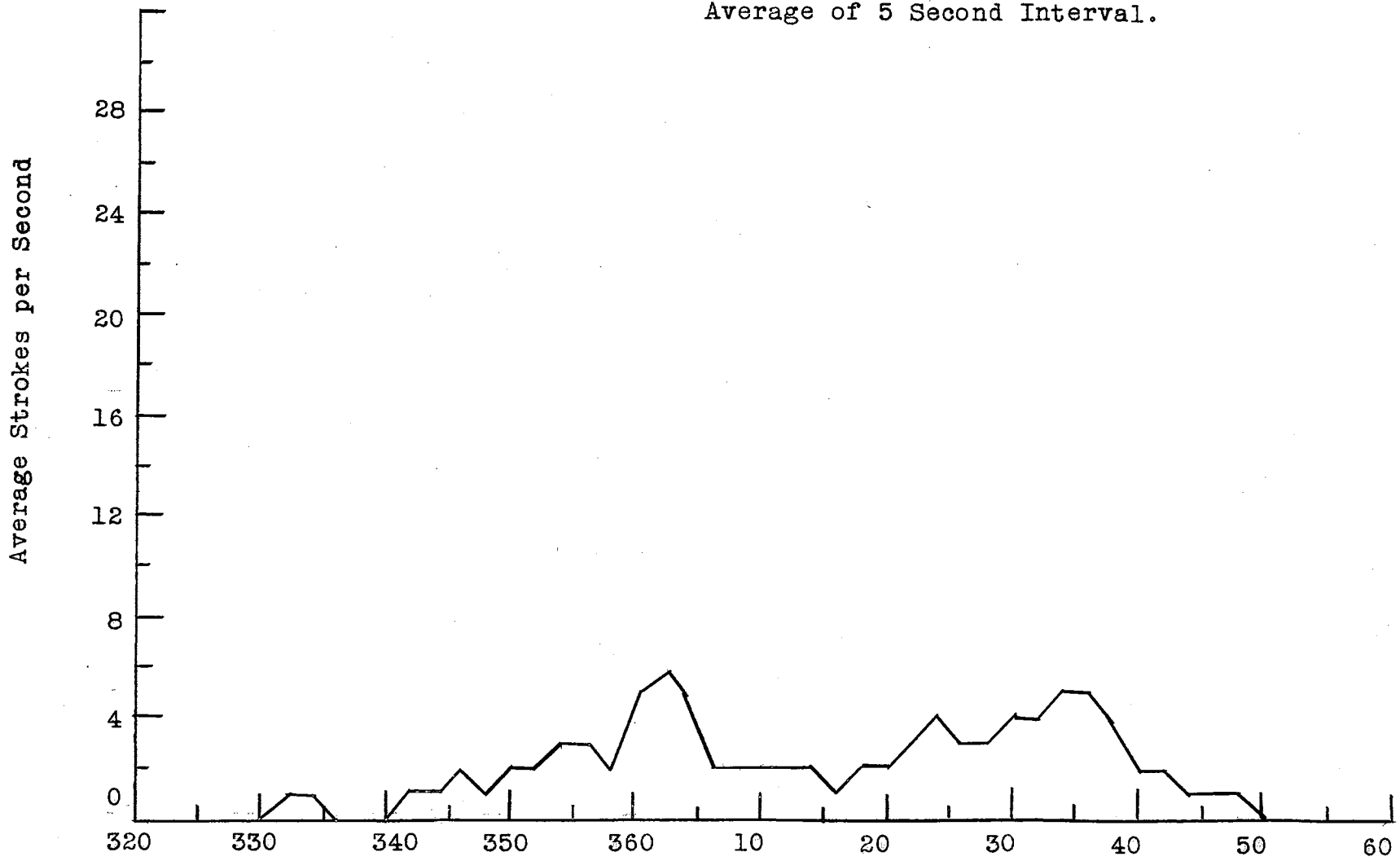

Figure 79

Azimuth Incidence Distribution of Sferic Activity Sampled by High Frequency Direction Finder, 27 May, 1955. Beginning with 2312 Hours, Average of 5 Second Interval.

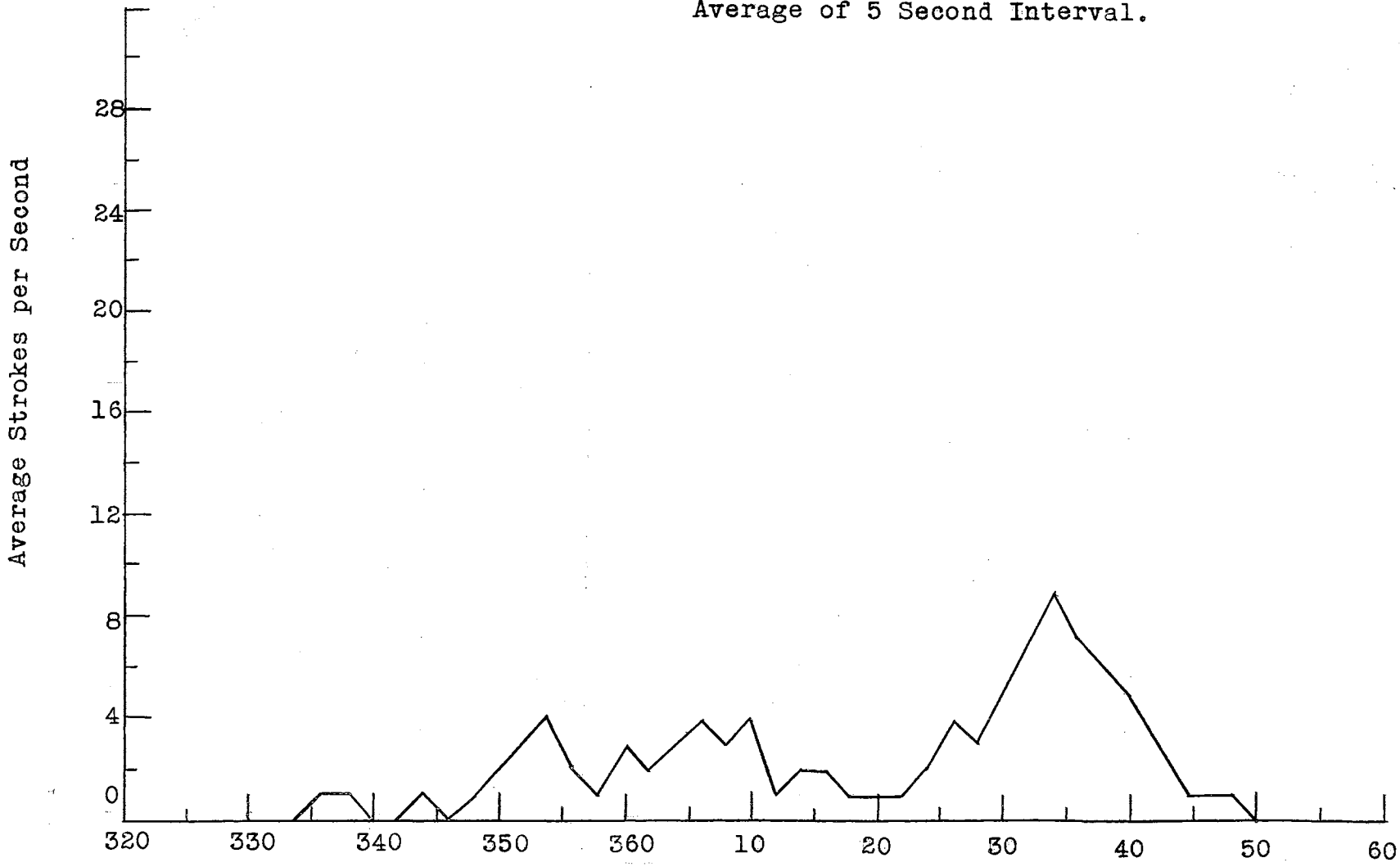

Figure 80

Azimuth Incidence Distribution of Sferic Activity Sampled by High Frequency Direction Finder, 27 May, 1955. Beginning with 2317 Hours, Average of 5 Second Interval.

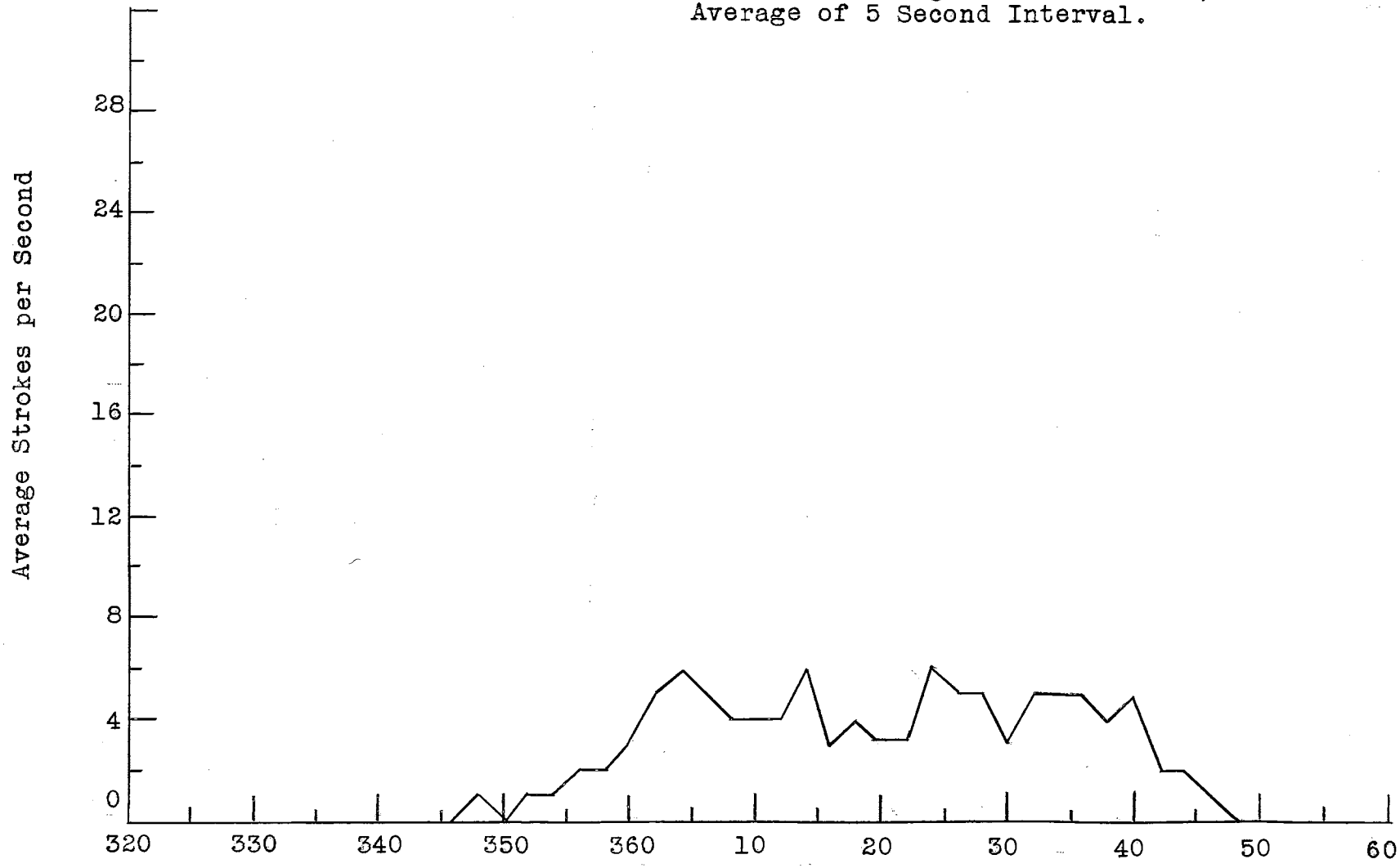

Figure 81

Azimuth Incidence Distribution of Sferic Activity Sampled by High Frequency Direction Finder, 27 May, 1955. Beginning with 2322 Hours, Average of 5 Second Interval.

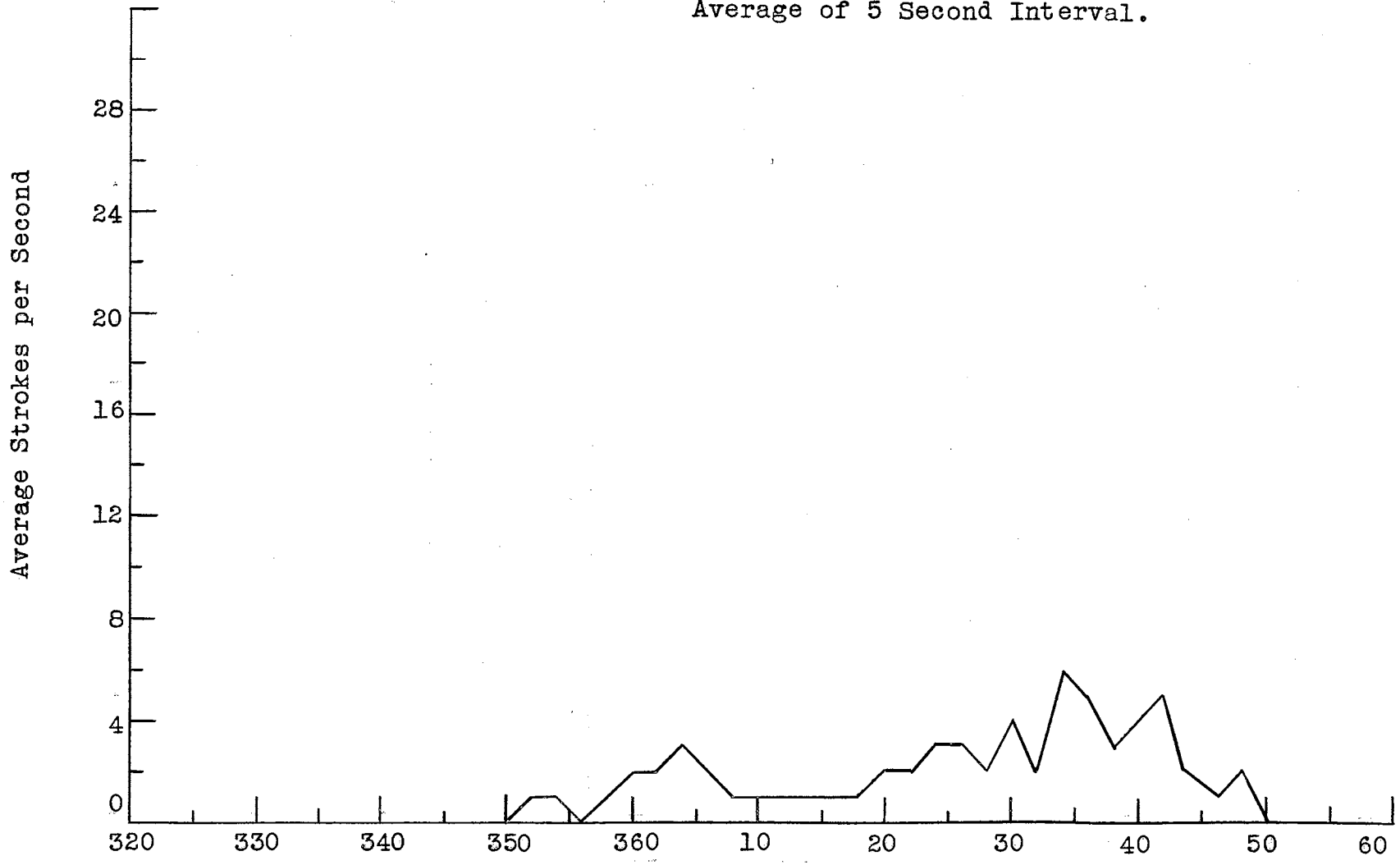

Figure 82

Azimuth Incidence Distribution of Sferic Activity Sampled by High Frequency Direction Finder, 27 May, 1955. Beginning with 2328 Hours, Average of 5 Second Interval.

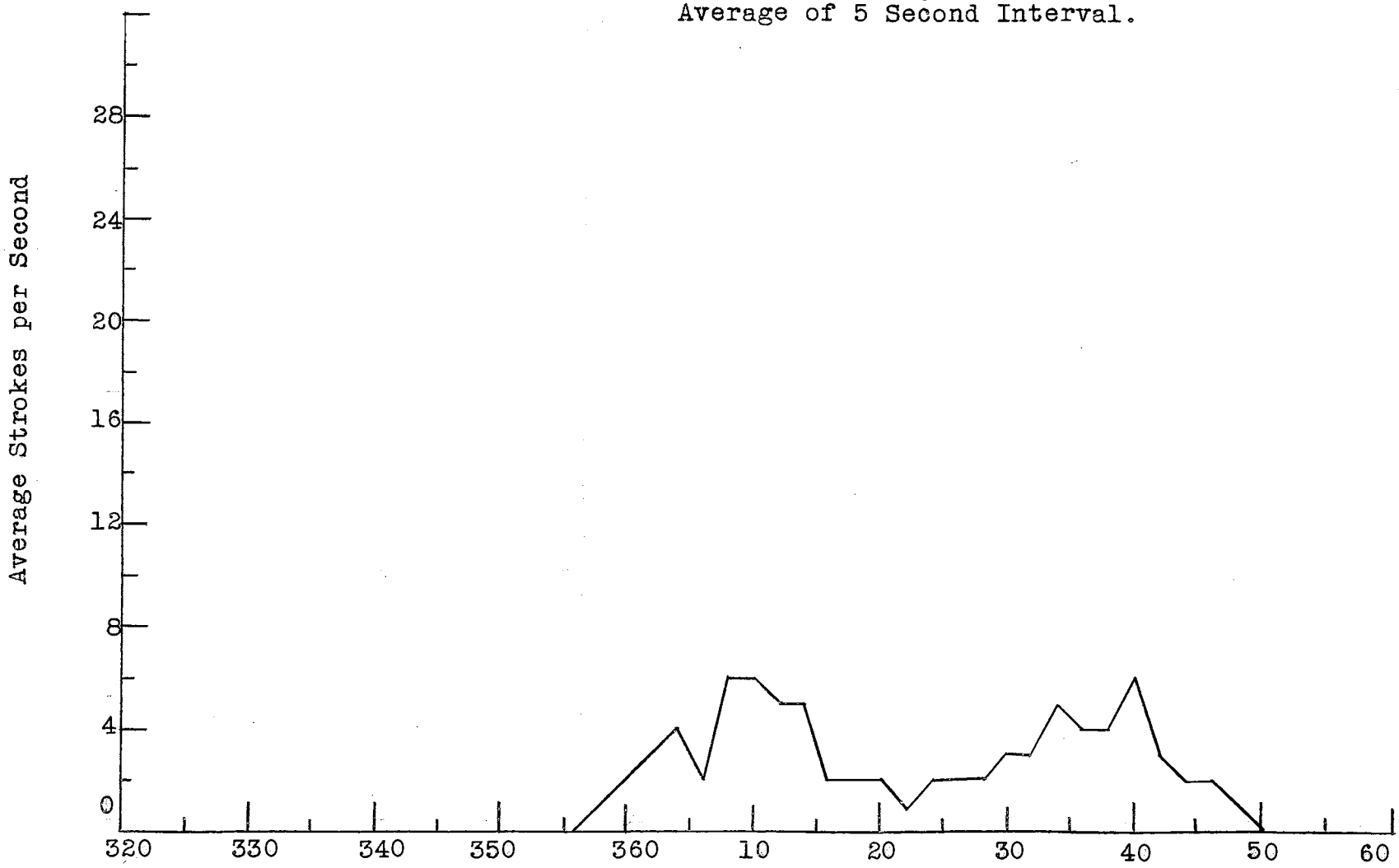

Figure 83

Azimuth Incidence Distribution of Sferic Activity Sampled by High Frequency Direction Finder, 27 May, 1955. Beginning with 2333 Hours, Average of 5 Second Interval.

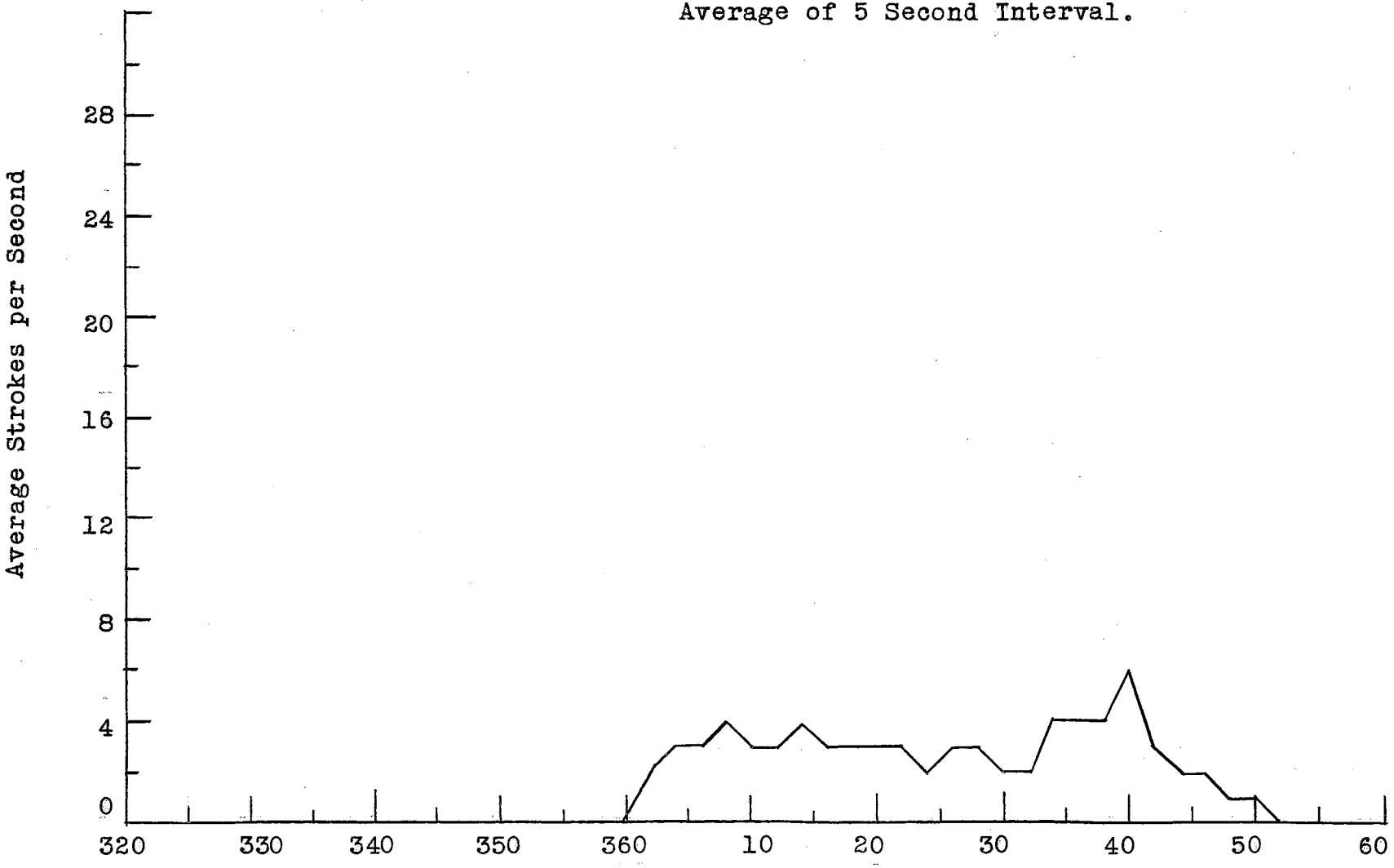

Figure 84

Azimuth Incidence Distribution of Sferic Activity Sampled by High Frequency Direction Finder 27 May, 1955. Beginning with 2338 Hours, Average of 5 Second Interval

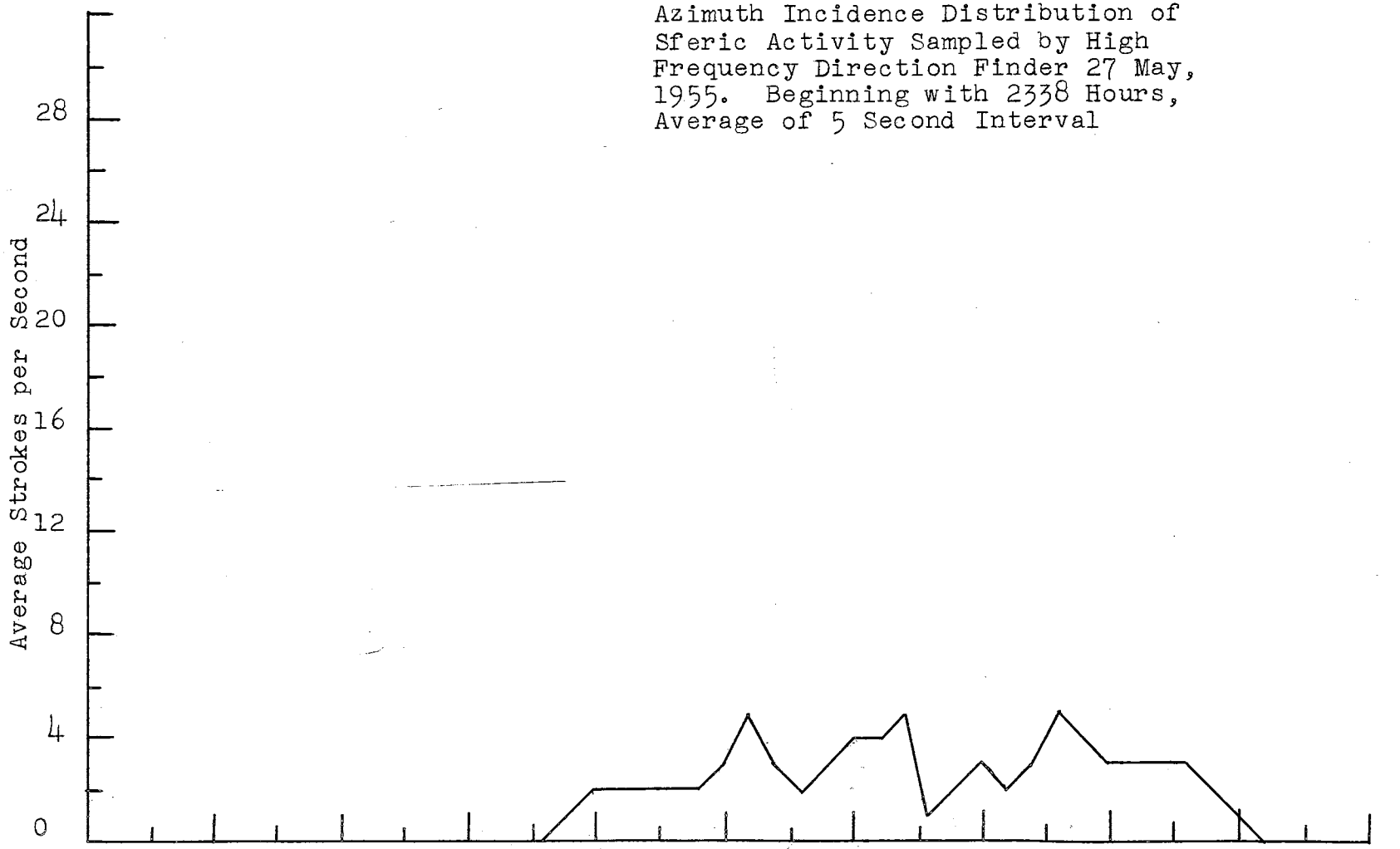

Figure 85

Azimuth Incidence Distribution of Sferic Activity Sampled by High Frequency Direction Finder, 27 May, 1955. Beginning with 2343 Hours, Average of 5 Second Interval.

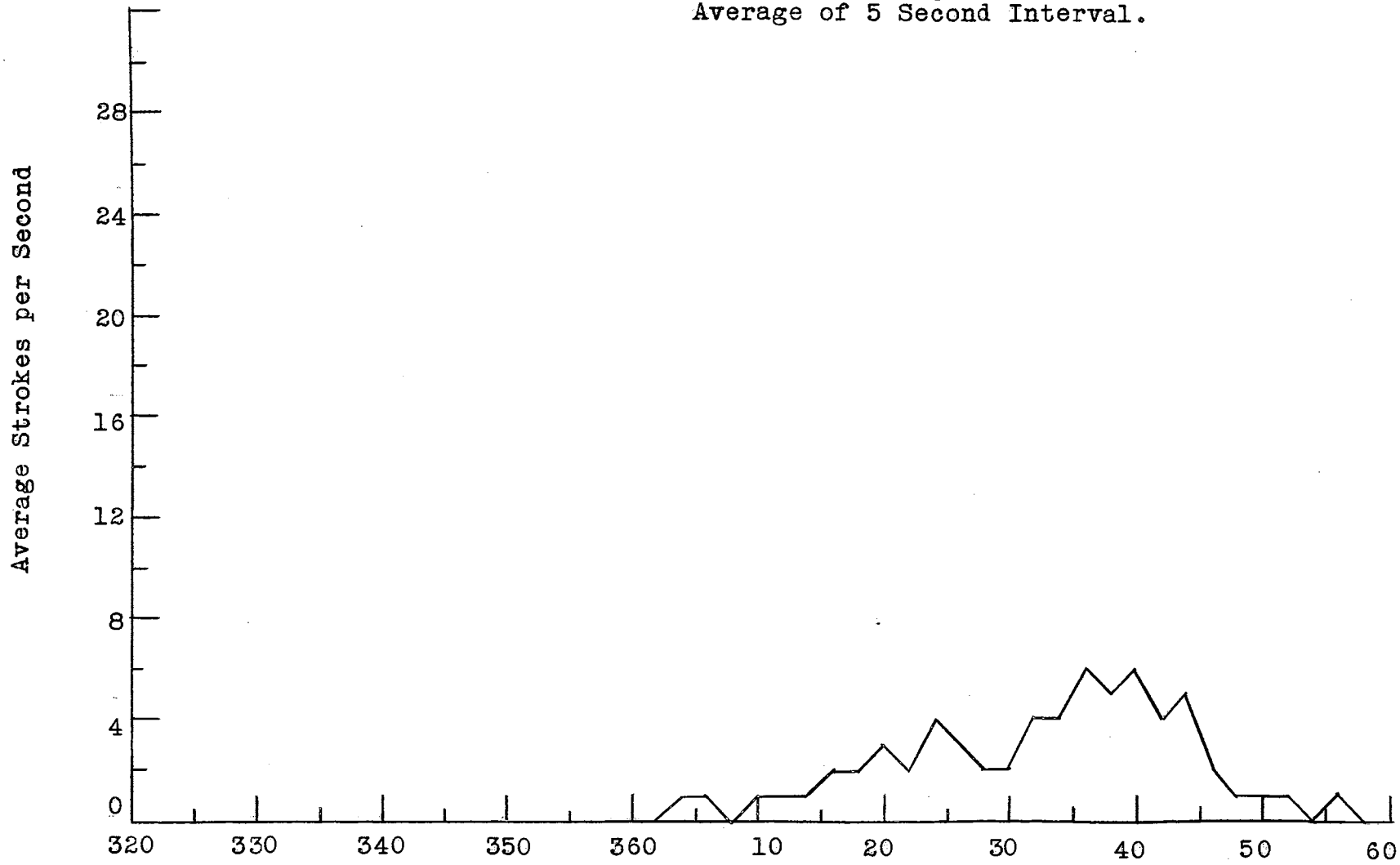

Figure 86

Azimuth Incidence Distribution of Sferic Activity Sampled by High Frequency Direction Finder, 27 May, 1955. Beginning with 2347 Hours, Average of 5 Second Interval.

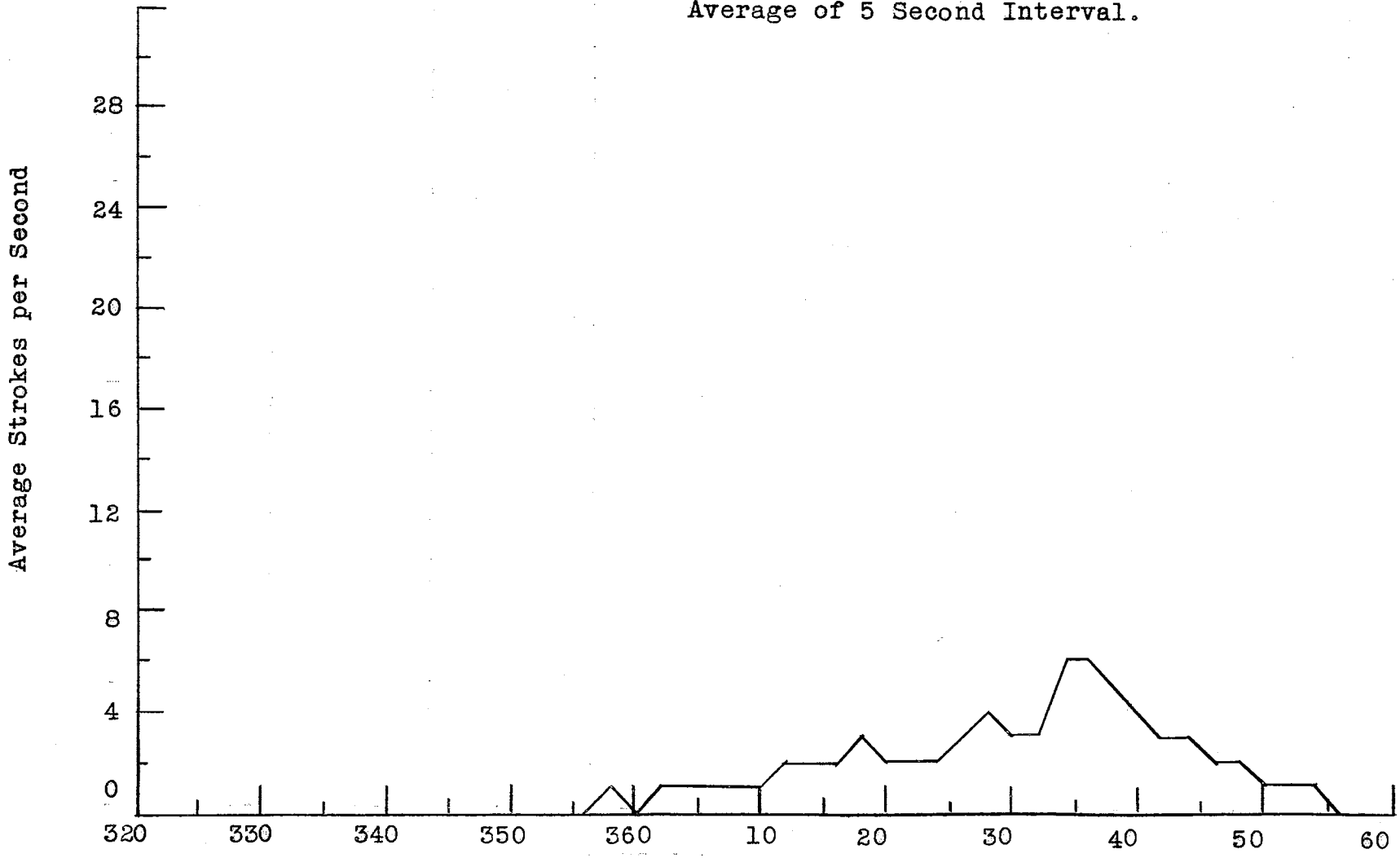

Figure 87

Azimuth Incidence Distribution of Sferic Activity Sampled by High Frequency Direction Finder, 27 May, 1955. Beginning with 2352 Hours, Average of 5 Second Interval.

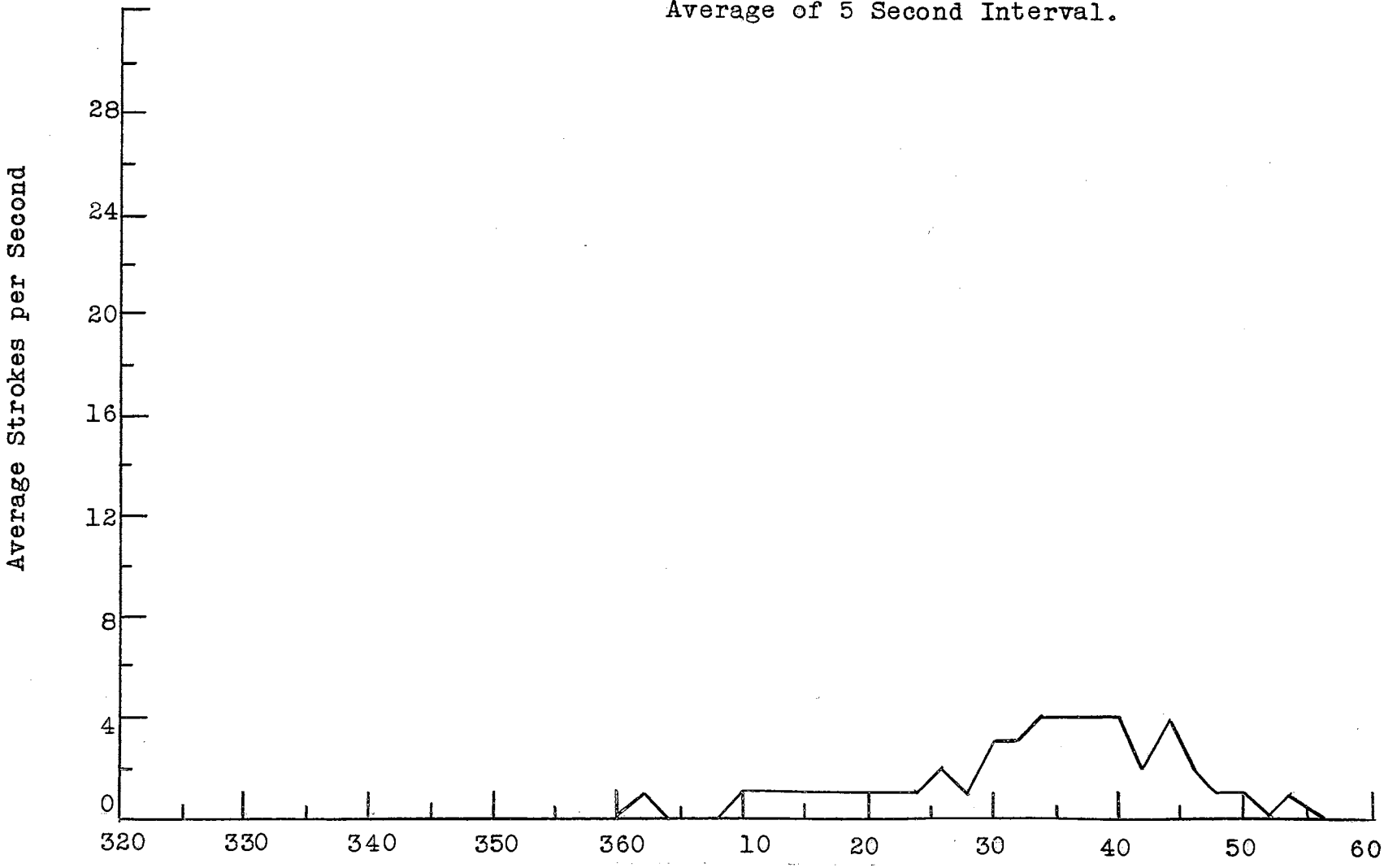

Figure 88

Azimuth Incidence Distribution of Sferic Activity Sampled by High Frequency Direction Finder, 27 May, 1955. Beginning with 2357 Hours, Average of 5 Second Interval.

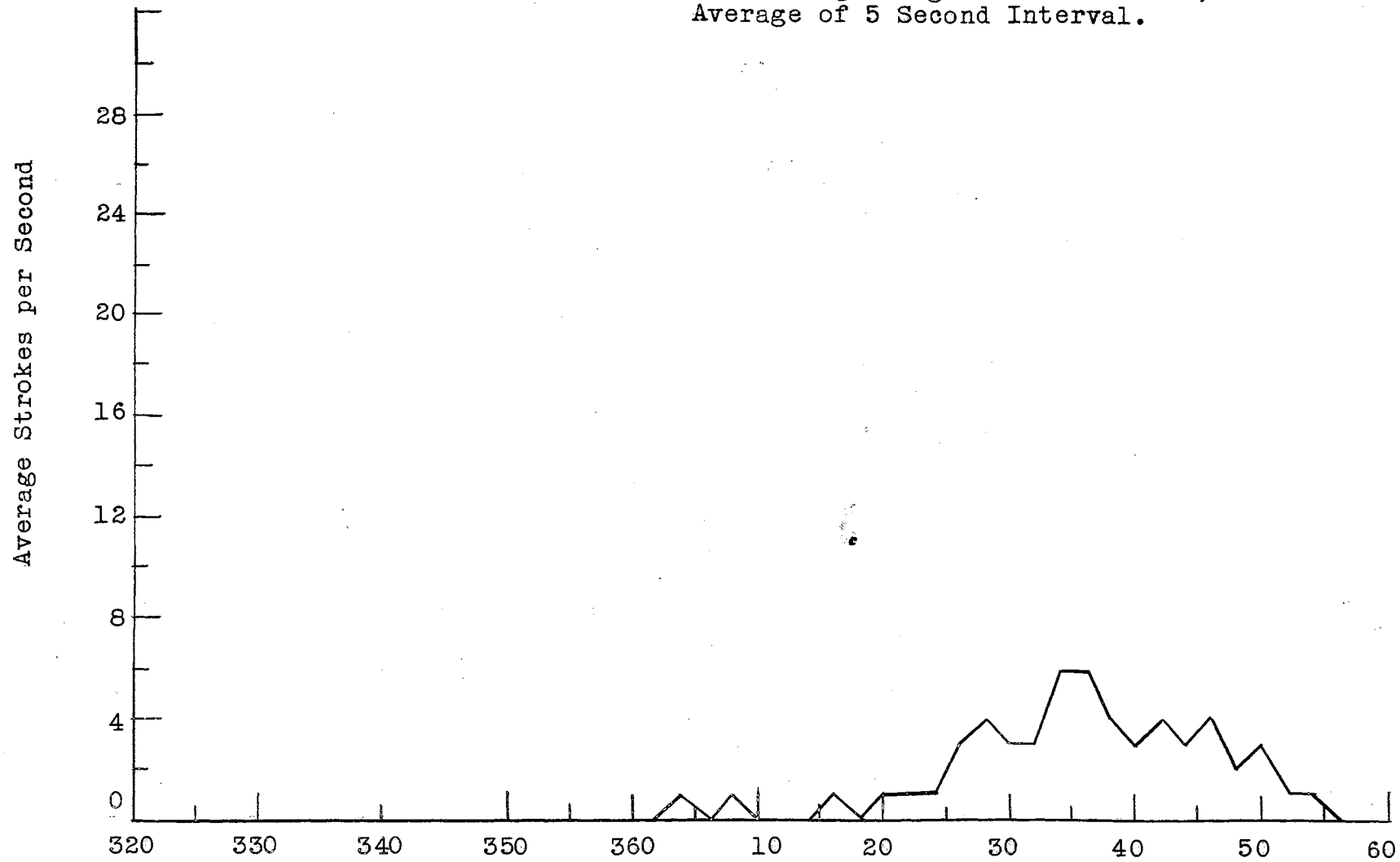

Figure 89

garded as a time sequence of storm events. The severe activity, as indicated by the peaks, was distributed over two major storm centers. In Figures 63 to 76 inclusive, there is only one peak in the azimuth plot of sferic intensity indicating only one major storm center. The lesser peaks of sferic intensity indicate minor thunderstorms or spurious disturbances. However, in Figure 77 (time 2257 CST) the azimuth distribution of sferics is seen to break up into two peaks, one at 356° and one at 30° indicating two storm centers of considerable magnitude. During the remainder of the time until 2357 CST, two storm centers are visible most of the time. The highest individual peak of average sferic activity occurred at 2233 CST at azimuth 25°. This peak reading of 13 strokes per second is still below the peak of 20 to 25 observed for most tornadoes.

In Figure 90 is shown how sferic activity builds up at a given location as a severe thunderstorm passes over. This graph shows the time distribution of sferics at azimuth 20° from 2140 CST until 2357 CST. There is no particular significance to this azimuth except that it is in the general region of interest. The graph shows that there was a background of about three strokes per second until about 2200 CST when the stroke rate suddenly increased to about 9 strokes per second and remained at that level for twenty minutes and then dropped to the background level of about three strokes per second. Unfortunately, there

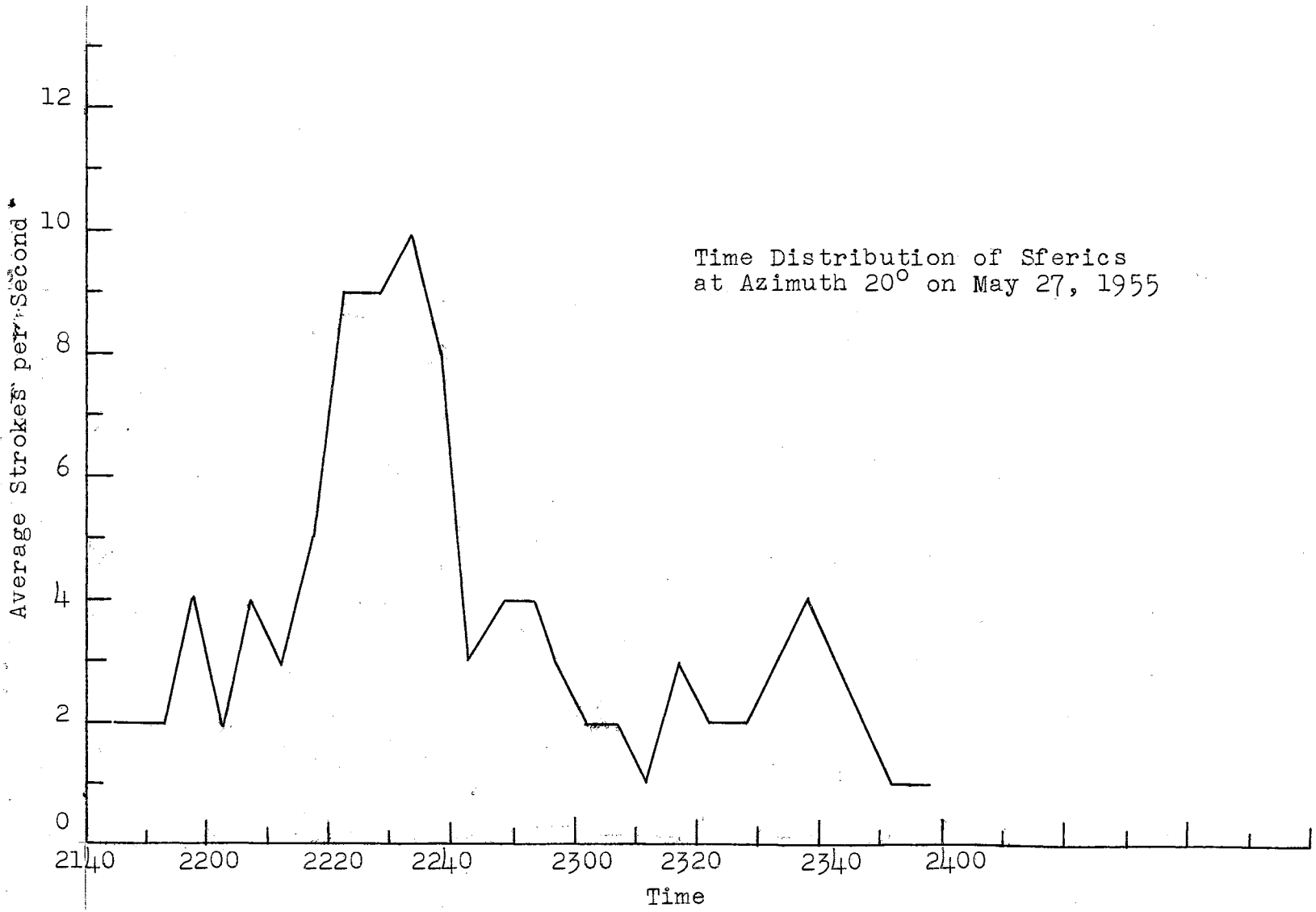
Time Distribution of Sferics
at Azimuth 20° on May 27, 1955
Average Strokes per Second
0
2
4
6
8
10
12
2140
2200
2220
2240
2300
2320
2340
2400
Time

Figure 90

is no data available to determine the actual weather conditions during this twenty-minute interval of time.

In Figures 91 to 97 inclusive are shown photographs of the radar screen at about 20-minute intervals during the lives of the storms. The azimuth distributions of sferics counts are shown at the tops of the pages for convenience. The position of the squall line may be observed on the photographs of the radar screen for successive intervals of time. A line intersecting the azimuth of maximum sferic intensity and the squall line indicates the storm center. The data shown in Figures 91 to 97 inclusive are summarized in Figure 98 which shows a plot of the squall line and the individual major storm centers at successive intervals of time. The motion of the squall line was generally southeast, but curved slightly more southward as it crossed north central Oklahoma. However, the motion of the two storm centers was almost straight east indicating that the storm centers were skidding along the squall line. This is a very interesting characteristic of severe storms which has been previously noted[2]. In one case it was observed that the thunderstorm suddenly reversed the direction of movement along the front. There is as yet no satisfactory theory to account for this component of velocity of a thunderstorm which is parallel to the direction of the

---

[2]"Research on Tornado Identification", Second Quarterly Progress Report, Signal Corps Research, Project No. 172 B, (1955), p. 14.

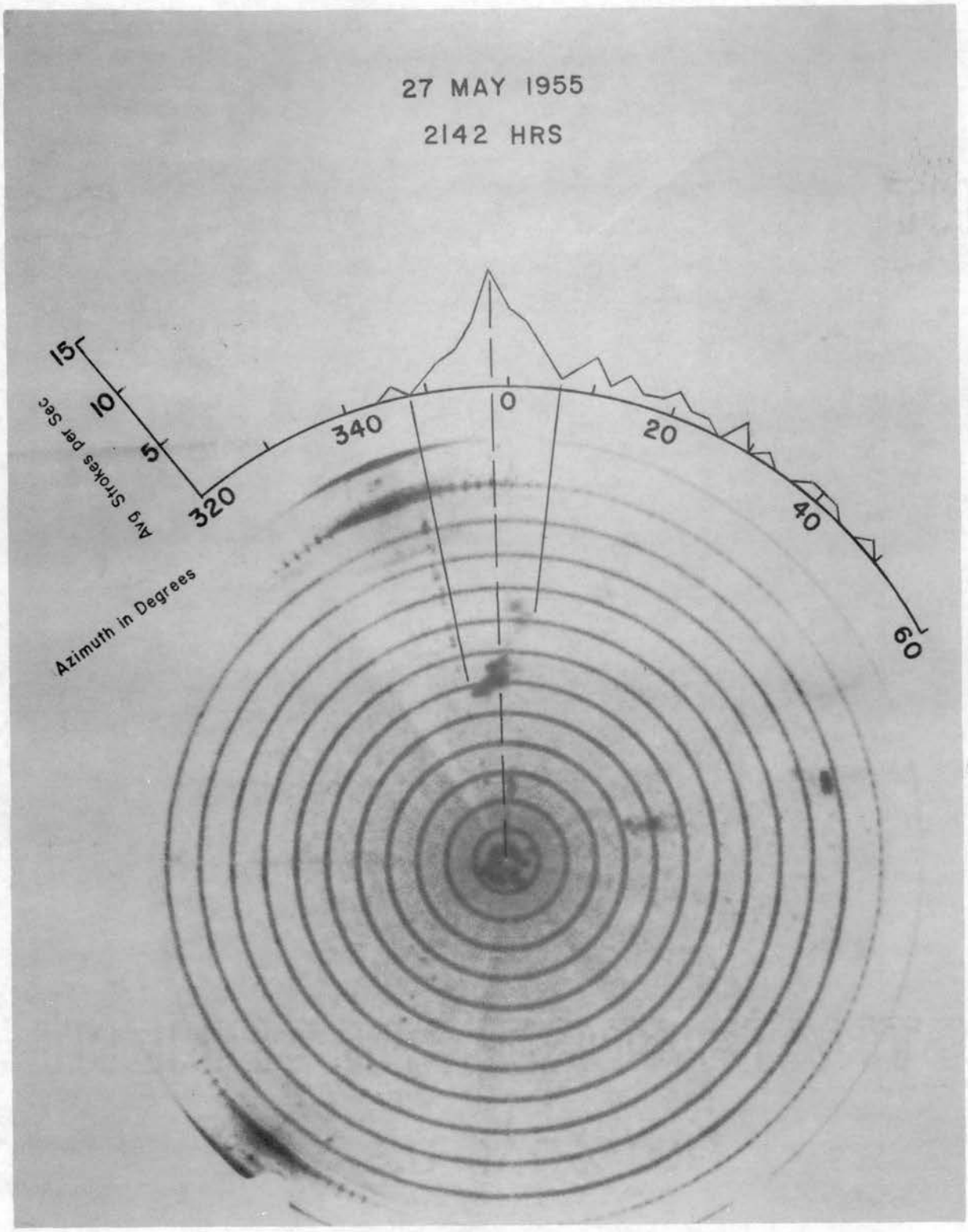

Figure 91. Radar-Sferics Composite for 2142 CST, 5-27-55.

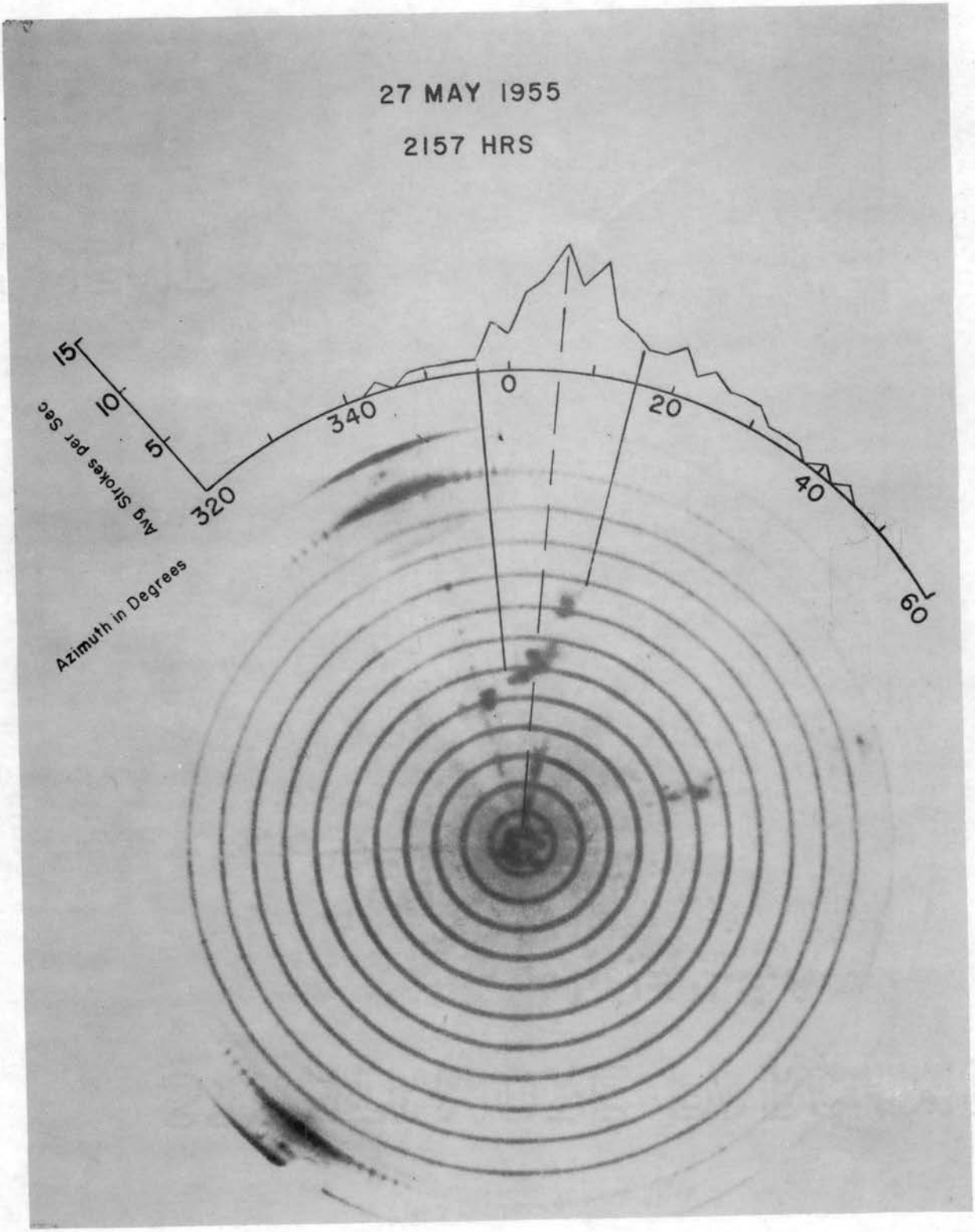

Figure 92. Radar-Sferics Composite for 2157 CST, 5-27-55.

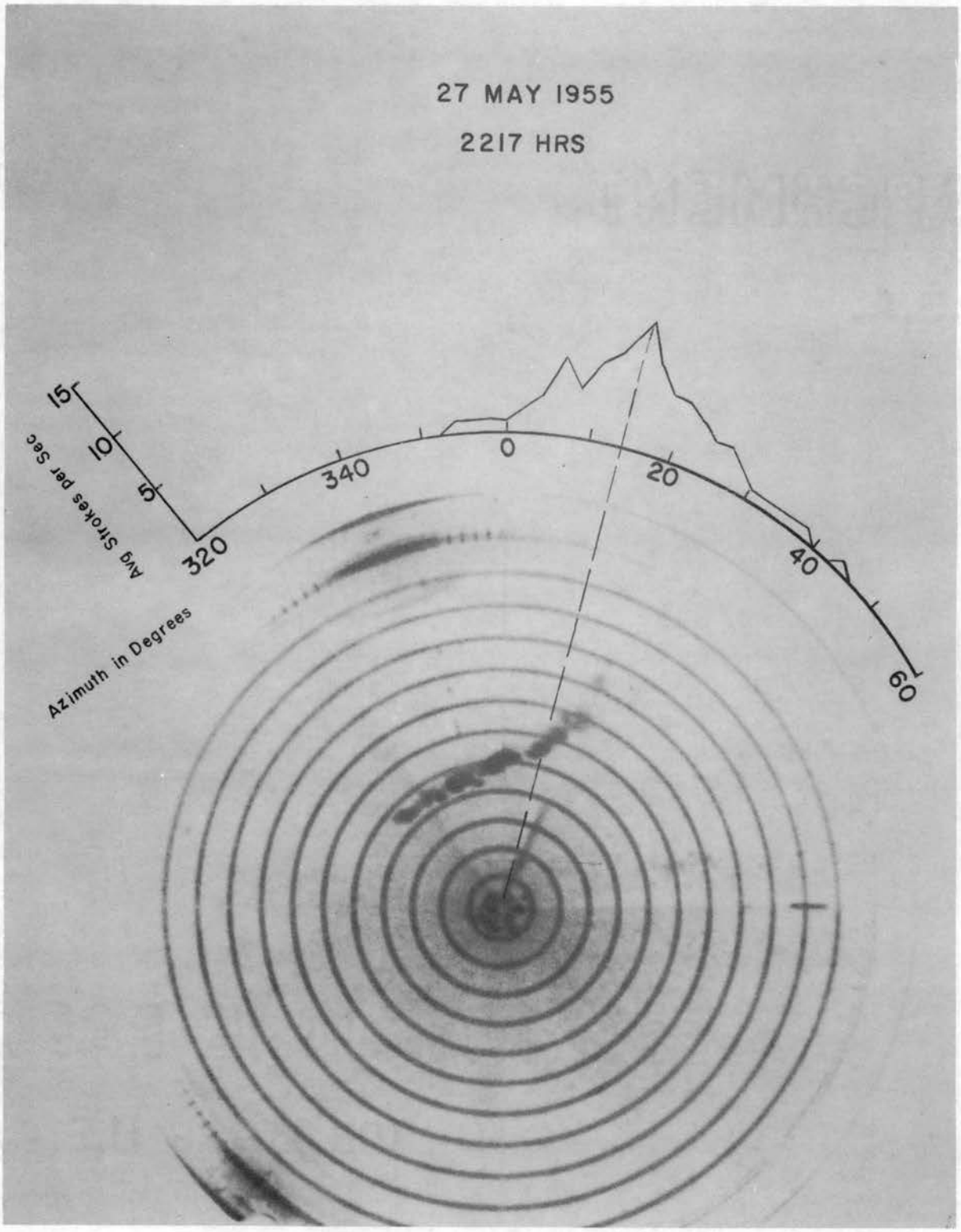

Figure 93. Radar-Sferics Composite for 2217 CST, 5-27-55.

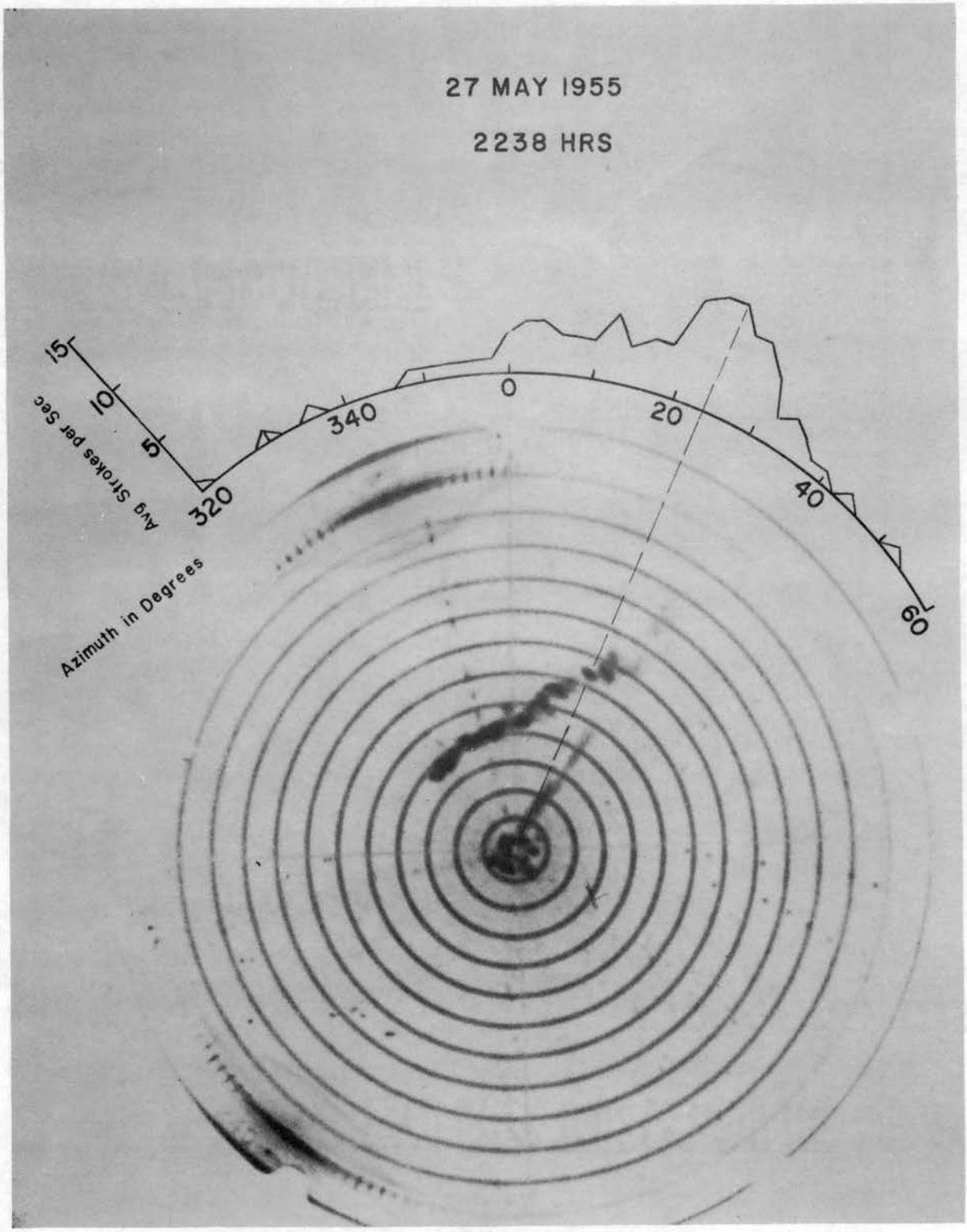

Figure 94. Radar-Sferics Composite for 2238 CST, 5-27-55.

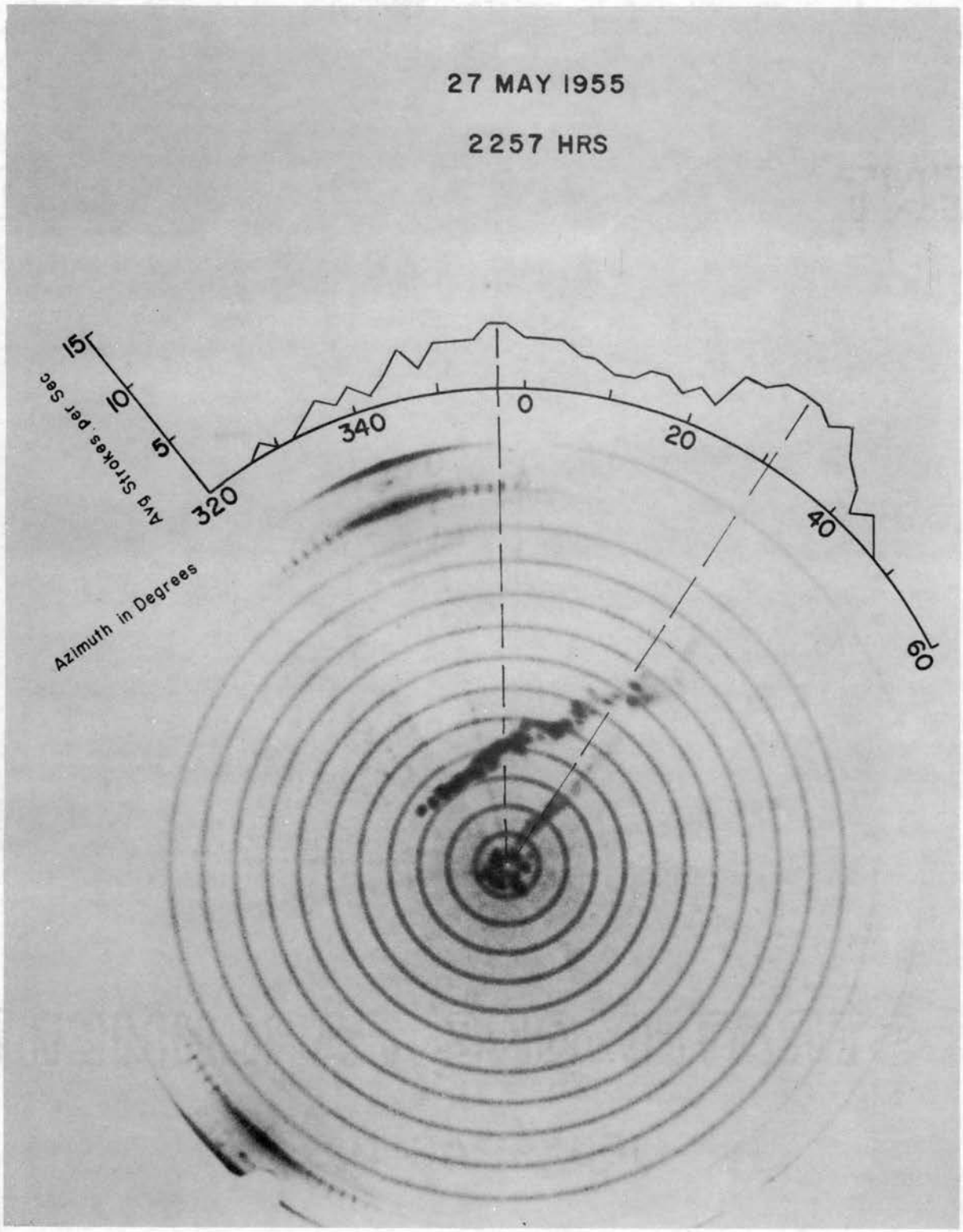

Figure 95. Radar-Sferics Composite for 2257 CST, 5-27-55.

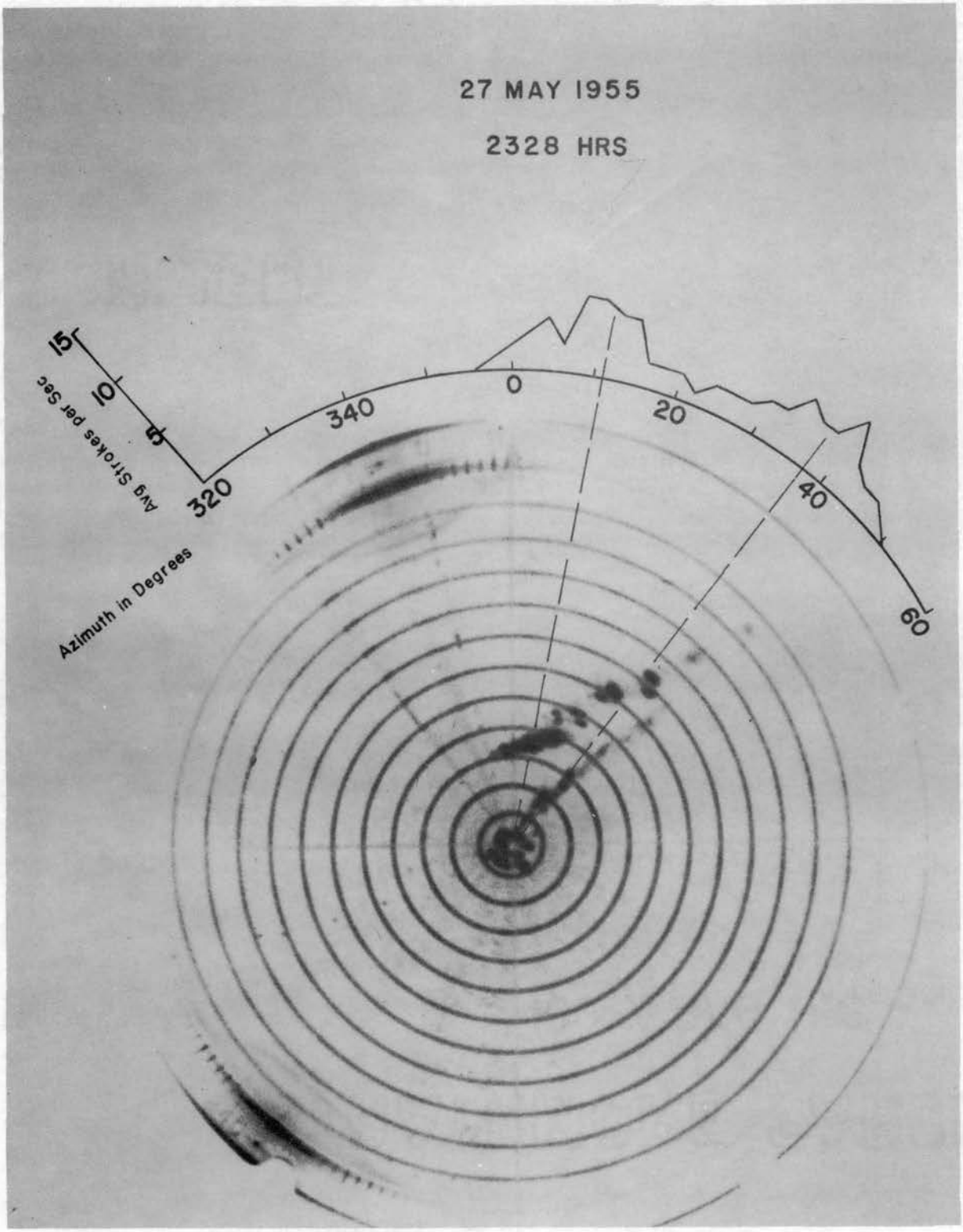

Figure 96. Radar-Sferics Composite for 2328 CST, 5-27-55.

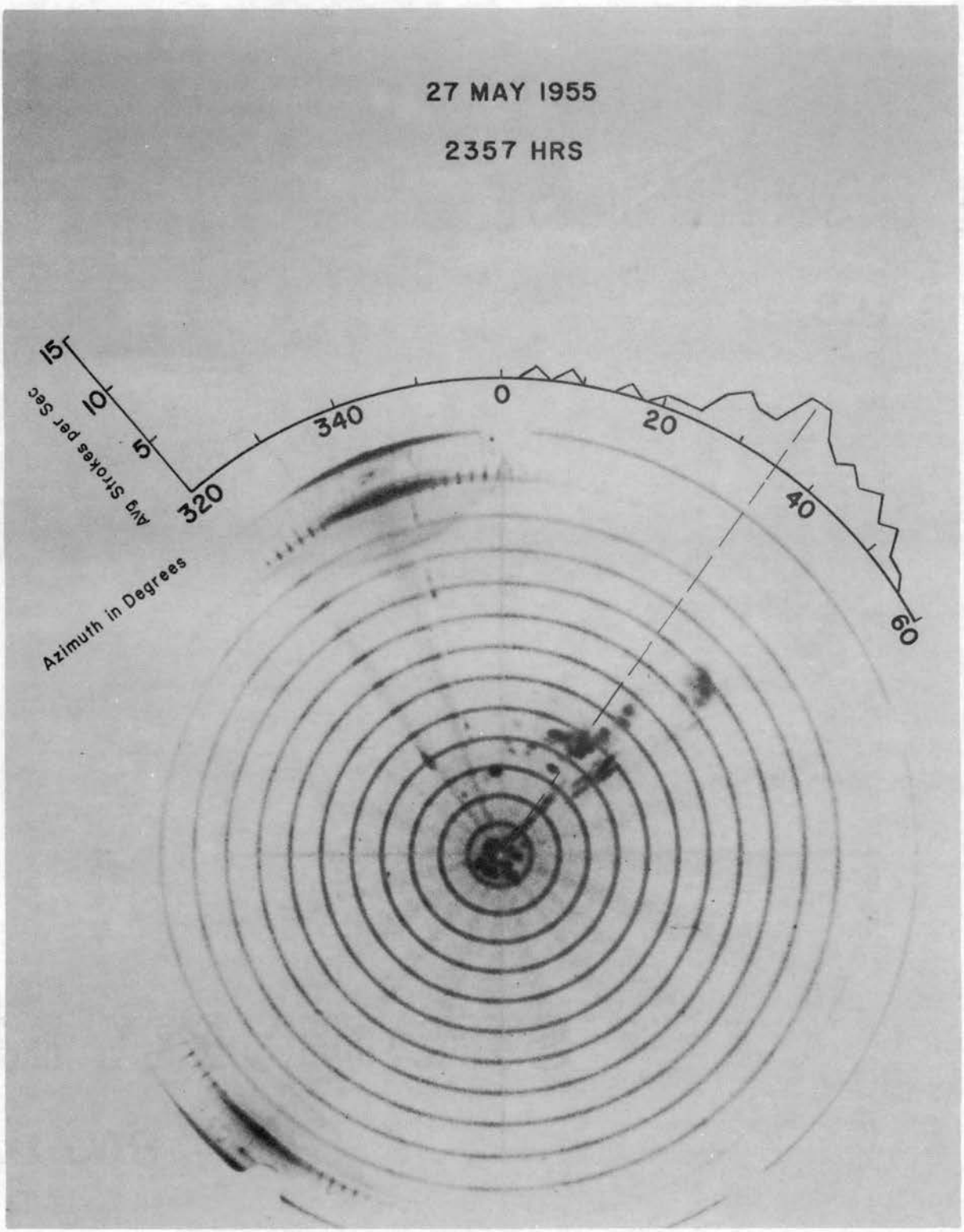

Figure 97. Radar-Sferics Composite for 2357 CST, 5-27-55.

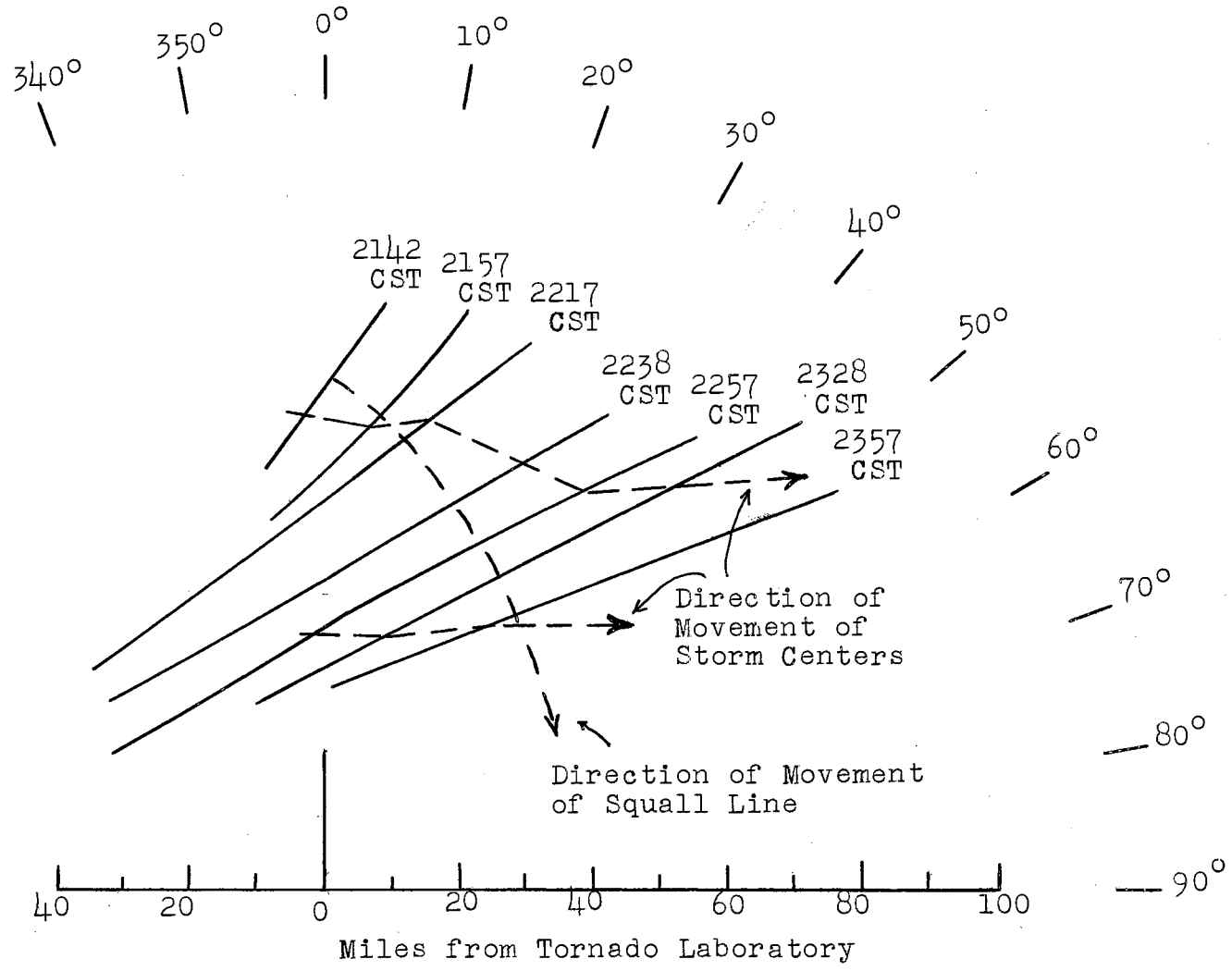

Figure 98. Plot of Movement of Storm Centers on May 27, 1955

squall line. (This problem would make a good subject for a doctoral thesis.)

The more northerly and intense of these two thunderstorms followed a path along US Highway 60, over Ponca City, then to Pawhuska and then to a point near Bartlesville. The second storm center passed just a few miles north of the Tornado Laboratory and likewise moved in an easterly direction.

Conclusions

The successful tracking of the storms of May 27, 1955 indicated that the combined radar-sferic method is entirely feasible as a practical method for locating and tracking all thunderstorms within range of the radar. The data presented here represents the first attempt to determine by the radar-sferics method the paths of thunderstorm centers in an advancing squall line. It is of importance that the paths determined at the time of the storm were quite similar to those determined by this later analysis of the data. These paths also agree with those determined by checking with the police departments of towns and cities in the general area of the storms.

CHAPTER VI

SUMMARY AND CONCLUSIONS

It has been the purpose of this study to improve the instrumentation used in identifying and tracking tornadoes by the radar-sferic method and to evaluate, not only the improved instruments, but also the usefulness of the method itself. In this thesis the emphasis has been placed on the sferic detector, or direction finder, and not on the radar which was already adequate for the purpose.

The first step in carrying out the objectives was to make an analysis of the available direction finder, the AN/GRD-1A. Past experience had found the AN/GRD-1A to be quite adequate for studying severe weather activity where long range was desirable, which is the case when hurricanes or other storms of large areal extent are being surveyed. For localized disturbances such as tornadoes, however, where the frequencies of the electrical discharges are high, the AN/GRD-1A was found to be of limited application. The analysis of the AN/GRD-1A was made in order to evaluate its usefulness in tornado identification and tracking and to determine the desirable characteristics of a new instrument to be designed more specifically for tornado work.

After the limitations of the AN/GRD-1A direction finder as applied to tornado studies were determined, a new sferic direction finder was designed which operates in the frequency range between 100 kilocycles per second and 300 kilocycles per second. The AN/GRD-1A is restricted in frequency response to the vicinity of 10 kilocycles per second. After some modification, the High Frequency Direction Finder was found to be well suited to the detection of the high frequency sferics generally associated with tornadoes and other localized severe weather activity.

The first real test of the new High Frequency Direction Finder occurred on the night of May 25, 1955 when a series of tornadoes swept across Texas, Oklahoma and Kansas. The separate tornadoes that struck Blackwell, Oklahoma, and Udall, Kansas, were particularly devastating. Although the meteorological conditions associated with these tornadoes were very complex, it was possible to identify them accurately and to plot their course by the radar-sferic method.

Two days later a squall line passed over the same general area as the tornadoes of May 25, 1955 and severe thunderstorm activity was noted. This squall line, with two widely separated storm cells, was almost ideal for evaluating the radar-sferic method. It was possible to identify the squall line on the radar and to obtain the direction of maximum sferic count from the High Frequency

Direction Finder. The intersection of the two lines was postulated as being the center of the storm cells. The path of these storm cells as plotted by the radar-sferic method was later verified by testimonies of eye witnesses.

It may be concluded that the radar-sferic method, using the High Frequency Direction Finder, is a powerful tool for identifying and tracking tornadoes and other severe weather activity that falls within the range of the instruments. It should be entirely possible to set up a warning system based on this method which would lessen the terrible loss of lives which has always plagued the inhabitants of the Great Plains region. It is hereby recommended that steps be taken to set up such a warning network.

It is recognized that there may, and probably will, be tornadoes which do not conform to the pattern of sferic and radar activity as treated in this study. Such inconsistencies are to be expected in almost any branch of Geophysics. For this reason it is strongly urged that research on the identification and tracking of tornadoes be continued. It is also suggested that research be initiated to study the physical forces which are present in the formation of a tornado and which determine the pattern that a tornado follows.

It is believed that the time is near when it will be possible to identify positively a tornado in the formative stage and then to take steps that will prevent

the formation of the tornado. The development of such a process would rank with the major scientific accomplishments of recent years. It is further believed that the Tornado Research Program at Oklahoma A & M College, of which this present study is but a small part, is capable of developing a method which may result in the destruction of tornadoes in the formative stage.

BIBLIOGRAPHY

Bode, H. W. Network Analysis and Feedback Amplifier Design. (D. Van Nostrand Company Inc., New York, 1945), pp. 22-30

Fawbush, Major E. J., Captain R. C. Miller, and Captain L. G. Starrett, "An Empirical Method of Forecasting Tornado Development", Bulletin of the American Meteorological Society, January, 1951, pp. 1-9

Flora, Snowden D. Tornadoes of the United States, (University of Oklahoma Press, Norman, 1953), p. 137

Goldman, Stanford, Transformation Calculus and Electrical Transients, (Prentice-Hall, Inc., New York, 1949) pp. 58-62, 102

Greenwood, I. A., Jr., J. V. Holdan, Jr., and Duncan MacRae, Jr., Electronic Instruments, (McGraw-Hill Book Company, Inc., New York, 1948), pp. 573-664

Lindsey, Joe Pat, "An Analysis of the Sferic Waveform", Unpublished Masters Thesis, Oklahoma Agricultural and Mechanical College, (1954), pp. 41-43

"Research on Tornado Identification", Sixth Quarterly Progress Report, Signal Corps Research Project No. 172B-0, 1953, pp. 18-19

"Research on Tornado Identification", Tenth Quarterly Progress Report, Signal Corps Research Project No. 172B-0, 1954, pp. 27

"Research on Tornado Identification", Eleventh Quarterly Progress Report, Signal Corps Research Project No. 172B-0, 1954, pp. 16-18

"Research on Tornado Identification", Second Quarterly Progress Report, Signal Corps Research Project No. 172B, 1955, pp. 12, 14, 17

Schelkunoff, Sergei A., Harald T. Friis, Antennas, Theory and Application, (John Wiley and Sons, New York, 1952) pp. 503-508

"Static Direction Finder AN/GRD-1A", War Department Technical Manual TM 11 - 2693, 1945

Turrentine, Charles M., "A Radar-Sferic Analysis of the Tornadoes of May 25, 1955", Unpublished Masters Thesis, Oklahoma Agricultural and Mechanical College, (1956) p. 27.

Valley, G. E., Jr., Henry Wallman, Vacuum Tube Amplifiers, (McGraw-Hill Book Company, Inc., New York, 1948) p. 44, 71-112

VITA

Henry Bradford Ferguson

Candidate for the Degree of

Doctor of Philosophy

Thesis: TORNADO TRACKING BY HIGH FREQUENCY SFERICS

Major Field: Electrical Engineering

Biographical:

Personal data: Born near Hulbert, Oklahoma, March 25, 1918, the son of Sam B. and Effie Lena Ferguson.

Education: Attended grade school in Cherokee County and Muskogee County, Oklahoma; graduated from the High School Department of Connors State Agricultural College in 1937; received the Bachelor of Science degree from Oklahoma Agricultural and Mechanical College, with a major in Electrical Engineering, in June, 1942; received the Master of Science degree from Oklahoma Agricultural and Mechanical College, with a major in Electrical Engineering, in June, 1948; completed requirements for the Doctor of Philosophy degree in May, 1956.

Professional Exerience: Employed by the General Electric Company in Schenectady, New York and Minneapolis, Minnesota, as a test Engineer and as a field Engineer, from June, 1942 until June, 1944. Entered the United States Navy in June, 1944, and served two years during which time was promoted from Ensign to Lieutenant (junior grade). Served as a technical radar officer attached to the Special Devices Division of the Naval Office of Research and Invention. Primary duty was the development of new radar equipment. Employed from June, 1946 until September, 1947 by Oklahoma Agricultural and Mechanical College as an Instructor in the Electrical Engineering Department.

Employed from September, 1947 until January, 1948 by Iowa State College as an Instructor in the Electrical Engineering Department. Employed since January, 1948 by The Carter Oil Company in the Research Department. Present position Head of the Geophysical Research Section.

TYPIST PAGE

THESIS TITLE: TORNADO TRACKING BY HIGH FREQUENCY SFERICS

AUTHOR: Henry Bradford Ferguson

THESIS ADVISER: Dr. Herbert L. Jones

The content and form have been checked and approved by the Author and Thesis Adviser. The Graduate School Office assumes no responsibility for errors either in form or content. The copies are sent to the bindery just as they are approved by the Author and Faculty Adviser.

TYPIST: Mrs. Doris Harding